Understanding projected salinity changes in the global ocean of the MPI-Earth system model under a global warming scenario

Dissertation

zur Erlangung des Doktorgrades der Naturwissenschaften
an der Fakultät für Mathematik, Informatik und Naturwissenschaftenan
Fachbereich Geowissenschaften
der Universität Hamburg

vorgelegt von Anju Sathyanarayanan
from Chalakudy, India

Hamburg, 2020

Als Dissertation angenommen am Fachbereich Geowissenschaften

Tag des Vollzugs der Promotion:	14-09-2020
Gutachter/Gutachterinnen:	Prof. Dr. Detlef Stammer Dr. Armin Köhl
Vorsitzender des Fachpromotionsausschusses Geowissenschaften:	Prof. Dr. Dirk Gajewski
Dekan der Fakultät MIN:	Prof. Dr. Heinrich Graener

Abstract

Salinity in the global ocean has started experiencing substantial changes related to the present-day warming and an associated intensification of the global water cycle. The resulting salinity trends which can be characterized as driven by "wet get wetter and dry get drier" are expected to continue over the next century, with a strength that will depend on the anthropogenic forcing. An assessment of the impact of the salinity changes on the general circulation requires to understand the mechanisms driving these changes, their attribution to changing surface fluxes, but also on the mechanisms influencing the rest of the physical ocean. In a projected climate, resulting in significant changes in the surface fluxes, each of these forcing mechanisms may drive a distinctly different salinity response.

The primary objective of this study is to distinguish between salinity changes resulting from warming, freshwater flux and wind-stress changes and to use this information to investigate mechanisms that are expected to drive future changes.

We investigated salinity change mechanisms that are simulated under strong climate change forcing conditions. This part of the study is based on the output of the Max Planck Institute Earth System Model (MPI-ESM) Medium Resolution run with RCP8.5 forcing conditions. In comparison to the present-day oceanic conditions, sea surface salinity (SSS) increases towards the end of the 21st century in the tropical and the subtropical Atlantic. In contrast, a basin-wide surface freshening can be observed in the Pacific and Indian Oceans. The RCP8.5 forcing scenario with a global surface warming of $\sim$2.3 °C marks a water cycle amplification of 19 % and a SSS signal amplification of 18 %. A dominant part of this amplification in SSS comes from the Atlantic Ocean (31 %), whereas the Pacific and Indian Oceans show a weaker amplification of 9 %.

On a large scale, the global water cycle drives global SSS changes by altering the surface freshwater flux. On smaller scales, advection related to circulation substantially affects near-surface changes. A large fraction of its associated advection changes is required to balance the advection change related to circulation changes. Subsurface salinity changes can be decomposed into the surface-forced changes in water masses (spice) and the heaving of isopycnals. We find that the changes in surface freshwater flux

dominate the upper 500 m subsurface salinity changes in the subtropical oceans by forcing the surface anomalies to subsurface through spice signal. While this is true for all the subtropical ocean basins, in the subtropical Atlantic Ocean, the dynamical response associated with wind-stress and circulation changes is equally important in driving subsurface salinity changes in the upper 1000 m. However, this mechanism is less significant for salinity adjustment in the Pacific and Indian oceans.

In a subsequent study, a set of Flux-Anomaly-Forced Model Intercomparison Project (FAFMIP) sensitivity experiments, are used to verify the salinity response to individual surface forcings. These sensitivity experiments from the high-resolution version of MPI-ESM indicate a similar response in salinity to surface freshwater flux in an RCP8.5 scenario. Analysing a small region of the South Atlantic Ocean, we find that freshwater flux changes alone were insufficient to see a significant SSS signal amplification. This indicates the strong role of surface warming in driving the Atlantic SSS response alongside the freshwater flux. However, the heat flux experiment in FAFMIP is unsuitable for isolating the salinity changes associated with warming in the global ocean. Finally, a passive tracer experiment perturbed with the same freshwater flux prescribed in the FAFMIP experiment shows the need to consider the role of ocean-atmosphere feedbacks and circulation changes in quantifying the salinity response to freshwater flux changes.

The results advance our knowledge about projected salinity changes by showing the consistently dominant role of the surface freshwater flux in forcing salinity changes in both depth and density levels for all the ocean basins. These results suggest that the water cycle changes under strong anthropogenic CO_2-forcing can lead to major changes in SSS and subsurface salinity over large parts of the global ocean.

Zusammenfassung

Der Salzgehalt im globalen Ozean hat im Zusammenhang mit der heutigen Erwärmung und einer damit verbundenen Intensivierung des globalen Wasserkreislaufs erhebliche Veränderungen erfahren. Die daraus resultierenden Salzgehaltstrends sind getrieben durch das Muster "nass wird nasser und trocken wird trockeneründ werden sich voraussichtlich im nächsten Jahrhundert fortsetzen, wobei die Stärke dieser Trends vom anthropogenen Einfluss abhängen wird. Eine Beurteilung der Auswirkungen der Salzgehaltsveränderungen auf die allgemeine Zirkulation erfordert das Verständnis der Mechanismen, die diese Veränderungen antreiben, ihre Zuordnung zu den sich ändernden Oberflächenflüssen, aber auch zu den Mechanismen, die den Rest des physikalischen Ozeans beeinflussen. In einem prognostizierten Klima, das zu signifikanten Veränderungen der Oberflächenflüsse führt, kann jeder dieser Antriebsmechanismen eine deutlich unterschiedliche Änderung des Salzgehalts bewirken.

Das primäre Ziel dieser Studie ist es, zwischen Salzgehaltsänderungen infolge von Erwärmung, Süßwasserflüssen und Windeinflussänderungen zu unterscheiden und diese Informationen zu nutzen, um Mechanismen zu untersuchen, von denen erwartet wird, dass sie zukünftige Veränderungen antreiben könnten.

Wir untersuchten Mechanismen der Salzgehaltsänderung, die unter Bedingungen eines starken Klimawandels simuliert werden. Dieser Teil der Studie basiert auf Ergebnissen des Erdsystemmodells des Max-Planck-Instituts für Meteorologie (MPI-ESM) in mittlerer Auflösung, das mit dem RCP8.5-Szenario angetrieben wurde. Im Vergleich zu den heutigen ozeanischen Bedingungen nimmt der Salzgehalt der Meeresoberfläche (SSS) im tropischen und subtropischen Atlantik gegen Ende des 21. Jahrhunderts zu. Im Gegensatz dazu ist im Pazifik und im Indischen Ozean eine beckenweite SSS-Abnahme zu beobachten. Das RCP8.5 Antriebsszenario mit einer globalen Oberflächenerwärmung von ∼2.3 °C markiert eine Wasserkreislaufverstärkung von 19 % und eine SSS-Signalverstärkung von 18 %. Ein dominanter Teil dieser SSS-Verstärkung kommt aus dem Atlantischen Ozean (31 %), während der Pazifische und Indische Ozean eine schwächere Verstärkung von 9 % aufweisen.

Großskalig treibt der Wasserkreislauf die globalen SSS-Veränderungen an, indem er den oberirdischen Süßwasserfluss verändert. Auf kleineren Skalen beeinflusst die Ad-

vektion im Zusammenhang mit der Zirkulation die oberflächennahen Veränderungen wesentlich. Ein großer Teil der damit verbundenen Advektionsänderung ist erforderlich, um die Advektionsänderung im Zusammenhang mit Zirkulationsänderungen auszugleichen. Salzgehaltsänderungen unterhalb der Oberfläche können in oberflächenbedingte Änderungen der Wassermassen (Spice) und die Hebung von Isopyknen zerlegt werden. Wir stellen fest, dass die Änderungen des oberirdischen Süßwasserflusses die oberen 500 m der unterirdischen Salzgehaltsänderungen in den subtropischen Ozeanen dominieren, indem die Oberflächenanomalien durch das Spicesignal nach unten gezwungen werden. Während dies für alle subtropischen Ozeanbecken gilt, ist im subtropischen Atlantischen Ozean die dynamische Reaktion, die mit Windeinfluss und Zirkulationsänderungen verbunden ist, ebenso wichtig, um die unterirdischen Salzgehaltsänderungen in den oberen 1000 m voranzutreiben. Dieser Mechanismus ist jedoch für die Salzgehaltsanpassung im Pazifischen und Indischen Ozean weniger ausgeprägt.

In einer anschließenden Studie wird eine Reihe von Sensitivitätsexperimenten des Flux-Anomaly-Forced Model Intercomparison Project (FAFMIP) verwendet, um die Reaktion des Salzgehalts auf individuelle Oberflächeneinflüsse zu verifizieren. Die Sensitivitätsexperimente, die mit der hochauflösenden Version von MPI-ESM durchgeführt wurden, weisen auf eine ähnliche Reaktion des Salzgehalts auf den Oberflächensüßwasserfluss in einem RCP8.5-Szenario hin. Eine kleine Region im Südatlantik zeigt, dass Süßwasserflussänderungen allein nicht ausreichten, um eine signifikante SSS-Signalverstärkung zu erkennen. Dies deutet auf die starke Rolle der Oberflächenerwärmung bei der Steuerung der atlantischen SSS-Reaktion neben dem Süßwasserflusses hin. Das Wärmeflussexperiment in FAFMIP ist jedoch ungeeignet, um die mit der Erwärmung im globalen Ozean verbundenen Salzgehaltsänderungen zu isolieren. Schließlich zeigt ein passives Tracer-Experiment, das mit demselben im FAFMIP-Experiment vorgeschriebenen Süßwasserfluss gestört wurde, die Notwendigkeit, die Rolle von Ozean-Atmosphäre-Rückkopplungen und Zirkulationsänderungen bei der Quantifizierung der Salzgehaltsreaktion auf Änderungen des Süßwasserflusses zu berücksichtigen.

Die Ergebnisse erweitern unser Wissen über prognostizierte Salzgehaltsänderungen, indem sie die durchweg dominante Rolle des Oberflächensüßwasserflusses bei der Erzwingung von Salzgehaltsänderungen sowohl in Tiefe- als auch in Dichteschichten für alle Ozeanbecken zeigen. Diese Ergebnisse deuten darauf hin, dass die Veränderungen des Wasserkreislaufs unter starkem anthropogenem CO_2-Antrieb zu großen Veränderungen des SSS und des unterirdischen Salzgehalts in weiten Teilen des globalen Ozeans führen können.

Contents

Chapter 1

Introduction

1.1 Motivation

As we dive into the ocean, the first thing we notice is the salty water. The salinification of the ocean happened over millions of years through sedimentation and riverine input from physical and chemical weathering of rocks over land. The global water cycle, which is the continuous exchange of water between ocean-atmosphere-land, modifies the ocean salinity. The regional and global changes in ocean salinity is determined by processes such as evaporation and precipitation over the ocean, river water input, and the melting of sea and land ice. This results in regions of low and high salinity, and a balanced salt exchange between them sets the horizontal distribution of salinity in the upper ocean. About 77 % of the global precipitation and 85 % of the global evaporation occur over the ocean (Schmitt, 2008). As a result, any changes in the water cycle, especially precipitation (P) and evaporation (E), affect the sea surface salinity (SSS), especially on regional scale.

An understanding on how salinity changes is important for two reasons. Firstly, salinity is closely linked to the water cycle. As a result, a better understanding of salinity changes would be required for a detailed estimation of changes in the water cycle. Secondly, salinity affects the ocean density and therefore the ocean circulation. The ocean circulation changes affect the heat transported from the tropics to the high-latitudes and thereby influence the climate.

According to the Fifth Assessment Report (AR5) of the Intergovernmental Panel for Climate Change (IPCC), the global ocean surface temperatures show an increasing trend of about 0.5 °C since the mid-20^{th} century (Solomon et al. 2007), which mostly comes from the anthropogenic forcing, associated with anthropogenic greenhouse gas emissions. This global warming has led to an intensification of the global water cycle

(Huntington 2006; Durack et al. 2012; Durack et al. 2014; Vinogradova and Ponte 2017), which involves changes in the rate of E and P and river runoff (R).

Many previous studies have addressed the importance of changes in surface forcing on SSS and subsurface salinity changes (Durack and Wijffels 2010; Lago et al. 2016; Zika et al. 2018). The observations and climate model simulations for the past decades have shown a substantial amplification in the mean pattern of SSS with an increasing salinity in evaporation dominated regions and a freshening in precipitation dominated regions (Durack et al., 2012), which is associated with an intensification of the water cycle (Helm et al. 2010; Hosoda et al. 2009; Durack and Wijffels 2010; Pierce et al. 2012); Bindoff and Mcdougall 1994; Curry et al. 2003; Hosoda et al. 2009; Helm et al. 2010; Durack et al. 2012).

To a large extent, patterns of the surface salinity field of the global ocean are imposed by the net surface freshwater flux, given by evaporation minus precipitation minus river runoff (E-P-R). For 0.5°C of surface warming and a water cycle amplification of around 4 % in the past 50 years, the global SSS has changed by about ±0.2 pss (Durack and Wijffels 2010). Moreover, subsurface ocean salinity in a warmer climate is driven by a combination of changes in surface forcings of freshwater flux, surface warming and wind stress. The effects of surface ocean warming and freshwater flux changes are already visible in the subsurface salinity (Durack and Wijffels 2010).

In the current scenario of global warming, during the 1950s to 2000s with a surface warming of 0.5°C (Solomon et al., 2007), Zika et al. (2018) find that the ocean warming attributes to almost half of the global SSS amplification along with the surface freshwater forcing. On multidecadal time scales, surface warming significantly impacts subsurface salinity changes (Durack and Wijffels 2010; Lago et al. 2016), along with surface freshwater flux changes. These changes were associated with the warming-induced lateral shift of the surface density outcrop locations. Hence, these studies show that in a 0.5°C warm world with a SSS amplification of 8 % (Durack et al. 2012), the surface warming and freshwater changes together combined almost linearly produce the subsurface salinity changes in the global ocean.

However, the previous studies on multidecadal time scales assumed the salinity changes associated with wind-stress and related circulation changes to be negligible. In a rapidly warming world, the wind-stress changes and related circulation might have a strong influence on multidecadal salinity changes. This draws our attention to how the salinity changes will be influenced by surface forcings in a future warmer world with an expected warming of 2-3°C and a 16-24 % amplification of the global water cycle (Durack et al. 2012). Under the global warming, in addition to the possibility of wind-stress related salinity changes, the contributions from warming and freshwater flux changes to salinity changes may also vary. Hence, there is a need to understand the role played by each surface forcing in their contribution to salinity changes.

With an expected increase in global warming, we need to determine which processes are involved in the associated adjustment of the salinity field in a future climate. This can be achieved by using climate projections from coupled climate models dependent on different climate change scenarios. With a continuing increase in greenhouse gas emissions, a climate projection under high greenhouse gas emission condition resulting in substantial changes in surface forcings will provide us with a global warming scenario to visualise the individual impact of surface forcings in salinity.

1.2 Thesis objectives

Under the pretext of significant forcing changes, the lack of understanding in how individual forcings influence the ocean salinities, in different basins, led to the development of the objectives behind this work. In this study, we aim at separating the surface flux contributions by distinguishing the surface and subsurface processes that contribute to salinity response under global warming. With the understanding that, in an ocean warming scenario, the total projected salinity response would be a combination of contributions from each surface forcing, we identify the impact and contributions from surface forcings on the projected global ocean salinity response. The high emission scenario used to study salinity projections is the Representative Concentration Pathway (RCP) 8.5 scenario (refer chapter 3, section 3.1).

The first part of the study answers the following questions:

- What are the mechanisms driving the salinity changes in the global ocean under global warming?
- Is the intensification of freshwater forcing the major driver of the global salinity changes in the RCP8.5 forced climate change scenario?
- If not, what are the relative contributions from each surface forcing in changing the ocean salinity?

The second part of the study uses the sensitivity experiments developed in Flux-Anomaly-Forced Intercomparison Project (FAFMIP). This set of experiments are forced with individual surface flux perturbations equivalent to a CO_2-forced climate change. They aim to identify the oceanic response to individual surface forcings (refer Chapter 3 for details). Therefore, the second part of the study answer the following question:

- What are the similarities and dissimilarities in the salinity contributions from surface forcings between an RCP8.5 scenario and individually-forced flux experiments in FAFMIP?

The second part helps to verify the contributions obtained from RCP8.5 scenario, in addition to providing any missing link between salinity changes and surface forcings.

1.3 Outline of the thesis

Chapter 2 provides a background on the salinity distribution in the global ocean, in addition to how the warming and the related changes in the hydrological cycle affect the salinity response in surface and sub-surface levels.

Chapter 3 briefly introduces the climate model used in this study, MPI-ESM, along with the individually forced surface flux experiments of FAFMIP, followed by a description of the passive tracer experiment setup. This chapter also explains the methods and mechanisms, related mathematical equations used to decompose surface flux impact on salinity changes on both depth and density levels.

Chapter 4 addresses the first part of the study by focusing on understanding the mechanisms affecting the salinity changes in each ocean basin under a high-emission scenario. To achieve this, we first look at the projected changes in SSS in comparison with the historical ocean run, which represents the present-day oceanic conditions. Subsequently, an analysis of the near-surface balance terms of freshwater to understand the impact of the large changes in projected freshwater flux.

Chapter 5 studies the impact of individual surface flux perturbations on the salinity response using FAFMIP runs and verifies the surface flux contributions identified for the RCP8.5 scenario of the MPI-ESM-MR model (chapter 4), thereby addressing the second part of the study. Additionally, we set up a passive tracer experiment, using salinity as a tracer, where we force the tracer with the prescribed freshwater flux, which is then analysed and compared with the freshwater perturbed FAFMIP run.

Chapter 6 concludes with a summary of the important findings from the Chapters 4 and 5 and provides the open questions and the possibilities for further research.

Chapter 2

Background

The global ocean salinity changes are driven by changes in surface forcings. Depending on the time scale, the individual surface forcings have varying impact on the salinity response. With the existing processes controlling the salinity distribution in the global ocean, the global warming causes additional changes in the surface forcings, such as the intensification of the global water cycle, which can lead to changes in their impact on salinity and thereby cause salinity changes.

Consequently, by using data from the climate change experiments in coupled models, we explain the mechanisms that produce the salinity responses. This chapter provides a background on the salinity changes associated with warming. As we focus on the multidecadal changes, we review the changes in salinity distribution that are associated with a warmer climate and its relation with the changing surface freshwater flux and other surface forcings (section 2.1). This will introduce the mechanisms associated with salinity changes. Finally, we close this chapter by looking at the ocean salinity response projected by coupled climate models towards the end of the 21^{st} century.

2.1 Salinity changes under global warming

Over the last several millions of years, earth's climate has experienced several changes, which is mainly attributed to changes in the solar energy received by the earth that is influenced by small variations in the earth's orbit. However, the beginning of human advancement was marked only about 11,700 years ago with the beginning of Holocene. Since the mid-20^{th} century, an unprecedented warming trend has been noticed which has been studied and attributed to be an influence of human activities (Santer et al. 1996; Hegerl et al. 1996; Ramaswamy et al. 2006; Santer et al. 2003; IPCC Fifth Assessment Report, Summary for Policymakers). The increase in greenhouse gases by human-emissions, especially CO_2, traps more heat in the earth's atmosphere, which

has resulted in an increase in our planet's surface temperature by about 0.5 °C since the 1950s (Solomon et al., 2007).

The ocean warming accounts for more than 90 % of the accumulated heat energy (Rhein et al., 2013a). As a result, an increase in temperature of more than 0.4 °C is estimated to have happened in the upper 700 meters of the ocean since 1969 (Levitus et al., 2017). In response to this warming, the ability of the atmosphere to hold more moisture (Willett et al. 2010) has driven substantial changes in the global water cycle over the past decades, leading to changes in E, P and R.

2.1.1 Changes in the global water cycle

Observational and climate model studies suggest that an intensification of the global water cycle has occurred over the last 50 years (Trenberth et al. 2007; Durack et al. 2012; Polson et al. 2013). This is also supported by the changes in E (Dai et al. 2004; Trenberth et al. 2007) and P (Held and Soden 2006; Zhang et al. 2007; Trenberth 2011; Donat et al. 2016) suggesting the "wet gets wetter and dry gets drier" paradigm.

The "rich get richer and poor get poorer" mechanism is a result of changes experienced by the global water cycle due to warming. The major driver of the global water cycle, the atmospheric water vapour, experiences changes in its distribution and concentration in the atmosphere. According to the Clausius–Clapeyron (CC) relation, the capacity of the atmosphere to hold water increases by 7 % for every 1 °C of warming (Held and Soden, 2006). Following this CC relation, modelling and observational studies have found an increase in the tropospheric water vapour concentration in association with a warmer climate in the last few decades (Willett et al. 2008; O'Gorman et al. 2012; Willett et al. 2010). This increase in the atmospheric water vapour primarily drives the strengthening of the global water cycle (Allen and Ingram 2002; Held and Soden 2006; Wentz et al. 2007).

Even though E and P over the ocean acts as the primary source and sink of the water vapour (Baumgartner and Reichel 1975; Schmitt 2008), due to sparse observational ocean data on P and E, the SSS has been widely used as a proxy to understand the changes in E-P and hence the water cycle.

The study of (Durack et al., 2012), using SSS observations to understand the water cycle changes, suggested that spatial pattern of SSS changes since 1950 already shows evidence for an intensified water cycle. They found that the "rich get richer" mechanism is already in place, and the salty regions are becoming saltier and fresh regions are becoming fresher. Their study estimated an intensification of the global water cycle, which is consistent with the CC relationship, at a rate of 8 ± 5 % for every 1 °C of surface warming causing a SSS amplification of about 16 % $°C^{-1}$. The study also

suggests a global water cycle amplification of about 16-24 % in a greenhouse gas forced warmer earth. This value suggests that the global water cycle is intensifying at a faster rate as it is nearly double the response estimated by the CMIP3 models.

The impacts of river runoff and melting of sea ice are limited to the coastal and higher latitude regions. Even the major issues, such as the glacial melting, associated with warming, contribute much less to the water cycle compared to the exchange of water between ocean and atmosphere (Peterson et al., 2006). However, the past decades have witnessed a significant increase in river discharges in the Arctic Ocean and the melting of Arctic sea ice and the Greenland sea ice, causing an increase in the freshwater content in the high-latitudes of the North Atlantic (Peterson et al. 2002; Stroeve et al. 2014; Serreze and Stroeve 2015; Perner et al. 2019). The increased river discharge was associated with the rise in global temperatures and the North Atlantic Oscillation (NOA). All these studies have led us to the conclusion that the intensification of the global water cycle due to warming bring forth substantial changes in the ocean salinity. Such changes in salinity have implications on the ocean circulation and therefore the climate.

A similar pattern amplification is also projected by climate model simulations towards the end of the 21st century (Trenberth 2011; Hsu et al. 2012; Donat et al. 2016; Bhowmick et al. 2019). However, the relation between the freshwater flux changes and SSS changes is complex (Vinogradova and Ponte, 2017). Under global warming, the changes in salinity are not only attributable to the freshwater flux changes associated with the global water cycle intensification but also with the ocean warming that drives density and ocean circulation changes.

2.1.2 Long-term changes in the global ocean salinity

At the ocean surface, the mean SSS distribution patterns reflect the E-P-R pattern in the global ocean (Schmitt, 2008) (Fig. 2.1). The changes brought out by the global warming on the surface forcings can significantly affect the ocean salinity not just on surface but also on subsurface levels. Large and consistent changes, both increasing and decreasing, on multi-decadal scales have already been documented for the global ocean salinity (Antonov et al. 2002; Curry et al. 2003; Boyer et al. 2005; Bindoff et al. 2007; Cravatte et al. 2009; Hosoda et al. 2009; Helm et al. 2010; Durack and Wijffels 2010; Delcroix et al. 2011; Skliris et al. 2014; Vinogradova and Ponte 2017; Zika et al. 2018).

The spatial mean SSS pattern has amplified since the 1950s in agreement with the intensification of the global water cycle (Durack et al. 2012; Skliris et al. 2014; Zika et al. 2018). Showing that the salinity is closely linked to the freshwater forcing we observe, the evaporation-dominated regions have increased salinities, such as the subtropical

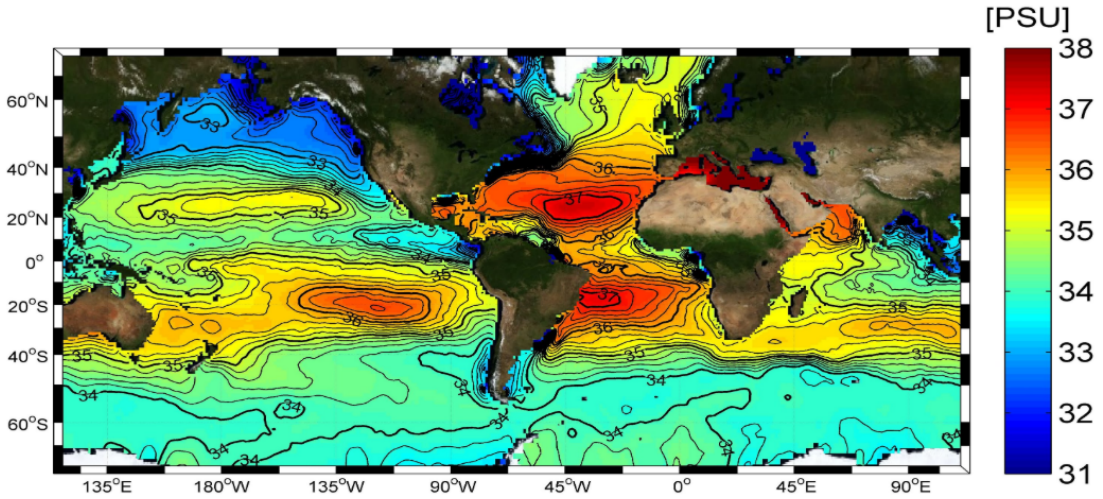

Figure 2.1: Annual mean of SSS distribution (World Ocean Atlas, 2005). Taken from the French Research Institute for Exploitation of the Sea (IFREMER).

gyres of the Pacific, the Atlantic and the Indian Oceans; whereas, the precipitation-dominated regions have decreased salinities, such as the Western Pacific Warm Pool, subpolar regions of the North Pacific and North Atlantic.

However, there are exceptions such as fresher waters in the eastern tropical Indian Ocean which do not follow the typical freshwater flux pattern. Since the focus of our study is to determine salinity contributions from the surface forcing changes, in the next section, we review the global changes in ocean salinity for different ocean basins and our present understanding of the impact determined for various forcing factors.

Pacific Ocean

The Pacific Ocean is relatively fresher compared to the Indian and Atlantic oceans. With the global warming, the Pacific Ocean over the past 50 years has experienced a decrease in SSS in the tropical and subpolar regions whereas the subtropical regions experienced an increase in SSS (Durack and Wijffels 2010; Delcroix et al. 2011; Skliris et al. 2014). Moreover, the salinity changes are mainly confined to the upper 500 m of the ocean with an exception south of 70°S, in the Ross Sea and coastal Antarctica, where there is evidence of deep freshening (Boyer et al., 2005). This freshening of the Ross Sea waters, towards the end of the 20^{th} century, was attributed to increased precipitation, reduced sea ice and increased melting of the Antarctic ice sheet (Jacobs et al., 2002), likely a result of atmospheric and ocean warming.

The major part of the Pacific basin, from 15°S to 60°N, has freshened in the past decades, typically up to a depth of 300 meters (Boyer et al., 2005). Notably, the western tropical Pacific Warm Pool (WP) which is typically a region of warm fresh

waters with high precipitation (Delcroix et al. 1996; Chen et al. 2004) has experienced intense freshening since 1955 (Cravatte et al., 2009) as a result of increased precipitation accompanied by warming. However, the North Pacific exhibits low salinities (Skliris et al. 2014), despite being a net evaporation region. Typically, the mean divergent Ekman drift causes the lower tropical salinities to advect to the entire western North and South Pacific (Huang et al., 2005). It is possible that with increased freshening of the tropical Pacific due to warming, the regions affected by the Ekman drift experience lower salinities than before.

In the subsurface levels, Wong et al. (1999) reported a freshening of the intermediate waters of the South Pacific, which is associated with a freshening of the AAIW source regions in the high latitudes. The decreased salinity in the Ross Sea might have contributed to the freshening of AAIW source regions in the Southern Ocean (Jacobs et al., 2002) which would then have changed the water mass characteristics of the deep and bottom water observed downstream. The subtropical South Pacific reports the largest area of salinity increase in the Pacific, which extends from the surface to 200 meters in conjunction with the increased E-P in the region.

Indian Ocean

For the Indian Ocean, Boyer et al. (2005) observed an increase in salinity from surface to about 150 meters in most of the latitudes. Similar to the Pacific, a freshening of the South Indian intermediate waters along 32°S was attributed to an increase in surface freshwater flux (Wong et al., 1999). The Pacific and Indian Ocean sectors of the Southern Ocean experience freshening where the E-P has a negative trend, however, the observational data in this region is subject to uncertainty due to sparse data availability (Durack and Wijffels 2010; Skliris et al. 2014).

The water masses in the northern Indian Ocean have become saline which is a result of the highly saline overflows from the marginal seas, Red Sea Water (RSW) and the Persian Gulf water (PGW) (Skliris et al. 2014; Durack and Wijffels 2010). Most of the near-surface salinity changes in the Indian Ocean are a result of advective transports of salinities from adjoining regions. The salinity changes in the northern tropical Indian Ocean are dominated by the advective-diffusive processes and less by the local freshwater forcing (Ponte and Vinogradova, 2016). Similarly, the advection of low salinity water of the western tropical Pacific, which serves as a source region of ITF (Valsala et al., 2011), causes freshening in the eastern tropical Indian Ocean. Therefore, the decrease or increase in salinities in the Indian Ocean reflects the impact of surface freshwater flux changes in the source regions.

Atlantic Ocean

Of all the ocean basins, the Atlantic Ocean has experienced the largest changes in salinity over the past decades. The tropical and subtropical Atlantic experienced a substantial increase in surface and subsurface salinities (Curry et al. 2003; Boyer et al. 2005; Durack and Wijffels 2010; Skliris et al. 2014). The increase in SSS, typically between the latitudes 20°S-20°N, was associated with a large loss of freshwater, i.e. an increase in net evaporation by 5-10 % associated with the warming of the upper ocean (Curry et al., 2003). In contrast, the higher latitudes of the North Atlantic experienced a freshening. This freshening is connected to an increase of the net rate of precipitation along with continental runoff from ice melting (Dickson et al. 2000; Peterson et al. 2002; Abdalati and Steffen 1997) and in some cases to the amplification of the North Atlantic Oscillation (NAO) (Marshall et al., 2001).

Similar to the Pacific and the Indian oceans, subsurface change in salinity is prominent in the upper 500 m of the Atlantic. Few observational studies have noticed an elevated North Atlantic salinity at depths around 1200 m (Boyer et al. 2005; Durack and Wijffels 2010), between the latitudes of 25°S and 40°N, at around neutral density 27.8 kg m^{-3}. This is the region of the Mediterranean Outflow Waters (MOW). The increasing salinity trend seen in the Mediterranean Sea over the last few decades (Painter and Tsimplis 2003; Maiyza and Kamel 2010) contributes to the increase in salinities of these water masses (Roether et al., 1996). While the North Atlantic has increased salinities in larger depths, the South Atlantic has maximum salinities only in the western subtropics at the surface ocean.

Salinity changes over the past decades in these three ocean basins have shown that there are substantial changes in the surface and subsurface salinities due to warming and associated changes in freshwater forcing. These observational studies from the 1950s have also concluded that the inter-basin contrast has increased with the Atlantic becoming saltier and the Pacific becoming fresher as a result of warming. The aforementioned has been associated with the increased moisture transport from the tropical Atlantic to the Pacific in response to warming (Richter and Xie, 2010).

All the above studies on salinity changes show the importance of warming and the impacts warming has on various other driving factors of salinity. There are few studies that focus on the contributions from different surface forcings that drive the salinity changes in the global ocean. An increase in ocean and atmospheric warming drives large changes in freshwater forcing and wind-driven circulation. Individually they cause salinity changes in different ocean basins with different degree. At the surface ocean, a study performed by Zika et al. (2018) combining both observational and numerical model simulations from 1956-2016, attributed about one-third of the total SSS amplification to ocean warming, one-sixth to ice mass loss and rest of the SSS

signal to the amplification of the water cycle by about 3.6 % ± 2.1 % for every 1°C rise in surface air temperature.

The ocean salinity set at the surface by various air-sea exchange, get carried into the subsurface ocean along the constant density surfaces. Provided the diapycnal mixing is weak, changes at the surface are mostly preserved in the ocean interior as they move along a given isopycnal surface (Ledwell et al., 1993). Durack and Wijffels (2010) used the subsurface salinity changes on isopycnals to distinguish and study the effect of global warming on the multidecadal salinity changes from the 1950s to 2000s. The period 1950-2000 marked with a surface warming of about 0.5°C except in the high latitudes which marked lesser magnitudes (Rhein et al., 2013b). Durack and Wijffels (2010) suggested that the rise in surface ocean temperature drive substantial changes in observed global subsurface salinity. During this period, the surface isopycnal outcrops shifted by about 50-100 km poleward and it was found that the surface warming drives a significant part of this shift (Durack and Wijffels, 2010). Such outcrop shifts cause changes in subducted salinity irrespective of changes at the surface due to freshwater flux changes.

The ocean warming-driven salinity changes are already visible in the mode waters of the global oceans (Durack and Wijffels, 2010). In support of the Durack and Wijffels (2010) study, a coupled global ocean and sea-ice model study done by Lago et al. (2016) shows similar results. They show that the changes caused by salinity and temperature changes are required to reproduce observed salinity changes in the subsurface ocean. However, their impact on density and depth levels are quite different. While SSS amplification dominates the subsurface salinity changes on depth levels, the salinity changes on density levels were explained by both warming and SSS amplification.

The wind stress-driven changes are more dominant on small time scales such as the interannual or seasonal. A recent study by Tesdal et al. (2018), for a period of 2005 to 2015, associated the decrease in near-surface salinity in the western subpolar North Atlantic with an increase in the eastern North Atlantic subpolar gyre strength. The subpolar gyre strength was connected to an increase in wind-stress curl driven by the NAO and Arctic Oscillation. A stronger gyre transports more freshwater into the Labrador Sea owing to an increase in the inflow of freshwater from East Greenland Current. Persisting over more extended periods, this potentially affects the deep convection and stratify the North Atlantic water column. However, on multidecadal time scales, wind-driven isopycnal changes do not dominate, and they act secondarily to other surface forcings (Häkkinen et al., 2016). As a result, the salinity studies mentioned earlier did not take into account the wind-driven changes assuming that shifts in circulation during their study period, the 1950s to 2000s, are less influential compared to the warming-related subduction.

2.1.3 Projected salinity changes over the 21st century

Climate projections are future scenarios simulated by climate models in order to understand the possible outcomes related to future changes in greenhouse gas emissions or their concentrations. A defined set of scenarios were developed by the IPCC to achieve better knowledge and to mitigate the risks associated with climate change. CMIP5 model studies include two periods of projections: Near-term (2006-2035) and long-term projections (2006-2100). Both projections reveal warming and associated enhancement of the global water cycle towards the end of the 21st century. This enhancement is associated with the expected rise in tropospheric temperatures, which hold and transport more water vapour.

Similar to observed intensification of the global SSS in the past decades, the high emission scenario of CMIP5 climate model projections show an amplification in SSS pattern. Near-term projections, for the next few decades (Figure not shown), and long-term projections (Fig. 2.2; IPCC climate change report 2013, Chapter 12, Fig. 12.34), until the end of the 21st century, in the climate models show substantial changes in the SSS with fresh regions becoming fresher and salty regions becoming salty. Even though

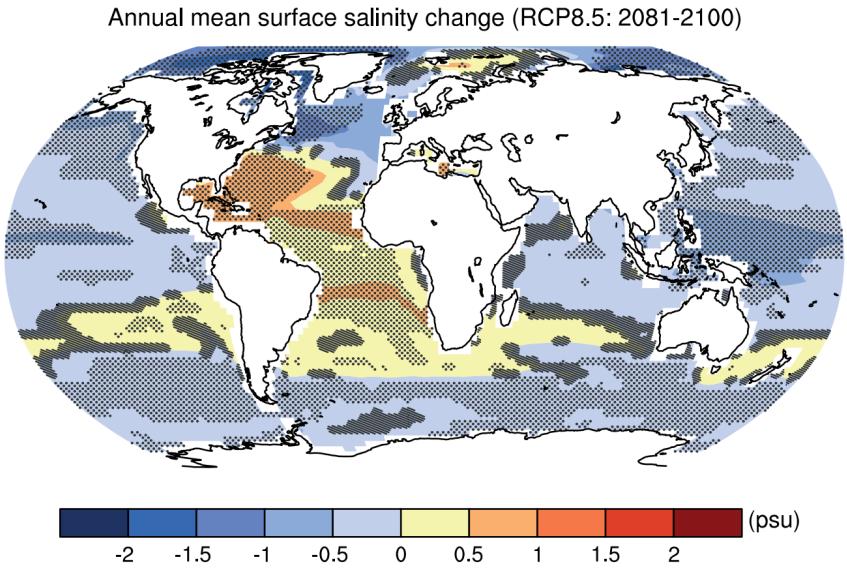

Figure 2.2: Projected SSS differences 2081–2100 for RCP 8.5 relative to 1986–2005 from CMIP5 models. Dark shaded regions correspond to regions where the change in the multi-model mean is less than one standard deviation of internal variability. Stippling indicates regions, where the change in the multi-model mean, is greater than two standard deviations of internal variability and also where $\geqslant 90\,\%$ of the models agree on the sign change (Taken from IPCC report, Chapter 12, Figure 12.34)

the SSS projections are consistent with the intensification of the water cycle (Terray

et al. 2012; Durack et al. 2012), the SSS pattern is different from the E-P projections (Levang and Schmitt, 2015) indicating possible contributions from the ocean warming, advection and mixing in addition to the surface freshwater flux changes.

The projections show an increase in the inter-basin salinity contrast between the Atlantic and the Pacific Ocean basins, with significant changes projected in the western Pacific WP and the North Atlantic (Terray et al., 2012). Near-term projections of increasing salinity in the North Atlantic and decreasing salinity in the western tropical Pacific are considered to be a likely scenario in the future. Therefore, the ocean salinity projections exhibit two main differences from the mean trend of the basin; an increase in south-east Pacific salinity and a freshening of the North Atlantic mid-latitudes.

The near-term projection of the North Atlantic, show an increase in the freshwater flux in the Arctic Ocean, which increases the freshwater transport into the North Atlantic Ocean (Holland et al. 2006; Holland et al. 2007; Vavrus et al. 2012). Such a freshwater increase at the surface can change the density and affect the deep ocean convection, thereby reduce the strength of the Atlantic Meridional Overturning Circulation (AMOC) in the near future. Changes in the AMOC affect the transport of salinities in the high latitudes and drive changes in the subsurface salinities of the North Atlantic. Given all this, it is important to recognise different factors that drive the salinity changes and their contributions to salinity changes in order to understand the effect global warming has on salinity.

Chapter 3

Model and methodology

3.1 Coupled Model Intercomparison Project

The Coupled Model Intercomparison Project (CMIP) was set up in 1995 under the sponsorship of the Working Group on Coupled Modelling. The objective of this project was to understand the climate changes which arise from natural variability or unforced or forced variabilities throughout various timelines. The intercomparison project has become a vital platform to assess the uncertainty and robustness of different climate models. Different phases of the project, CMIP Phases 3 through 6, in different stages envisioned to address the major climate change-related issues in the past and for the future. Each of these phases setup a new framework to fill the gaps and to advance the understanding of climate change.

CMIP Phase 5 (CMIP5) includes more than 20 modelling groups and over 50 climate models performing a set of simulations. The CMIP5 models perform two types of experiments on climate change: one with near-term projections, for 10-30 years which is also called decadal predictions, second with long-term projections which are on century time scale (Taylor et al., 2012).

The long-term experiments in CMIP5 consist of different runs which include several experiments such as a control run, a historical run and a set of future projections which are forced by specific radiative forcings defined by "Representative Concentration Pathways" (RCPs) and the RCP scenarios were developed by Moss et al. (2010). The detailed overview of the CMIP5 experiments are provided by Taylor et al. (2012). The historical runs, referred to as 20^{th} century runs, starts from the mid-19^{th} and is forced with observed atmospheric parameters which include the natural and anthropogenic changes. However, the RCP runs were developed for mitigation, which enables policymakers to take appropriate actions to avoid or achieve specific emission targets. They, therefore, are designed based on the expected population growth, emission rate,

societal and technological developments by the end of the 21st century. The RCPs are named based on their roughly estimated radiative forcing by 2100. The high-emission scenario of RCP8.5 means that the radiative forcing reaches a level of about 8.5 W m^{-2} by 2100, likewise for the RCP4.5 and RCP2.6 runs. For these RCP forced runs, the atmospheric CO_2 concentration is not specified but instead calculated by the climate model.

In this thesis, long-term projections for the RCP8.5 run of the Max Planck Institute-ESM (MPI-ESM), one of the ESMs that participated in CMIP5, are used to study salinity changes and their associated mechanisms.

3.2 Model and experiments

3.2.1 Max Planck Institute - Earth System Model

The Max Planck Institute Earth System Model (MPI-ESM) was one of the CMIP5 models and comprises of the general circulation models for the atmosphere (ECHAM6; Stevens et al. (2013)) and the ocean (MPIOM; Jungclaus et al. (2013)) along with the biogeochemistry (HAMOCC5; Ilyina et al. (2013)), land and vegetation (JSBACH; Reick et al. (2013); Schneck et al. (2013)) modules (Fig. 3.1). The details of model coupling and configuration are described in the papers of Jungclaus et al. (2006) and Giorgetta et al. (2013).

Here, the study uses the MPI-ESM Medium resolution (MR) version, specifically the ocean and sea-ice model - MPIOM component. The MR version has a higher vertical and horizontal resolution in the atmosphere and the ocean, respectively in comparison with LR. However, LR was used in most of the CMIP5 experiments and MR was used much less with fewer realisations. The MR has 95 vertical atmospheric levels and a horizontal ocean grid of 0.4°. The spin-up procedure for MPI-ESM-MR went on for 1500 years. This is required to make sure the model reaches an equilibrium, especially in the deep ocean, and to minimise model drift before the start of the control simulations. Through the 1500 years spin-up procedure, the control run trends were minimised and MR produced a relatively small linear trend of the order of 0.03 °C and 0.003 psu over 1000 years of control simulations in comparison with what was reported in other CMIP5 models (e.g. Griffies et al. 2011; Sterl et al. 2012). The Max Planck Institute Ocean Module (MPIOM) MR oceanic grid is quasi-isotropic with three poles, two of which is residing in Siberia and Canada and the third pole is located at the South Pole. The MPIOM-MR has 40 unevenly spaced depth levels starting from 12 meters to several hundreds of meters with a horizontal resolution of 0.4 °; i.e., the higher resolution quasi-isotropic grid is eddy-permitting in most of the regions in the global

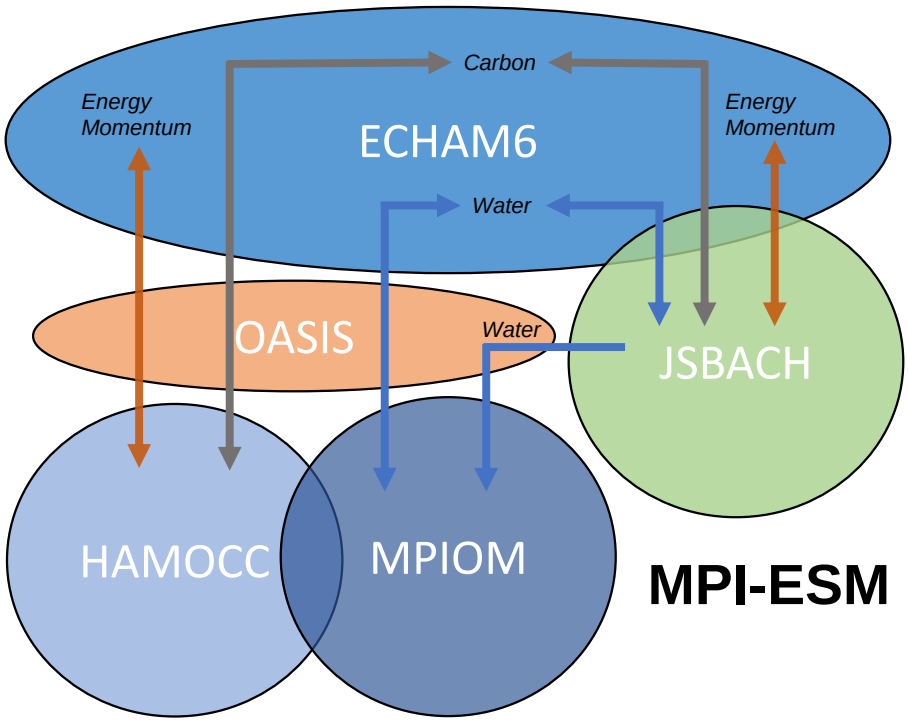

Figure 3.1: Schematics of MPI-ESM showing all modules and their interaction, redrawn from Giorgetta et al. (2013).

ocean. The historical run simulates the climate from 1850-2005, and the RCP8.5 run simulates from 2006-2100.

This thesis also uses the MPI-ESM1.2-HR, referred to as MPI-ESM-HR, which is the high resolution (HR) version of MPI-ESM. MPI-ESM-HR has an atmospheric resolution of 100 km or 1.65 ° and 95 vertical levels (ECHAM6.3 T127L95). The HR version is used in the sensitivity experiments described in section 3.2.2. The model related details are described in the paper by Müller et al. (2018). The ocean component MPIOM with the tripolar grid has the same resolution as the MPI-ESM-MR version of the model (Jungclaus et al., 2013), with a resolution of 40 km or 0.4 ° (MPIOM1.6 TP04/L40) with 40 unevenly spaced vertical levels. This high-resolution model was spun-up for several thousand years. The MPIOM component of the CMIP6 remains unchanged in comparison to the CMIP5 version. Further description and details of HR version of the model can be obtained from the paper by Jungclaus et al. (2013).

To understand all the changes and processes related to salinity, the difference between the last 20 years time mean of the RCP8.5 run (2081-2100), referred as "RCP period" in the following, and the last 20 years time mean of the historical run (1986-2005), referred as "historical period", is assessed. The MPI-ESM-MR has only a single realisation

of the RCP8.5 run. Hence only the changes that are above two times the natural variability of the model's control run are considered significant. Since focus of the study is to understand salinity contribution of surface forcings in a global warming scenario and their associated mechanism, the use of only a single MR realisation should not affect the interpretation of mechanisms and their contributions to the projected salinity response. Moreover, the period used in this study is long enough to filter out the inter-annual, inter-decadal and multi-decadal natural variabilities in the ocean climate system. Section 3.3 describes in detail the methods used to analyse the model data.

3.2.2 Flux-Anomaly-Forced Model Intercomparison Project

The Flux-Anomaly-Forced Model Intercomparison Project (FAFMIP) is part of the CMIP Phase 6 (CMIP6) whose main objective is to address the spread observed in CO_2-forced climate projections and to study the sea level and the ocean climate changes. Projected oceanic responses of different AOGCMs are different due to a difference in models' surface ocean fluxes, which creates wide model spread and difficulties in understanding the oceanic responses. In FAFMIP, a set of climate models uses CO_2-forced climate conditions to calculate surface flux perturbations which are then imposed on a given model's respective surface fluxes (Gregory et al., 2016).

Seventeen models participate in the FAFMIP experiments, and the data provided by them are used for the CMIP6 analysis. The 17 models participating in this study by the end of 2019 are ACCESS-CM2, CCCma CanESM2, CCCma CanESM5, CNRM-CN6-1, GFDL-CM4, GFDL-ESM2M, GISS2.1, HadCM3, HadGEM2-ES, HadGEM3-lr, HadGEM3-hr, IPSL-CM6-LR, MIROC6, MPI-ESM1.2-LR, MPI-ESM1.2-HR, MPI-ESM2, NCAR CCSM. Out of these, nine models have completed the experiments, including the MPI-ESM-HR.

FAFMIP consists of a set of experiments which separate the effect of surface flux changes for freshwater flux, momentum and heat flux on ocean response. The experiments are categorised as FAFMIP tier-1, which consists: faf-stress, faf-heat and faf-water and FAFMIP tier-2, which consists of 2 experiments; faf-passiveheat and faf-all (Table 3.1). The surface flux perturbations are derived from the 1pctCO2 experiments of the CMIP5 models. The 1pctCO2 experiment begins from a control state, with an increase in CO_2 concentration by 1 % every year. The perturbations are derived from the years 61-80 of these 1pctCO2 runs, which are taken from 13 CMIP5 models. This period was chosen as the 70 years in a 1pctCO2 experiment run is the time at which the CO_2 concentration doubles compared to the control state (Gregory et al., 2016).

The faf-stress, faf-water and faf-heat experiments are where perturbations of the surface zonal and meridional component of the momentum flux, surface freshwater flux and

Experiment name	surface flux perturbation
Tier-1	
faf-stress	Zonal and meridional wind stress (F_s)
faf-water	Freshwater (F_w)
faf-heat	Heat (F_h)
faf-heat-NA50pct	F_h reduced by 50 % over the North Atlantic (F_{h50})
Tier-2	
faf-all	perturbed with all surface forcings from Tier-1
faf-passiveheat	heat added as passive tracer
faf-passivesalt	salinity as a passive tracer (S_t)

Table 3.1: Summary of FAFMIP experiments; Adopted from Gregory et al. (2016). The faf-passivesalt experiment is set up for the tracer study described in this thesis.

surface heat flux are applied on a model's surface fluxes respectively (Table 3.1). The faf-passiveheat experiment introduces a passive heat tracer at the ocean surface forced by the same perturbation as the faf-heat experiment. The faf-all run imposes all the above surface flux perturbations of momentum, heat and freshwater simultaneously. Table 3.1 highlights the experiments used for this thesis in grey. Further details of the FAFMIP design and experiment setup can be found in Gregory et al. (2016).

In case of a heat flux experiment, when the heat flux perturbation (F_h) is applied at the ocean surface, it causes the surface air temperature to rise, which then increases the net heat flux into the ocean. This feedback opposes the F_h thereby enhancing the perturbation added into the ocean. Therefore, in the faf-heat experiment, the model's surface heat flux is calculated from a passive temperature tracer which was introduced to mitigate the feedback associated with F_h. This passive tracer was set up such that it does not see F_h; hence, avoid the feedback and helps to add F_h entirely into the ocean. However, this addition causes a reduction in the AMOC of the North Atlantic, which causes extra F_h to be added over the North Atlantic. In order to rectify this, we use faf-heat-NA50pct, which reduces the surface heat flux over the North Atlantic by 50 %. Details of their difference and impacts on other oceanic response are discussed in Chapter 5.

The Chapter 5 uses the aforementioned tier-1 experiments performed on MPI-ESM-HR, hereby referred to as FAFMIP-HR data, to understand the individual impact of each of the surface forcings on salinity changes. The FAFMIP data has been primarily used for sea level studies so far; however, we make use of this sensitivity experiments by using the difference of the time mean of the last 20 years, of the 70-year FAFMIP run, relative to the control run to analyse the salinity response in a warming climate.

3.2.3 Passive salinity tracer experiment

The passive salinity tracer experiment setup in this study follows a similar idea as the set up of faf-passiveheat experiment in FAFMIP. In faf-passiveheat, the surface heat flux perturbation is imposed on a passive tracer, referred to as "added heat" tracer, which is initialised to zero (Gregory et al. 2016; Griffies et al. 2016). This heat tracer does not change the other oceanic parameters in the model; hence, it is the same as a control run. Similarly, in the passive tracer experiment for salinity, a passive tracer is imposed with the same freshwater surface flux perturbation, F_w, given in faf-water experiment. The setup is implemented in the MPI-ESM-HR model, and the experiment is run for a total period of 150 years.

The passive tracer experiment in this study is given by the name "faf-passivesalt". Here, unlike in faf-passiveheat, the tracer is initialised to the salinity field of the control run (S_a). Therefore, we call it S_T, the total tracer field. This S_T does not affect the density of the seawater nor does the imposed F_w affect the model's salinity field or other surface fluxes. The rest of the model parameters related to the tracer experiment run are same as in the control experiment run. The tracer is diluted by the P+R-E field, keeping it unchanged from the model's actual dynamics. Hence, the tracer evolves in the same way as the control salinity plus the perturbation induced changes. The evolution of S_T is associated with the perturbation flux F_w. Therefore, the total tracer field is given by,

$$S_T = S_a + S_t \tag{3.1}$$

where S_t is the change in the total tracer field resulting from the perturbation flux, F_w and S_a is the salinity field of the control run. From here on, S_t is referred to as "passive tracer". This means if $F_w = 0$ then, $S_t = 0$.

Thus, a comparison of faf-passivesalt with faf-water allows to interpret changes in the salinity transport and influence of F_w-induced surface flux changes in F_s and F_h on salinity in the faf-water run.

3.3 Theory and methodology

In order to perform zonal-average for each ocean basin, of the MPI-ESM data which is on a curvilinear grid, the required fields (scalar and vector) were carefully transformed from curvilinear grid to rectilinear grid with a global ocean resolution of 0.5°, using the Climate Data Operators (CDO). The original grid resolution for MPIOM (MR/HR) is 0.4°; hence, this resolution change is unlikely to affect the global scale analysis and inference.

3.3.1 Surface analysis

The changes in freshwater budget terms are calculated using the budget equation. Advection and freshwater forcing components of the balance equation are calculated in the original model grid (curvilinear) using the finite volume method (control-volume approach) to minimise errors. The freshwater balance equation is given as

$$(P - E + R) = \int_{-h}^{0} u\ FW\ dz\ +\ \int_{-h}^{0} v\ FW\ dz\ +\ w\ FW\ |_{z=-h}\ + F \tag{3.2}$$

where the first term on the left side of the equation (lhs) is the surface freshwater flux term, FW is the freshwater calculated from salinity and is given by $1 - S/S_{ref}$, where S_{ref} is 35 psu, u and v are the zonal and meridional ocean currents respectively, h is the layer from surface (12 meters) to 122.5 m of the model and F accounts for the rest of the processes such as diffusion and mixing. The total advection term includes the horizontal and vertical advection components (first three terms on rhs). The terms are integrated over every grid cell in the finite volume method and are represented in terms of flux, expressed in unit $\mathrm{kgm^{-2}s^{-1}}$.

Since the salinity changes are calculated from RCP minus historical period and given the substantial changes in freshwater flux, what we would like to see is the new balance created majorly by changes in the freshwater term and the advection term. The balance between changes in the freshwater and advection terms create the freshwater changes occurring between these two periods. In order to simplify the understanding, the equation can be simplified to read:

$$FW_{rcp} - FW_{hist} = ADV_{rcp} - ADV_{hist} + F_{rcp-hist} \tag{3.3}$$

Here FW_{rcp} is the freshwater flux term for RCP8.5 and FW_{hist} is for the historical period, ADV_{rcp} and ADV_{hist} represent the advection term in the RCP8.5 and historical period, respectively. The advection term in eq: 3.2 can be further divided into four transport terms:

$$ADV = ADV_{mean}\ +\ ADV''\ +\ ADV_{FW'}\ +\ ADV_{U'} \tag{3.4}$$

where ADV_{mean} is the transport due to mean flow and mean freshwater, ADV'' is the changes in flow and changes in freshwater, $ADV_{FW'}$ is the transport due to mean flow and changes in freshwater and $ADV_{U'}$ is the changes in flow and mean freshwater.

3.3.2 Subsurface analysis

The subsurface salinity changes can be associated with the surface forcings such as freshwater flux, heat flux and wind-stress and how they change under the global warming. All the related salinity changes are reflected in both depth and isopycnal surfaces. According to this, the subsurface mechanisms leading to salinity changes can be categorised as heave and spice changes of salinity (Bindoff and Mcdougall, 1994). In the following, the spice-related salinity changes are calculated on neutral density surfaces. The neutral density, γ^n, which is a function of in-situ temperature (°C), salinity, latitude, longitude and pressure/depth (Jackett and McDougall, 1997), is the currently used best representation of density surfaces to perform ocean water-mass analyses (McDougall 1987; Jackett and McDougall 1997). The neutral density surfaces are calculated using the MATLAB package developed by Jackett and McDougall (1997).

Bindoff and Mcdougall (1994) provide a framework to understand the subsurface salinity changes on neutral density surfaces from processes of 1) pure warming, 2) pure freshening and 3) pure heave. The current study uses this framework to deduce the projected subsurface salinity changes.

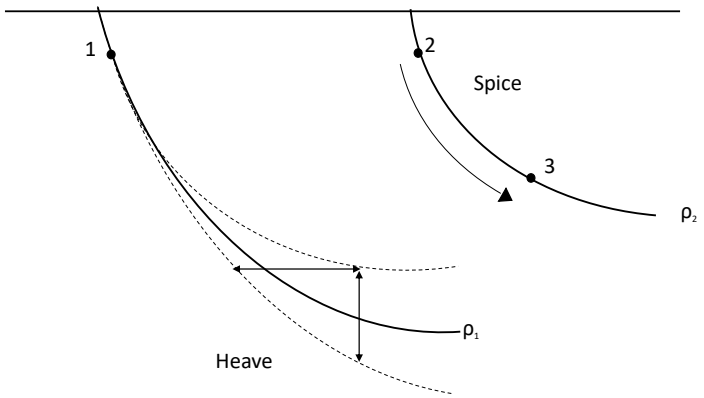

Figure 3.2: Processes of heave and spice. In spice, the parcel subducts along a given density surface, say ρ_2; whereas, in heave the parcel experiences horizontal and vertical displacement in position over time.

Heave and spice

A heave signal gives the changes in the isopycnal position resulting from their vertical or lateral motions over time. This can result from dynamical changes such as wind-stress changes and also from warming or freshwater changes which causes density changes as a result of changes in temperature and salinity. However, spiciness does not include the isopycnal motion. The surface properties are carried along a given isopycnal (Fig. 3.2), and this subducted surface salinities along a given isopycnal can be associated with warming and freshwater flux changes. So changes seen along a given isopycnal would depict water-mass changes or changes in the θ-S relationship.

Equation 3.5 shows the total salinity change decomposed into two signals: the spice and the heave driven salinity changes using the approach from Durack and Wijffels (2010). Hence, decomposition of the total salinity change can be written as:

$$dS = dS_{\gamma^a} + \frac{\partial \overline{S}}{\partial \gamma^a}(d\gamma^a) \tag{3.5}$$

where dS is the total salinity change, dS_{γ^a} is the salinity changes on density levels, $\partial \overline{S}/\partial \gamma^a$ is the local gradient of mean salinity against density, $d\gamma^a$ is the change in density

The changes on the isopycnals are related to changes at the surface which are separated for a given isopycnal outcrop into the salinity changes due to the migration (lateral shift) of a that outcrop and the local SSS changes. The salinity changes associated with zonal and meridional migration of isopycnal outcrops are related to the presence of the horizontal salinity gradients. Here, we only consider the meridional shift of density outcrops since most of the isopycnal migrations are towards the pole and the zonal gradient in salinity are smaller than the meridional gradients. The total surface salinity changes at a given isopycnal outcrop can be expressed as:

$$dS = \frac{d\overline{S}}{\partial y}(\delta y) + dS', \tag{3.6}$$

dS is the total change in the surface salinity which includes the changes due to migration $(d\overline{S}/\partial y)(\delta y)$ and the temporal salinity changes (dS'), likely caused by the freshwater flux changes. The (δy) is the meridional migration of the outcrop. Let's define the first term as the $migration - term$ and the second term on R.H.S as $freshwater - term$. To calculate the changes due to lateral shift of a given isopycnal outcrop (first term on rhs), we used the outcrop locations for the RCP period 2081-2100 and historical period 1986-2005 to find (δy) along with the mean salinity for the period 1986-2100. (δy) is calculated by the change in the neutral density over the meridional gradient of the mean neutral density for the whole period.

The caveat of applying this method to the case in which most of the signal is related to warming is, as the schematic in Fig. 3.2 shows, that the warming signal causes a signal related to lateral and vertical shift of surface isopycnal outcrops that is compensated by the signal related to the changes in spice. Hence, the analysis masks the effects of wind and freshwater changes, which do leave a change on depth coordinates. In order to better address the impact of freshwater flux and wind changes the decomposition into the pure processes according to Bindoff and Mcdougall (1994) is applied.

Pure warming, pure freshening and pure heave

Bindoff and Mcdougall (1994) proposed the three ventilation processes of pure warming, pure freshening and pure heave which provide a kinematic approach to approximate the contributions of the three surface forcings: heat flux, freshwater flux and wind stress.

The **pure warming** process represents a change in the ocean temperature across the ocean-atmospheric interface without changes in the freshwater flux and wind stress curl (Bindoff and Mcdougall 1994; Bindoff and McDougall 2000). The surface warming causes changes in density, where a water parcel previously of a given density (ρ_1) now subducts on a less dense surface (ρ_2). This displaces the water column, between the surfaces ρ_1 and ρ_2, which moves slightly downward without any change in the total volume and subduction rate (Fig. 3.3a). As a result of no changes in salinity of the subducted water parcel, the volume averaged salinity of water column also remains unchanged; whereas the subducted parcel experiences an increase in volume averaged potential temperature on depth surfaces. Hence, surface warming followed by subduction is similar to a scenario where thermocline parcels experience warming at a given depth without salinity changes.

To describe one of the cases, on the $\theta - S$ diagram (Fig. 3.3a), the water parcel in position 1 has a salinity and temperature of θ1-S1, which on warming, moves to position 2, θ2-S1, without any change in salinity ($S'|_z$) but experiences an increase in potential temperature ($\theta'|_z$). Interpreting on density surfaces, a parcel 1 which would have subducted on density level ρ_1, due to warming followed by subduction, will now subduct on a lighter density level ρ_2 (Fig. 3.3a, parcel 1 moved to position 2). This results in cooling and freshening of the parcel compared to another parcel at the same density surface ρ_2 (parcel 2 is cooler and fresher than parcel 3).

Similarly, in a **pure freshening** process, the freshwater flux changes while the heat flux and the wind-stress curl remains constant. That means in freshening followed by subduction, the volume averaged salinity changes while the potential temperature is held constant. For example, with freshening, a parcel is subducted along a lighter density surface and the subducted parcel will now have a fresher and cooler profile than

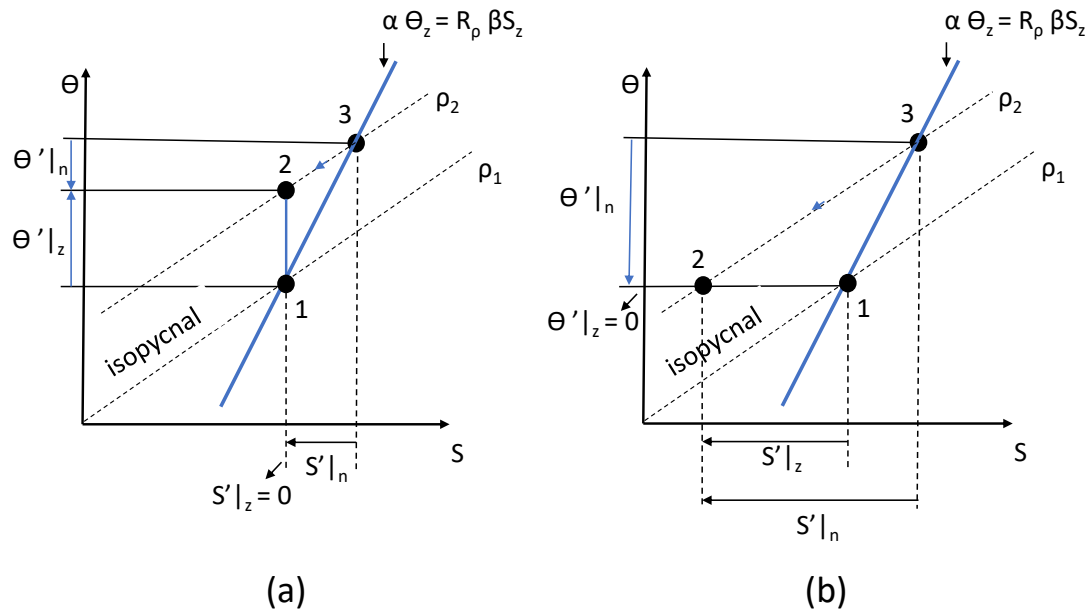

Figure 3.3: Schematics of processes redrawn from Bindoff and Mcdougall (1994). The parcel 1 in (a) upon warming acquires the properties at point 2, with no changes in salinity, moving to a density level same as parcel 3 and becoming cooler and fresher, in (b) a similar case for pure freshening where parcel moves to position 2 with no change in θ, however, becoming cooler and fresher than the parcel at 3.

another parcel of the same density surface with no change in potential temperature (parcel 2 is cooler and fresher than parcel 3, Fig. 3.3b). These two cases show that the pure warming and pure freshening processes can result in indistinguishable signals along density surfaces. However, the difference in their relationships on depth-related and density surface-related changes can help in distinguishing the processes.

In case of a **pure heave** process, unlike the pure warming and pure freshening process, the isopycnal positions change without any change in the water mass properties. This can be a result of the changes in the rate of subduction, eddies, or circulation changes (Bindoff and Mcdougall, 1994) that are driven by wind-stress curl changes. Thus, pure heave results in no visible changes in the θ-S diagram but causes a change in salinity or temperature at a constant depth level. The detailed description of the three ventilation processes is given by Bindoff and Mcdougall (1994). Below given mathematical equations taken from Bindoff and Mcdougall (1994) demonstrate the pure warming, pure freshening and pure heave processes and how to find the related

salinity changes.

The salinity and temperature changes on depth levels can be expressed in terms of their changes on isopycnals ($\theta'|_n$, $S'|_n$) and changes due to isopycnal movement (N'θ_z, N'S_z),

$$\begin{aligned} S'|_z &= S'|_n - N'S_z \\ \theta'|_z &= \theta'|_n - N'\theta_z \end{aligned} \tag{3.7}$$

For a pure warming process, change in salinity on depth levels is zero, hence,

$$\begin{aligned} \beta S'|_z &= 0 \\ \beta S'|_n &= N'\beta S_z \\ \frac{\alpha\theta'|n}{\alpha\theta'|_z} &= -(R_\rho - 1)^{-1} \end{aligned} \tag{3.8}$$

where R_ρ is the stability ratio given by $R_\rho = \alpha\theta_z/\beta S_z$. α and β are the thermal expansion coefficient and the haline contraction coefficient, respectively.

The pure freshening process is defined as

$$\begin{aligned} \alpha\theta'|_z &= 0 \\ \alpha\theta'|_n &= N'\alpha\theta_z \\ \frac{\beta S'|n}{\beta S'|_z} &= -(1 - R_\rho^{-1})^{-1} \end{aligned} \tag{3.9}$$

The pure heave process is defined as

$$\begin{aligned} \alpha\theta'|_n = \beta S'|_n &= 0 \\ \beta S'|_z &= -N'\beta S_z \\ \alpha\theta'|_z &= -N'\alpha\theta_z \end{aligned} \tag{3.10}$$

The details of each of these equations are given by Bindoff and Mcdougall (1994). Putting together the mathematical formulations of the above three processes 3.8, 3.9, 3.10 into a matrix form gives:

$$\frac{\rho^{-1}\rho'|_z}{R_\rho - 1} \begin{bmatrix} -(R_\rho - 1) & 0 & -R_\rho \\ 1 & R_\rho & 0 \\ R_\rho & R_\rho & R_\rho \\ 0 & (R_\rho - 1) & -1 \\ 1 & R_\rho & 0 \\ 1 & 1 & 1 \end{bmatrix} \begin{bmatrix} A^w \\ A^f \\ A^h \end{bmatrix} = \begin{bmatrix} \alpha\theta'|_z \\ \alpha\theta'|_n \\ N'\alpha\theta_z \\ \beta S'|_z \\ \beta S'|n \\ N'\beta S_z \end{bmatrix} \tag{3.11}$$

where $A^w\ \rho^{-1}\rho'|_z$, $A^f\ \rho^{-1}\rho'|_z$, $A^h\ \rho^{-1}\rho'|_z$ gives the contribution of the in-situ density change due to warming, freshening and heave processes. The terms on the rhs of the equation are called "observable" quantities. These quantities are the temperature and salinity changes on density and depth levels along with their heave components. From the equations 3.7 - 3.10 it is clear that they are dependent variables and only provide two independent sets of information. Hence, this linear system of equations is rank deficient with rank 2 and therefore underdetermined. The three processes can be determined using inverse methods following Bindoff and Mcdougall (1994) and the system is solved using the singular value decomposition (SVD) method. The SVD is performed at each grid point of the global ocean and then the zonal average for each ocean basin is calculated.

On solving the above equation (3.11) and obtaining the density changes ($\rho^{-1}\rho'|_z$), corresponding to each process (i.e., $A^w\ \rho^{-1}\rho'|_z$, $A^f\ \rho^{-1}\rho'|_z$, $A^h\ \rho^{-1}\rho'|_z$), I calculated the change in salinity on the depth and density levels for pure warming, pure freshening and pure heave. For pure warming, the change in salinity on depth levels is zero as pure warming cannot cause salinity changes on pressure/depth surfaces. Therefore,

$$S'|_z = 0 \tag{3.12}$$

The spice contribution of pure warming is given by:

$$S'|_n = \frac{A_w(\rho^{-1}\rho'|_z)}{\beta(R_p - 1)} \tag{3.13}$$

The salinity changes in depth and density levels due to pure freshening are given by:

$$S'|_z = \frac{A_f(\rho^{-1}\rho'|_z)}{\beta} \tag{3.14}$$

$$S'|_n = \frac{Rp\ A_f(\rho^{-1}\rho'|_z)}{\beta(R_p - 1)} \tag{3.15}$$

Determination of salinity changes due to pure heave will help to distinguish the contributions by changes in wind, circulation changes, eddies etc from total heave (Equation 3.5) which includes effects of warming and freshening. The salinity changes in depth levels due to pure heave are given by:

$$S'|_z = \frac{-A_h(\rho^{-1}\rho'|_z)}{\beta(R_p - 1)} \tag{3.16}$$

Chapter 4

Mechanisms for salinity change in the global ocean under global warming conditions[1]

4.1 Introduction

In this chapter, we investigate mechanisms that drive salinity changes at surface and subsurface levels under the high emission RCP8.5 forcing scenario of the MPI-ESM-MR. Studies performed in Coupled Model Intercomparison Project Phase 3 (CMIP3) and Phase 5 (CMIP5) indicate that, under global warming conditions, the subtropics, which historically are net evaporation dominated regions, could become more saline in the future; and the tropics and the high latitudes which are precipitation dominated regions could freshen towards the end of the 21st century (Terray et al. 2012; IPCC Report Chapter 12). The surface freshwater flux (FWF) changes play a significant role in long-term surface salinity changes (e.g. Lagerloef et al. 2010; Durack et al. 2012). However, dissimilarities in the projected SSS changes with respect to the freshwater forcing in a CMIP5 study by Levang and Schmitt (2015) show the significance of ocean processes in setting the long-term salinity response. In addition, the warming of the global ocean in recent decades has gained much attention in salinity studies. The previous studies suggest that surface warming has played a significant role in the multidecadal subsurface salinity changes in the global ocean (Durack and Wijffels 2010; Lago et al. 2016).

Durack and Wijffels (2010) used observational data and analysed subsurface salinity changes, for 1958 through 2005, in a neutral density framework. In their study, a significant shift in the isopycnal outcrops of the subtropical oceans was associated with the broad-scale ocean warming. As a result, the fresh or salty water at new outcrop

locations gets subducted into the subsurface levels by mean wind-driven subduction (Ledwell et al. 1993; Drijfhout et al. 2013). The authors suggest that the observed changes in subsurface salinity on isopycnals are not only driven by the surface FWF changes but also by the poleward shift of surface isopycnal outcrops resulting from surface warming alone. Moreover, the study of Lago et al. (2016) shows that changes in subsurface salinity could only be explained by both surface salinity changes and surface warming. In their idealised experiments, the authors varied surface temperature and salinity to analyse the associated subsurface changes observed in salinity. The study shows that present-day surface salinity changes act as a primary driver on depth level changes and surface warming, which causes a lateral shift of isopycnals, act primarily on density level changes. An increase in surface temperature and an amplification of salinity patterns were found to act almost linearly on subsurface salinity changes, given that changes in wind and circulation are negligible. In short, there are several studies that associate SSS changes with an intensification of the global water cycle (Durack et al. 2012; Rhein et al. 2013b; Skliris et al. 2014) and long-term changes in ocean salinity with the global warming signal (Curry et al. 2003; Boyer et al. 2005; Hosoda et al. 2009; Helm et al. 2010; Pierce et al. 2012; Zika et al. 2018).

However, the global ocean salinity changes are driven by a combination of the surface forcings of FWF, heat flux and wind-stress. A shift in outcrop location can result from a deepening of the isopycnal surfaces, which can result from all the three surface forcings. Although Durack and Wijffels (2010) and Lago et al. (2016) show the importance of a warming-induced poleward shift of isopycnal outcrops on salinity changes, their approach does not entirely resolve the surface forcing contributions, especially for the changes in wind-stress. The changes in wind-stress contribute to salinity changes by affecting ocean currents and thereby changing the circulation. While wind-stress related density changes dominate the changes in ocean heat content and salinity on inter-annual or decadal time scales, they play only a secondary role on multidecadal time scales (Häkkinen et al. 2016; Durack and Wijffels 2010). Moreover, on multidecadal time scales, along with warming and wind-stress changes, a substantial change in freshwater forcing could also contribute to the isopycnal movement.

Therefore, it is still unclear how exactly changes in each of these surface forcings contribute to salinity changes on the depth and density levels, especially under the global warming scenario. This chapter investigates the mechanisms driving the global ocean salinity changes under global warming. Subsequently, we identify the major drivers and their contributions to the projected salinity changes. We achieve this objective by using Bindoff and Mcdougall (1994) (BM's) approach of pure warming, pure freshening and pure heave processes (described in chapter 3, section 3.3.2), which we think is currently the best available approach to quantitatively estimate the contributions from the FWF, heat flux and wind-stress changes on a subsurface level. Hence, decomposing the total salinity changes, "total salinity" in the following, on the subsurface

depth and density levels to contributions from each of these processes will signify the impact of the corresponding surface forcings. Additionally, using the RCP8.5 scenario provides us with a strong signal, which gives a magnified perspective of the respective surface forcing contributions, especially of wind-stress, which is otherwise weaker in the current state of ocean warming.

4.2 Projected changes in SSS and freshwater flux

The relationship between the future SSS changes and the respective changes in FWF differs with ocean basin under the RCP8.5 scenario (Fig. 4.1), similar to the CMIP5 study of Levang and Schmitt (2015), specifically for the Pacific and Indian oceans. However, for the Atlantic Ocean, an increase (decrease) in zonally averaged SSS concur with a decrease (increase) in FWF. The lack of correspondence between SSS and FWF changes in the Indo-Pacific region strongly points to mechanisms for salinity changes other than surface freshwater forcing. Moreover, at some latitudes, we observe strong local anomalies in FWF changes, specifically near the Equator and 10 °S in the Atlantic Ocean. These variations could be due to strong latitudinal FWF changes in the eastern border of the tropical Atlantic which mark a river outlet and high precipitation zone. The SSS changes in the Indo-Pacific, which often show no apparent relation to the corresponding FWF changes, illustrate the existence of a more complex relation between salinity and surface FWF changes.

The projected spatial SSS changes of the MPI-ESM-MR (Fig. 4.2 a) are reasonably consistent with the projected SSS changes from 31 CMIP5 models shown by Levang and Schmitt (2015) in their Figure 3. The FWF, accumulated over decades, should have led to an extensive freshening of the western equatorial Pacific. However, this is not the case, affirming that, in a quasi-stationary balance the changes in oceanic processes must also play an essential role in regulating the salinity. Respective SSS and FWF changes are discussed in the following by basin.

4.2.1 Atlantic Ocean

The Atlantic Ocean exhibits significant SSS changes in the subtropics and tropics of both hemispheres over the 21st century, following a similar spatial pattern as the surface FWF anomalies. The tropical east Atlantic shows a decrease in SSS which is consistent with the slight increase in the FWF (Fig. 4.2 b) and with the E-P changes in this region which show increased precipitation over land and coastal regions (not shown). The increased freshening of the northern North Atlantic and the Arctic regions corresponds to a increase in FWF in the region. However, a substantial salinity decrease in this

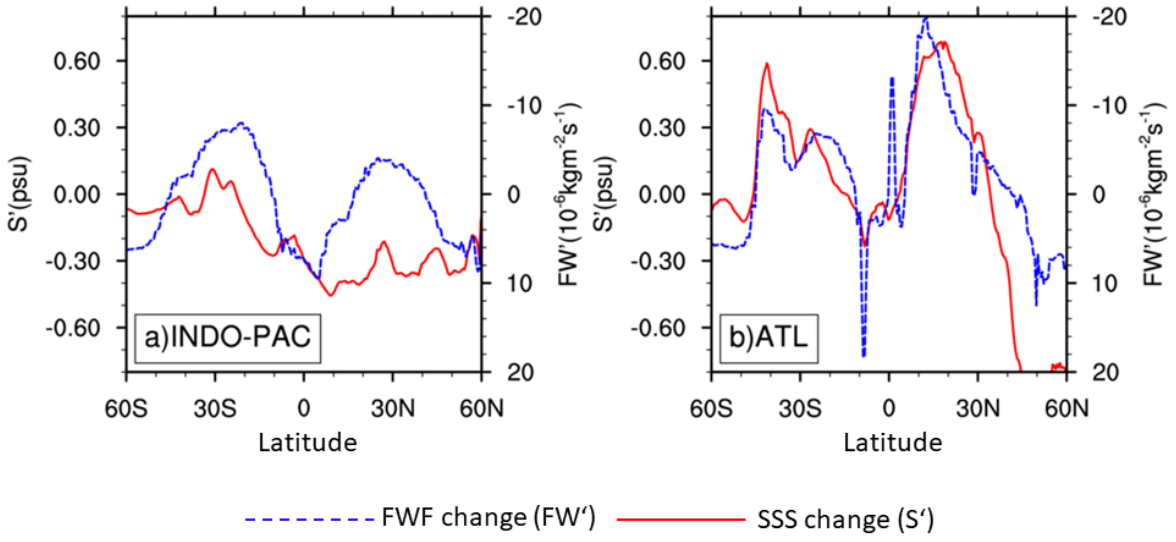

Figure 4.1: Zonally averaged SSS (red) and FWF (blue) changes (positive into the ocean) shown separately for the Atlantic and Indo-Pacific basins as the change of the means over the historical period (1986-2005) to the RCP 8.5 period (2081-2100). Units of SSS in psu and FWF in 10^{-6} kg m^{-2} s^{-1}). Results are shown separately for (a) the Indo-Pacific and (b) the Atlantic Oceans.

region suggests the role of other processes. However, the freshening anomalies in this region could result from a decrease in deep convection. A decrease in deep convection can result from a weakening of the overturning circulation, which can affect the mixing of the fresh surface waters into deeper layers and result in their accumulation at the surface (Häkkinen, 2002). Since a weakening of the Atlantic meridional overturning circulation (AMOC) is evident in a global warming scenario (Sévellec et al. 2017; Caesar et al. 2018), likely, this explanation also holds in our case. Moreover, the subpolar North Atlantic freshening extends southward where it enters the North Atlantic subtropical gyre by the southward Ekman transport.

4.2.2 Pacific and Indian Oceans

For the western equatorial Pacific Ocean, the figure reveals a consistent and distinctive freshening to take place over the next century. Already over the past decades, this

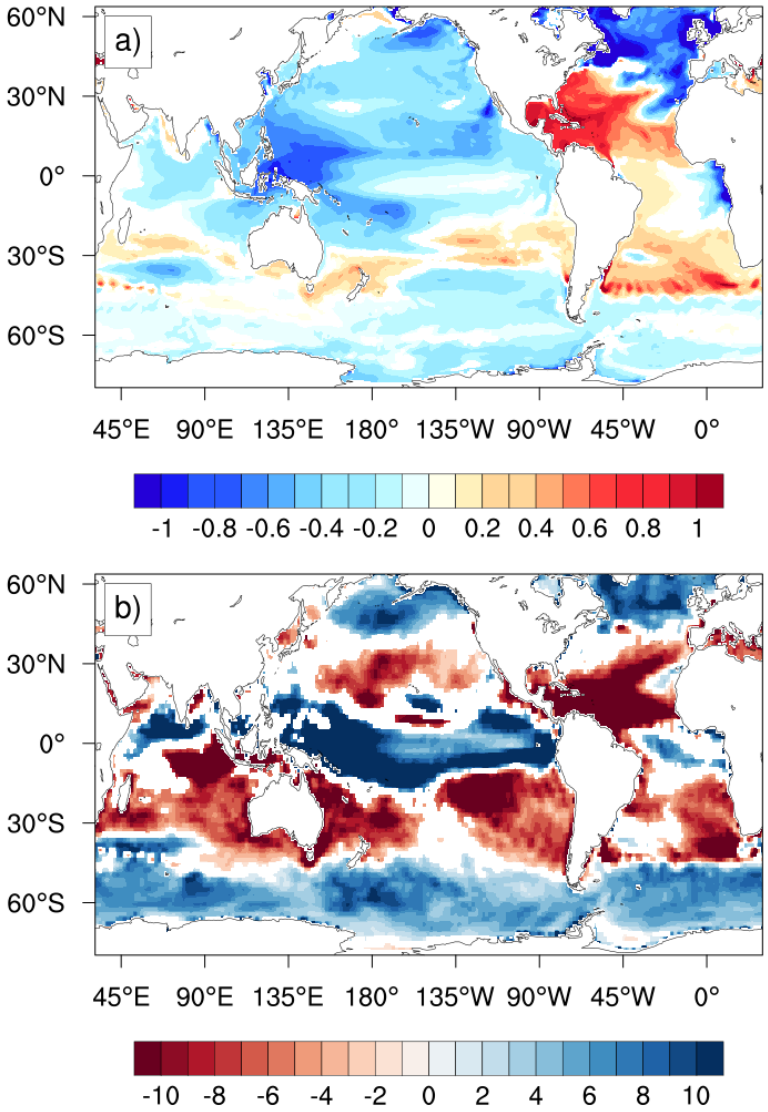

Figure 4.2: (a) SSS changes (psu) and (b) FWF changes (10^{-6} kg m^{-2} s^{-1}) of RCP8.5 period relative to historical period (1986-2005). Salinity values less than twice the standard deviation of respective control runs are not shown.

region of warm and fresh waters has experienced a freshening due to warming-induced increase in the mean hydrological cycle (Cravatte et al., 2009) which Terray et al. (2012) partially attributed to anthropogenic influence. Projected FWF changes in this region are even more substantial (Fig. 4.2 b). Accumulated over decades, they should lead to extensive freshening in the western equatorial Pacific; however, this is not the case, suggesting that strong compensating effects must play an important role. We also note a noticeable freshening extending further north and south of the western equatorial Pacific (Fig. 4.2 a). Huang et al. (2005) explained this by a poleward drift of anomalous surface waters in this region by the mean divergent Ekman flows near the Equator. Hence, the advection of western tropical Pacific fresher anomalies towards the east may explain the simulated significantly negative SSS anomalies in the subtropical gyres of the southern and northern hemispheres despite the decrease in the FWF (Fig. 4.2).

The changes in the Indian Ocean basin remain smaller than those seen in the Pacific or the Atlantic Ocean basins with no clear local correspondence between the SSS and surface FWF changes present. One consistent feature over the 21st century is the negative SSS anomalies in the eastern tropical Indian Ocean which appear uncorrelated with significantly negative surface FWF anomalies there. Instead, the western equatorial Pacific serves as a source region of the Indonesian Throughflow (ITF) water communicated via a freshwater transport through the ITF (Valsala et al., 2011). Gupta et al. (2016) suggests a decrease in the ITF strength by approximately 1 to 6 Sv in future projections of CMIP5 models (including MPI-ESM-MR). However, with a strong decrease in FWF anomalies in the east one must expect a strong advective process in play to see the observed decrease in SSS changes. Hence, we can consider both changes in salt advection and the decrease in SSS in the western equatorial Pacific play a role in the freshening of the eastern tropical Indian Ocean.

4.3 Surface salinity amplification

To express the amplification of salinity changes quantitatively, we calculated the pattern amplification (PA) introduced by Durack et al. (2012). The PA is defined as the slope of a linear regression of zonal mean of SSS changes versus SSS climatological mean anomaly from the global mean SSS. To be consistent with Durack et al. (2012), the high-latitude (>65°) and marginal seas are not included in the zonal average of the global basin due to the strong influence of local variabilities in such regions. Under RCP8.5 run, our study reports an 18 % PA with a correlation (R) of 0.73 to occur over 115 years (1986-2100) (Fig. 4.3 a), in comparison with Durack et al. (2012) who reported an 8 % PA over 1950-2000. The correlation value is almost the same as the correlation reported by Durack et al. (2012), which is ∼0.7. This change in PA could

be a result of strong multidecadal SSS changes projected in the RCP8.5 period over the weaker SSS changes in 1950-2000 reported by Durack and Wijffels (2010). The salinity PA result suggests that the ocean under global warming experiences a large SSS amplification, with a high R value suggesting that the SSS change reasonably matches the mean climatological SSS pattern.

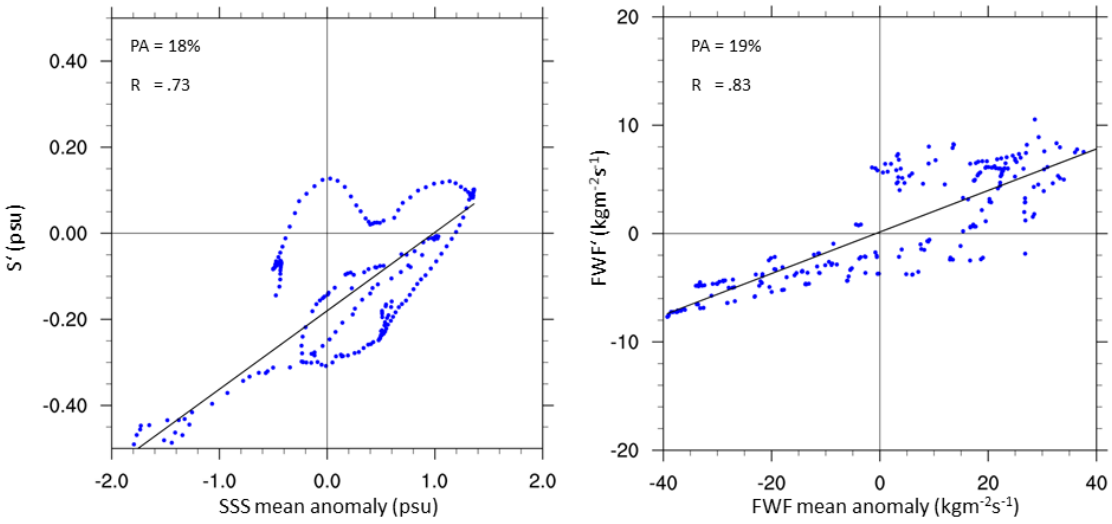

Figure 4.3: (Left) SSS changes (S') between the RCP8.5 and historical period (y axis) against the SSS mean anomaly (y axis). (Right) FWF (FWF) changes versus FWF mean anomaly. The correlation (R) and pattern amplification (PA) are also provided.

The SSS PA value in our study is similar to the study performed by Zika et al. (2018), where they reported a ∼13-15 % PA in the SSS forced by changes in the water cycle, surface warming and ice mass loss by the end of a 100-year model simulation. They claim that approximately half of the SSS amplification during 1957-2016 is due to surface ocean warming, which causes a stable stratification (Kara et al. 2003). In their experiments, a stable stratification, which inhibits the deepening of the mixed layer (ML) (Capotondi et al. 2012), is primarily driven by surface warming rather than freshwater forcing. In our study, we observe a shoaling of the ML in most of the global ocean during the RCP8.5 period (Fig. 4.5). Since in CMIP5 model projections, an increase in temperature is the dominant contributor to the increase in buoyancy flux (Levang and Schmitt 2020, Figure 1), a shoaling seen in most parts of the global ocean in our study can be associated with surface warming, except in the subpolar North Atlantic (Levang and Schmitt 2020).

Therefore, a global mean SST change of ∼2.3 °C in the RCP8.5 run (Fig. 4.4) could be causing the shoaling of the ML in most of the global ocean during the RCP8.5 period

(Fig. 4.5). It is challenging to deduce the quantitative contribution from warming in our case.

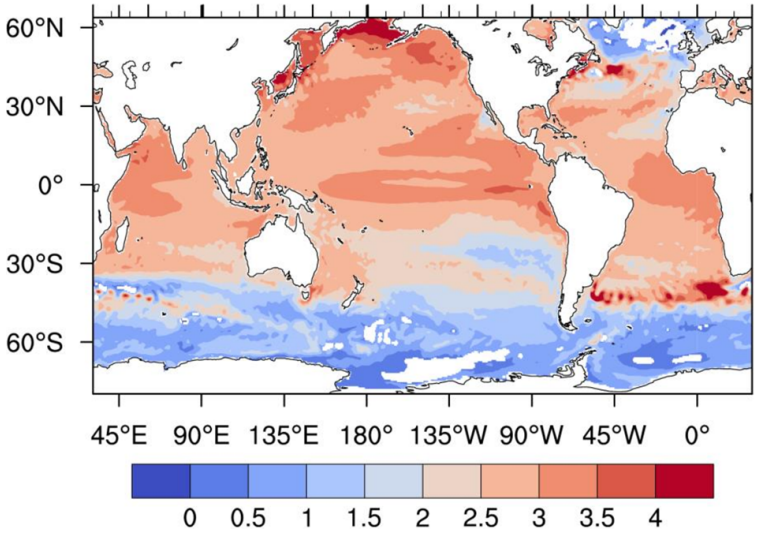

Figure 4.4: SST anomalies (°C) in the RCP8.5 period relative to the historical period. Values less than twice the standard deviation of the control run have been masked.

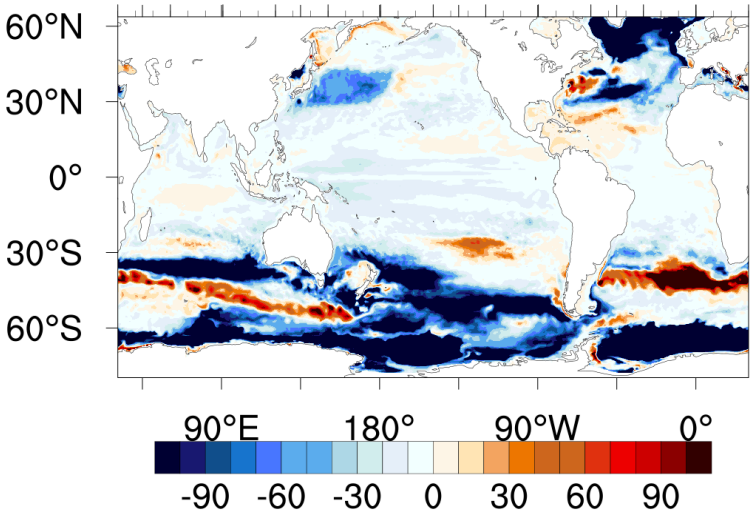

Figure 4.5: The maximum (winter) mixed layer depth (MLD) differences in meter between the RCP8.5 and historical period.

However, if we were to roughly estimate the warming contribution, Zika et al. (2018)

claims that surface warming during 1957-2016, roughly 0.5 °C increase (Durack and Wijffels 2010), causes a SSS PA of around 2 %. Assuming that the changes are linear over the projected scenario, the surface warming may contribute to a SSS PA of around 9.2 %, which is approximately half of the total SSS PA of 18 %. This suggests that the warming-related SSS amplification would not change in the projected climate.

We calculated the PA for FWF changes, and for a global surface warming of ∼2.3°C, the FWF amplification is 19 % (R=0.83), which would be ∼8 %°C^{-1} and is close to the water cycle amplification predicted according to the CC relationship (∼7°C^{-1}). For a similar water flux amplification in Durack et al. (2012), the SSS PA derived from a CMIP3 ensemble was double the value of the water flux PA. However, because we estimated an almost one-to-one ratio for the global zonal mean SSS PA and FWF PA, the changes in each ocean basin perhaps could explain this difference. Although all three ocean basins, the Atlantic, Pacific and Indian oceans, experience an amplification, the SSS changes in the Pacific and Indian Oceans are much weaker than in the Atlantic Ocean, which experiences the most substantial SSS changes (Table 4.1). The R value in the Pacific Ocean denotes a weak correlation of the SSS changes to the mean climatological SSS of the basin. This could be a result of the subtropical Pacific and east Indian Oceans experiencing a decrease in SSS despite a decrease in FWF, thus pointing to a significant role played by the other oceanic processes in these regions.

PA (R)	Global	Atlantic	Pacific	Indian
SSS	18 % (0.72)	31 % (0.88)	9 % (0.54)	9 % (0.79)
FWF	19 % (0.83)	18 % (0.68)	20 % (0.72)	11 % (.54)

Table 4.1: SSS PA for each ocean basin. The correlation coefficient (R) is given in brackets.

4.3.1 Near-surface salinity adjustment processes

For long-term changes in the ocean salinity, the tendency term in the balance equation can be considered small and a balance reflecting only changes in the surface FWF, oceanic advection and mixing can be considered. Previously, several studies have documented the importance of oceanic advection on observed regional salinity changes (Johnson et al. 2002; Rao and Sivakumar 2003; Bingham et al. 2010) and the dominance of E-P on salinity changes in the ITCZ regions (Cravatte et al. 2009; Bingham et al. 2010). Under the hypothesis that mixing is not changing substantially, we first consider in Fig. 4.6 only the contribution to the freshwater balance term from the freshwater advection flux changes and the FWF changes given in Fig. 4.2 b.

The tropics and most of the subtropics show a reasonable balance between the changes in the advective and surface FWF terms (Fig. 4.6 a and Fig. 4.2 b). Note that the

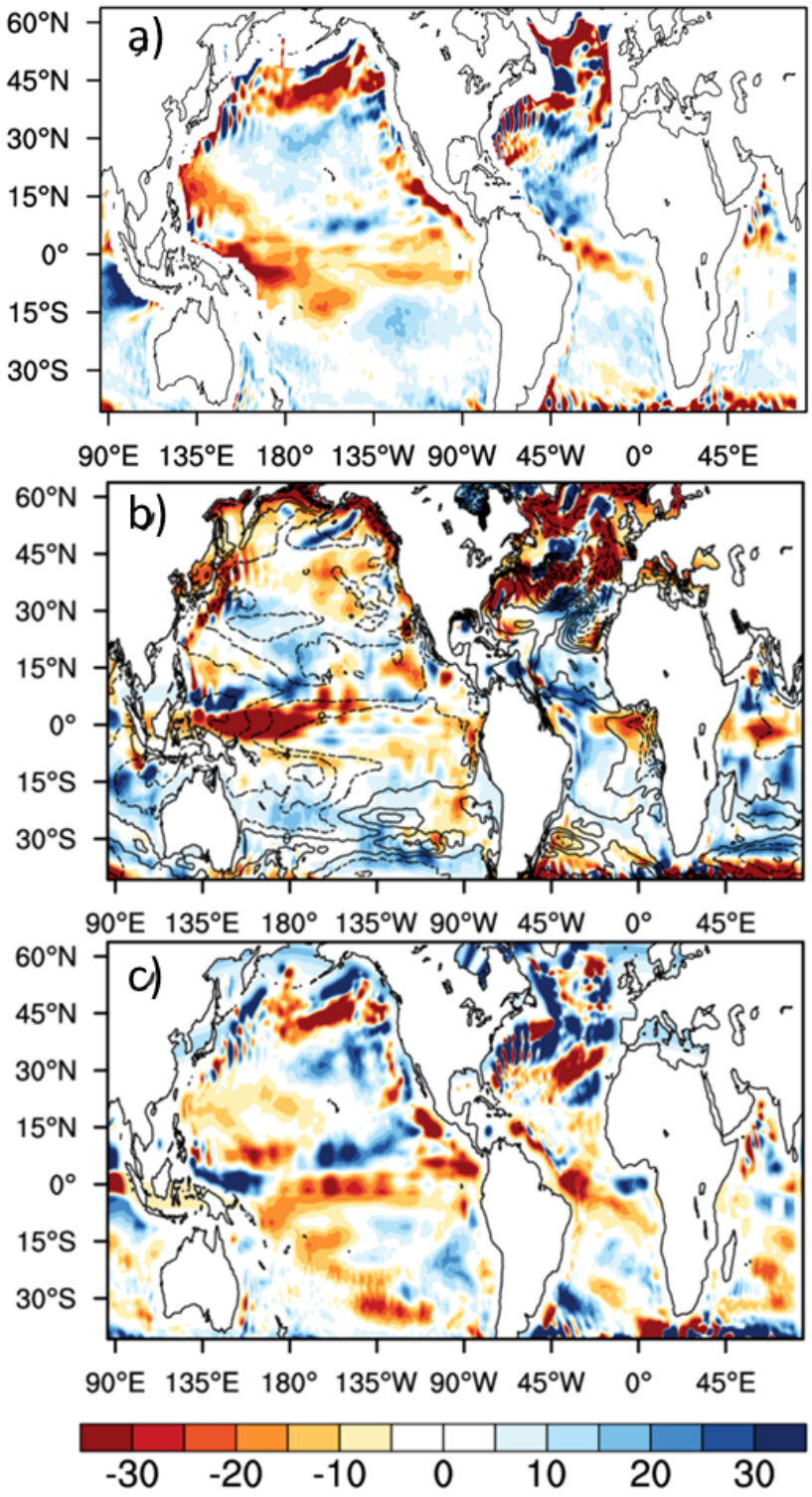

Figure 4.6: (a) Total freshwater advection flux changes. The components of the total freshwater advection flux given by (b) the freshwater advection changes due to changes in the near-surface salinity over-contoured by the SSS changes (solid lines are positive and dashed for negative values) and (c) the freshwater advection changes due to changes in the ocean currents. Units are in 10^{-6} kg m^{-2} s^{-1}.

balance was calculated for the upper 122.5 m, which includes the layers below the ML for most of the tropics and subtropics. The vertical transport associated with an intense mixing in the ML is therefore mostly excluded in this region. Consequently, at latitudes higher than 40 ° poleward, the advection signal significantly exceeds the surface flux term, suggesting a significant additional contribution from mixing processes. In the following, we will focus on the latitudes equatorward of 40 ° where this simple balance between the advective and surface FWF terms holds.

If changes to the balance are primarily driven by changes of the surface FWF as hypothesized by the expectation of using salinity as a rain gauge, the changed surface flux is expected to build up salinity changes which modify the advection term until it balances the contribution from a changing FWF. However, additional changes in the circulation driven by wind and heat flux changes interfere and lead to changes in magnitude of ocean currents. To evaluate the importance of these mechanisms, we split the advection changes into three contributions, one due to changes only in the circulation, the second due to changes in only salinity and a term with changes in salinity and ocean currents. The third term turns out to be small (not shown) and the remaining first two terms are of similar size and are equally relevant for the total advective transport of freshwater (Fig. 4.6b,c). Both terms are often anti-correlated rather than complementary. The negative signal of the total advection changes in the subtropics most consistently is related to surface salinity changes. This supports the simple idea of the increasing contrast between relatively salty and relatively fresh regions associated with the enhancing hydrological cycle will enhance the transports. The anti-correlation of the signal suggests that salinity changes are also partly driven by circulation changes. Assuming that circulation changes driven by FWF changes are smaller than those driven by wind and heat flux changes (Gregory et al., 2016), we can rationalise the SSS changes in the tropics and subtropics as those changes in SSS that are necessary to create advection fluxes that can balance the combination of the surface flux (Figure 4.6 a) and the changes in advection related to circulation changes (Figure 4.6c). However, in some regions, for instance, the positive signals in the tropical southern hemisphere, circulation changes balance surface flux changes and therefore require smaller SSS changes.

4.4 Subsurface salinity changes

The vertical averages over different depth ranges (Fig. 4.7a−d) and zonally averaged (Fig. 4.7e−g) salinity changes down to 2000 m depict that subsurface changes occur mostly in the upper 500 m, which closely resemble the spatial pattern of the SSS changes (Fig. 4.2a). The subtropical North Atlantic is the only basin where significant subsurface salinity changes reach as deep as 1200 m. The Pacific Ocean experiences

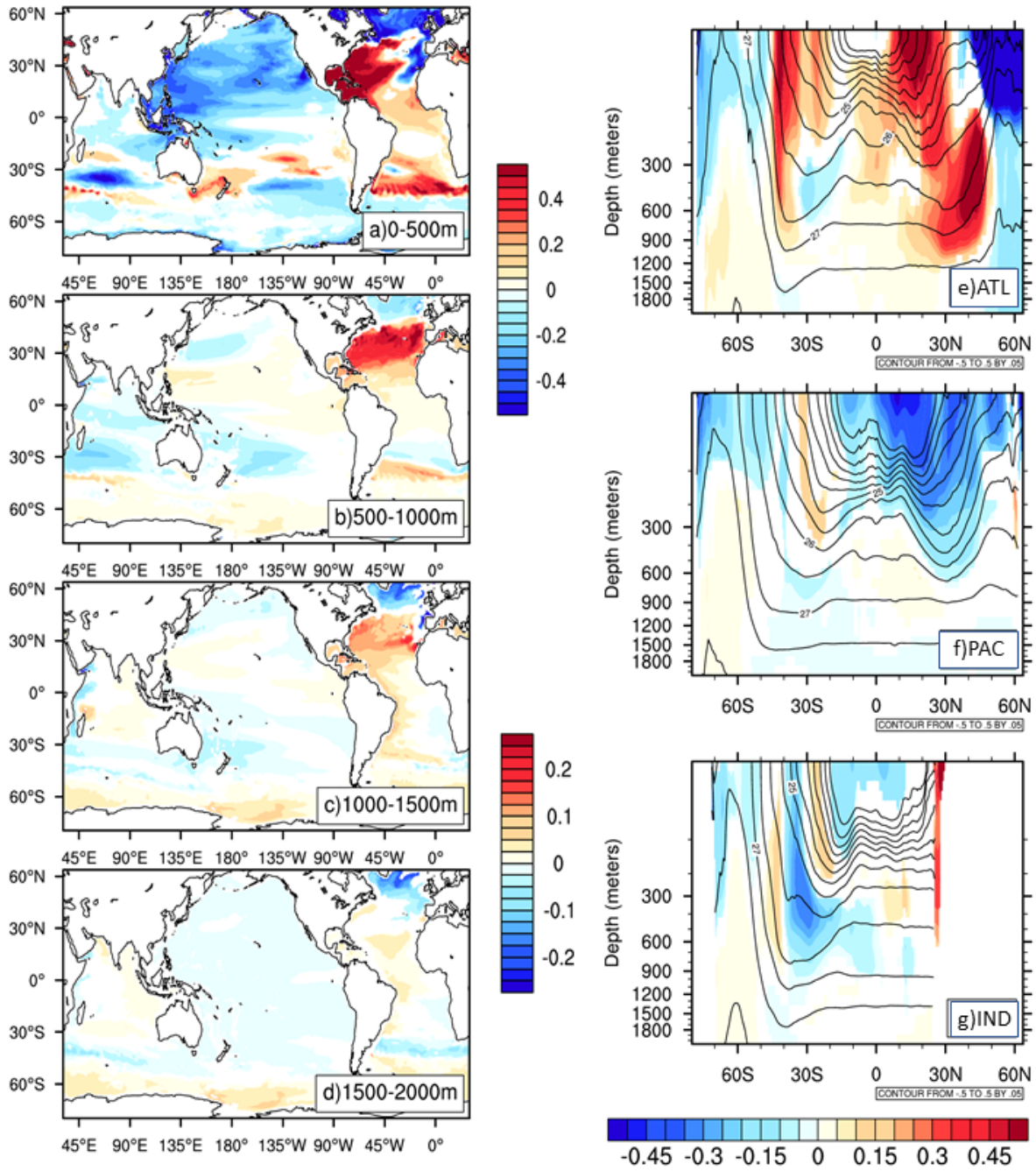

Figure 4.7: Left panel: Salinity changes (psu) between the RCP8.5 period (2081-2100) and historical period (1986-2005) averaged over four depth levels (a) surface−500 m, (b) 500−1000 m, (c) 1000−1500 m, and (d) 1500−2000 m. Note that the values from 1000−2000 m depth (c, d) are shown at half the scale of the upper 1000 m (a, b). Right panel: Zonal average of subsurface salinity changes between the RCP8.5 period (2081−2100) and historical period (1986−2005) of the model data in (e) the Atlantic Ocean, (f) the Pacific Ocean and (g) the Indian Ocean basins. Values have been masked that are below two times the standard deviation of the control run.

an almost basin-wide freshening in the upper 500 m with a slightly positive signal in the southern subtropical gyre. The upper ocean of the subtropical South Indian Ocean experiences a decrease in salinity, similar to that at the surface, extending down to a depth of 700-900 m. This decrease is different from the increase in salinity the region has experienced during the period from 1950s to 2000s (Durack and Wijffels 2010; Skliris et al. 2014). As the surface changes here correspond to a positive surface freshwater forcing, freshening in those intermediate depths must have resulted from the subduction of these lower surface salinities, which is supported by an increase in the Ekman pumping velocities (Fig. 4.8b) in these latitudes which can drive the fresher surface waters into the interior.

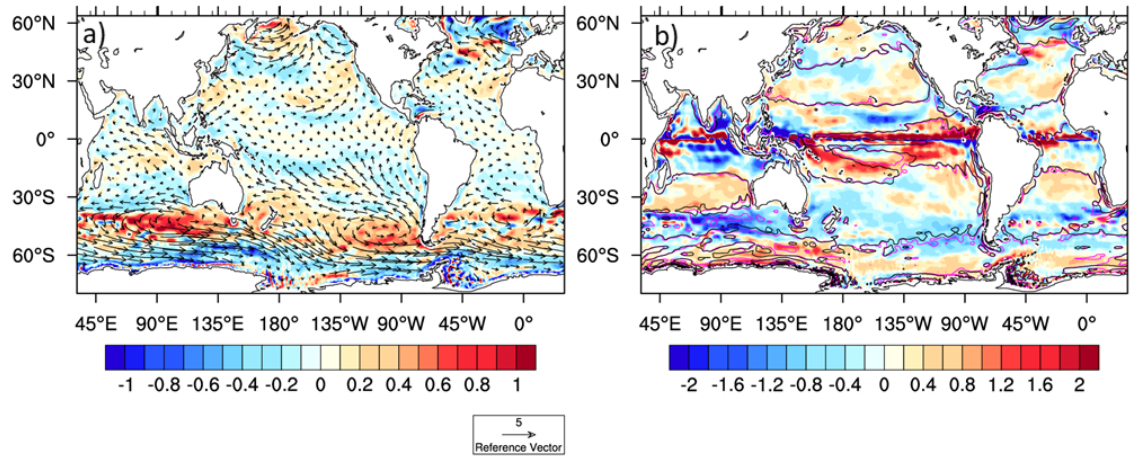

Figure 4.8: (a) Changes in the wind-stress curl (10^{-7} N m^{-3}) and wind-stress (10^{-2} N m^{-2}), (b) changes in the Ekman pumping velocity (10^{-6} m s^{-1}). The zero wind-stress curl for the RCP8.5 (black) and historical (magenta) periods are overlaid on (b).

The Atlantic Ocean experiences the largest subsurface salinity changes, in comparison to the Pacific and Indian oceans, under the RCP8.5 scenario, especially in the northern subtropical latitudes. The subtropical increase in salinity corresponds to an increase in SSS, which can be caused be increasing evaporation due to ocean warming (Curry et al. 2003). A majority of the increase in the upper 500 m of the subtropical gyre focuses on the western North Atlantic (Fig. 4.7 a), where the winter ML reaches a depth of 300−350 m (Fig. 4.5). Together with an equatorward extension of the salinity maximum (35 °N and 400 m; Fig. 4.7 e), due to subduction and circulation of these saline waters in the subtropical gyre, resulted in the salinification of the upper 500 m of the subtropical North Atlantic. Hence, the salinity change observed in these latitudes, at around 300−600 m depth, could be driven mainly by an intense near-surface salinification due to a substantial decrease in surface FWF over the subtropical North Atlantic. The significant salinity changes in the subtropical North Atlantic extends

to a depth of approximately 1200 m, between the latitudes 30 °N-50 °N (Fig. 4.7 e). Boyer et al. (2005) observed a similar but weaker positive salinity trend in the North Atlantic during 1950-2000, extending down to a depth of 1500 m, which was connected to a possible outflow of Mediterranean waters that are increasing in salinity (Béthoux et al. 1998).

A similar case holds true for the salinity increase from 500 m and downwards and could be associated with salinity changes in the Mediterranean Outflow Waters (MOW). The figure 4.9 shows the vertical profile at 36 °N, where the high saline Mediterranean waters enter the North Atlantic. Fig. 4.9 c demonstrates an upward shift in the MOW saline waters resulting in fresher water beneath (below 1100 m) the high saline signal. Alongside, the westward flowing component of the MOW extends further westward in the RCP8.5 scenario compared to the historical period giving rise to the maximum salinity west of the outflow region centred around the depth of 700 m. This characteristic shift in MOW was reported by Thorpe and Bigg (2000). They found a reduction in salinity projections at depths of 1000−1500 m and an increase in salinity between 500-1000 m. Their study connected the shallowing feature of the MOW to a reduction in the density of the Mediterranean water owing to anthropogenic warming (Thorpe and Bigg, 2000). With a strong ocean warming in the RCP8.5 run, it is plausible that their warming explains the upward shift in MOW in our study. This upward shift in MOW could also justify why a strong signal is present in the 500−1000 m of the North Atlantic subtropical region.

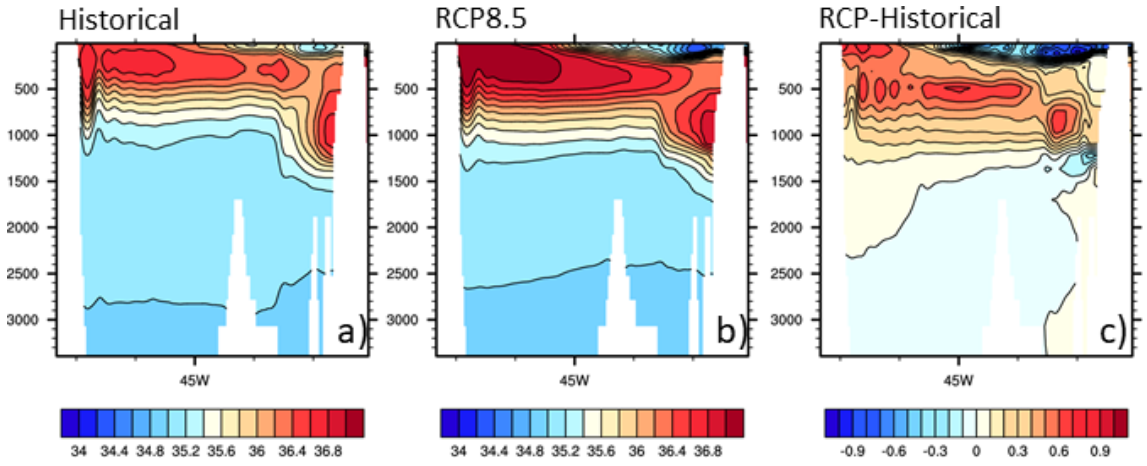

Figure 4.9: The depth-longitude section of (a) salinity (psu) in the historical, (b) salinity (psu) in the RCP8.5 and the (c) changes in salinity (RCP8.5 minus Historical) at 36 °N in the North Atlantic.

The subpolar and eastern subtropical North Atlantic experience intense freshening at the surface (Fig. 4.2 a) down to a depth of 150 m (Fig. 4.7 a, g). This fresh signal, extending to the eastern subtropical latitudes, is projected by many CMIP5 models (Fig. 2.2) (Levang and Schmitt 2020). The strong fresh signal in the subpolar North

Atlantic is limited to the upper layers, which is mostly in the ML, after which the signal becomes extremely weak (Fig. 4.7 e). This sudden weakening can be connected to a decrease in deep convection as already mentioned in the section 4.2 for projected surface changes (Häkkinen, 2002). The distinct saline-fresh partition at the surface (Fig. 4.2 a) continues in the subsurface levels supporting the impact of a weakened AMOC. The freshening noticed in the higher northern latitudes ($> 40\,^{\circ}$N) is not an observed feature in many observational studies (e.g. Durack and Wijffels 2010; Skliris et al. 2014), but there has been a large addition of freshwater into the northern North Atlantic since the 1960s (Dickson et al. 2002; Curry and Mauritzen 2005) from ice melting and increased freshwater from river inflow, which supports the positive FWF projected in this region and therefore the decrease in salinity.

The changes in the rest of the Atlantic are also large, but relatively weaker than the subtropical North Atlantic. The South Atlantic subsurface salinity changes, which corresponds to the positive SSS changes, are larger in the ML and gradually weaken below the ML. Additionally, we notice a slight freshening at $30\,^{\circ}$S over a depth range of 300-600 m, which could be related to the Agulhas leakage. The South Atlantic Ocean receives saline waters from the Indian Ocean via Agulhas leakage, the part of the Agulhas Current that enters the South Atlantic (Gordon et al. 1992; De Ruijter et al. 1999). Few studies have established that the sources of the Agulhas Current are dominated by the south-west "subgyre" of the South Indian Ocean, which extends to $65\,^{\circ}$E (Harris 1972; Stramma and Lutjeharms 1997), and not by the east Madagascar Current (Lutjeharms, 1988) or the Mozambique Current (Sætre and Da Silva, 1984). Hence, with a freshening of intermediate water masses in the South Indian subtropical gyre (Fig. 4.7 a), the fresher waters get transported to the South Atlantic via the Agulhas leakage. Once the Benguela Current picks up these fresher waters, they enter the subtropical gyre of the South Atlantic Ocean (Fig. 4.7 b, c). The fresh signal is weaker further down (1000-1500 m) but persists in the eastern South Atlantic region.

In comparison with the Atlantic Ocean, the Pacific and Indian Oceans experience much weaker subsurface salinity changes, especially below 500 m where changes are quite unremarkable. Much of the freshening in the upper 200 m of the subtropical North Pacific Ocean occurs in the winter ML. The increased SST (Fig. 4.4) and freshening of the surface subtropical North Pacific create stable stratification and hence a shallower mixed layer, which could likely be a driving factor for the near-surface freshening. The freshening signal extends further down to 500-600 m, and the equatorward slope of the fresh signal depicts an equatorward propagation of the subducted subtropical gyre waters (Fig. 4.7 a, f).

The South Pacific and South Indian oceans experience a freshening of the intermediate levels, albeit weaker for the Pacific. The study of Wong et al. (1999) reported a similar freshening of the Pacific and Indian intermediate waters. The intermediate freshening

in their study was attributed to an increase in precipitation in the source regions of AAIW (centred around 800 m) and North Pacific Intermediate Water (NPIW; centred around 500 m). The precipitation was estimated to have increased by 31 mm yr^{-1} between the latitudes 55° and 65°S, which was three times more than the increase estimated by coupled models for the same period. In addition, a decrease in salinity of AAIW alongside an increase in salinity in the upwelling Circumpolar Deep Water was to an increase in the northward transport of the Antarctic sea-ice by Haumann et al. (2016). From these studies it can be presumed that increase in the surface FWF in the high-latitude southern oceans in our study (Fig. 4.2 a) could drive a freshening of the intermediate waters (Fig. 4.7 f, g). However, the South Indian Ocean also experiences surface freshening north of the source region. Therefore, it is possible that the subsurface freshening here may be a direct result of this surface freshening, especially as the subsurface signal can be seen connecting to the surface (Fig. 4.7 g).

The subsurface salinity changes below the ML are a combination of changes that occurred from changes in the $\theta - S$ relationship and changes due to changes in the isopycnal movement. As explained before, these changes are driven by changes in surface forcings. In order to distinguish contributions from the surface forcings and related circulation changes, in the following section, we decompose the above-explained changes in the subsurface salinity (Fig. 4.7 e, f, g) and examine different mechanisms associated with the changes in different ocean basins.

4.4.1 Heave and spice

The total changes in subsurface salinity can be determined by decomposing changes into changes along constant isopycnal surfaces and changes caused by isopycnal movements. Any change in surface forcings can affect the density surfaces and lead to changes in subducted water either by deepening or shoaling the isopycnal surfaces. Fig. 4.10 shows the changes in depth of isopycnal surfaces for each ocean basin, where the positive values correspond to deepening, and the negative values correspond to shoaling of isopycnal surface. On multidecadal time scales, if there is a deepening throughout the oceans, then it is very likely due to warming (Häkkinen et al., 2016), and circulation changes play only a secondary role in these changes.

A deepening of the isopycnal surfaces can be a result of changes in temperature and salinity and/or due to wind-stress changes. However, the wind-related heave changes have a dominant impact on shorter time scales such as in seasonal, interannual or decadal scales (Bindoff and Mcdougall 1994; Evans et al. 2017) and as already mentioned, play a weaker role on multidecadal time scales compared to warming. It is assumed that the freshwater forcing drives weak isopycnal movement, which is later confirmed in section 4.4.3. As a result, most of the isopycnal deepening and associated

subsurface salinity changes were determined to be majorly driven by ocean warming (Durack and Wijffels 2010).

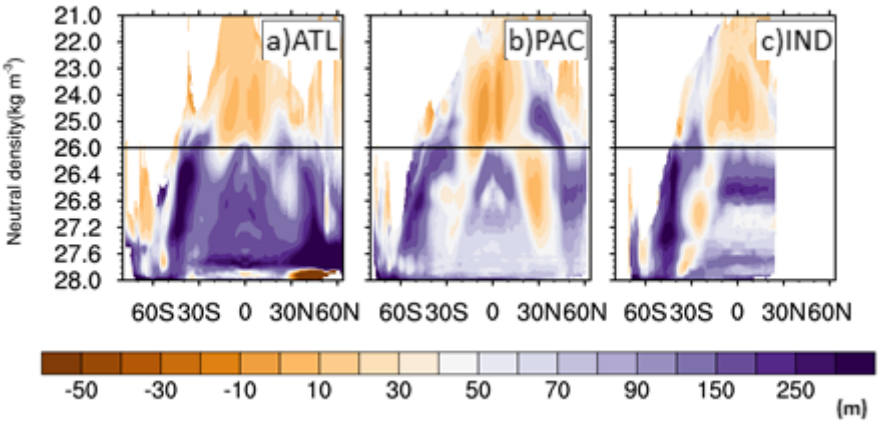

Figure 4.10: Zonally averaged depth changes of constant neutral density surfaces in meter for (a) the Atlantic Ocean, (b) the Pacific Ocean and (c) the Indian Ocean.

On the other hand, the changes along constant isopycnal surfaces, i.e. spice-related changes, can occur from changes in temperature and salinity on isopycnals, hence, associated with surface warming and FWF related changes together with ocean mixing. We assume that wind-stress changes play no role in the spice changes. Therefore, as the first step, partitioning the total salinity into heave and spice components isolates surface buoyancy flux changes from wind-related changes in subsurface salinity changes.

Except for small regions near the surface and in tropical regions of the Pacific at a depth of the equatorial thermocline, all ocean basins experience a deepening (Fig. 4.10). The deepening in the transition from subtropical to subpolar regions entails due to the large isopycnal slopes horizontal, i.e. poleward, shift of isopycnals which again entails the poleward outcrop migration. Hence, we can assume that downward motion by warming is a dominant cause for the motion of the isopycnals.

The zonal average of heave and spice components of salinity change are clearly anti-correlated (Fig. 4.11). However, from a quick view of the zonal and depth average of the upper 500 m given in Fig. 4.12, where the contributions are largest, the total salinity signal marks a dominance by heave for the Atlantic Ocean, particularly in the 500-1000 m. For the Pacific and Indian Oceans, the total signal contribution appears to be mainly from the spice component.

In the high latitudes, poleward of 40 ° North and South, the upper ocean experiences freshening that is dominated by the heave component (Fig. 4.11 a, c, e). Most of the heave signal here is compensated by the spice component, which is consistent with warming.

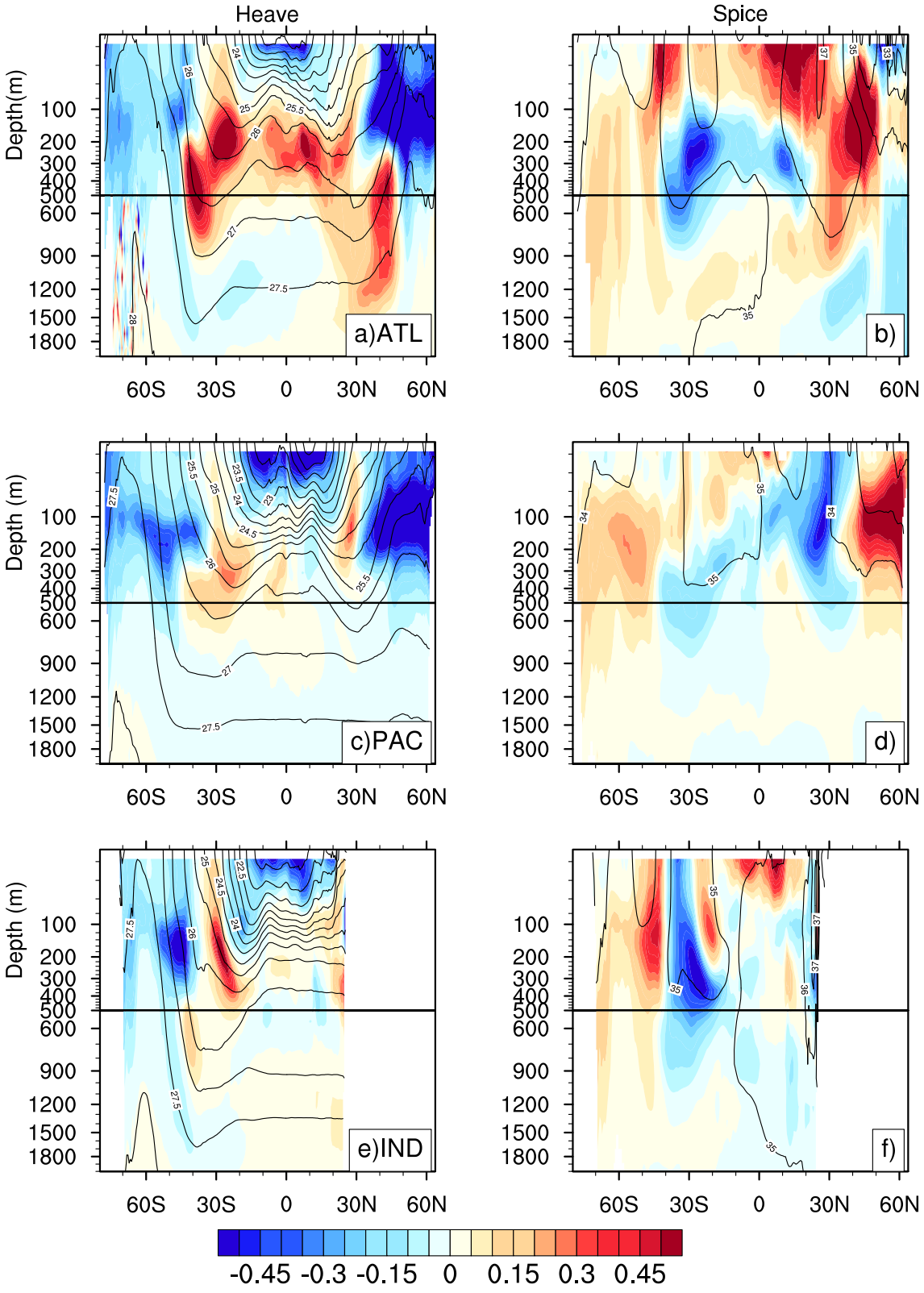

Figure 4.11: Zonally averaged salinity changes (psu) for (a,b) the Atlantic Ocean, (c,d) the Pacific Ocean and (e,f) the Indian Ocean between the RCP 8.5 (2081−2100) and historical (1986−2005) period. Heave-driven changes are calculated and over-contoured with the isopycnals (a,c,e). Changes in salinity analyzed on the neutral density surfaces (shown as contours) and the spice signal mapped back to depth levels shown in (b, d, f) over-contoured with climatological mean salinity. Note the break in depth axis at 500 m.

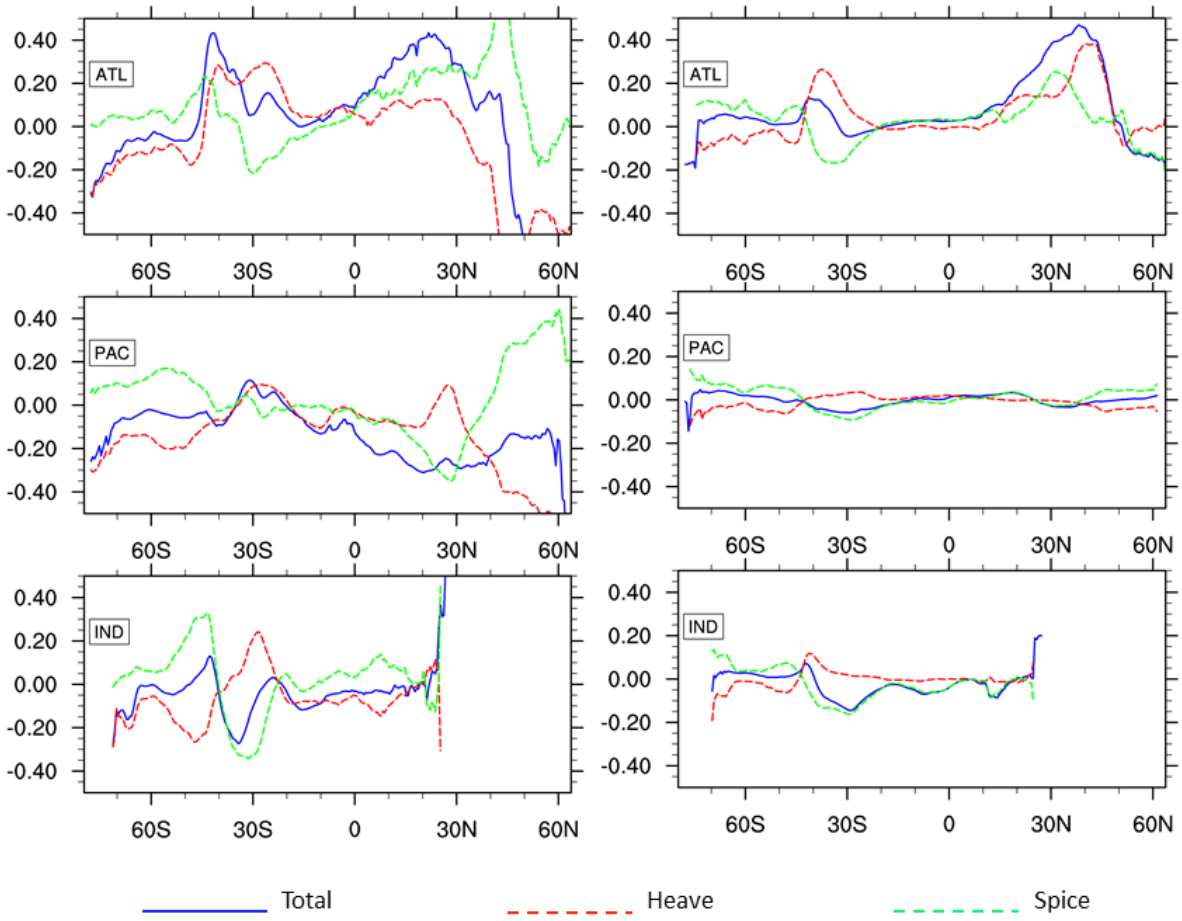

Figure 4.12: Lines show the effects of zonally averaged total salinity (blue), spice (green) and heave (red) on salinity (psu) between RCP8.5 (2081−2100) and historical period (1986−2005) for Atlantic (top), Pacific (middle) and Indian Ocean (bottom) at 0−500 m depth (left panel) and at 500-1000 m (right panel).

For the Atlantic Ocean, the total signal remains in the order of the heave and the spice contributions (Fig. 4.11a,b and Fig. 4.7e). Notably, in the upper 100 m of the subtropical gyres, the spice signal is responsible for the salinification in agreement with the expected enhancement of the hydrological cycle. In the subtropical North Atlantic, there is a possibility that the freshening dominated by heave (Fig. 4.12) has a contribution from wind-driven changes. We notice a shift in the zero wind-stress curl in the northern boundary of the North Atlantic subtropical gyre (Fig. 4.8b). This shift is marked by a dipole-like structure in both the curl and Ekman velocity changes (Fig. 4.8a,b). The resulting Ekman downwelling in the north of the subtropical gyre suggests an increase gyre circulation due to a northward shift (Fig. 4.8b) that could drive a deepening or poleward shift of the isopycnal surfaces in the subtropical gyre. Hence, from the wind-related circulation changes and the heave domination in the North Atlantic, there is a possibility that wind-driven changes play an important role

in North Atlantic subsurface salinity increase.

The upper 500 m of the Pacific shows predominantly freshening. Although freshening also dominates in the heave contribution, as explained before, the signal is larger and strikingly appears to a large extent anti-correlated with the spiciness contribution (Fig. 4.11 c, d). This mainly occurs in the high-latitude of all ocean basins. Thus, freshening appears when there is imperfect compensation, which renders the decomposition as little useful for exploring the origin of the freshening. At surface, these regions experience a surface warming of around 0.5 °C (Fig. 4.4), together with surface freshening (Fig. 4.2 b). Apart from this, the increase in westerly winds in the southern hemisphere pushes the fresher high-latitude waters further north by Ekman transport. This could result in displacing the surface waters with fresher waters from southern latitudes (Fig. 4.8 a, b).

A similar compensating effect is visible for the Indian Ocean, in which the compensation is even more evident, leaving a small residual effect on the total salinity (Fig. 4.11e,f). However, in the subtropical South Indian Ocean, centred around 30°S, the negative total salinity appear to be dominated by the negative spice component (Fig. 4.12). As the positive heave-driven changes compensate with an increase in salinity, the freshening caused by negative spice dominates and leaves a freshening in the total salinity of the subtropical South Indian Ocean.

The total subsurface salinity changes are pronounced in the upper 500 m of all the ocean basins (Fig. 4.7 e, f, g). This is the case for the Pacific and Indian oceans (Fig. 4.12). However, for the Atlantic, heaving component dominates below the depth of 500 m (Fig. 4.12; Right panel). At 500−1000 m depth, the subtropics in both hemispheres are dominated by heave-driven changes with positive spice signal, also adding to the total salinity in the subtropical North Atlantic. The heave domination in 500-1000 m could very likely be a result of gyre circulation changes or AMOC weakening or warming. The patterns visible in heave and spiciness appear to have a strong signature of the warming. As a result, this decomposition approach fails to identify or distinguish the contributions from different surface forcings. This highlights the key problem with a simple decomposition into heave and spice signals in determining the surface forcing contribution and, therefore, the need to use Bindoff and Mcdougall (1994) approach discussed in section 4.4.3.

4.4.2 Spiciness and water mass changes

As a consequence of heating playing a substantial role in salinity changes, heaving and spiciness changes are largely coupled. This can be rationalized because isopycnal migration leads to changes in the lateral positions of the surface density outcrops affecting the characteristics of water transported into the subsurface of the ocean and

thus influencing subsurface changes on isopycnals. The changes of the mean winter surface isopycnal outcrops from the historical (1986−2005) to the RCP8.5 (2081−2100) period (Fig. 4.13) show a large lateral shift in isopycnal outcrop locations, mainly shifting poleward for which heating is the dominant cause. However, note that not all migration changes are related to heating and not all spiciness changes are associated with the associated change in outcrop position. In particular, changes of subducted salinity are also driven by the temporal changes in SSS, including freshwater forcing changes.

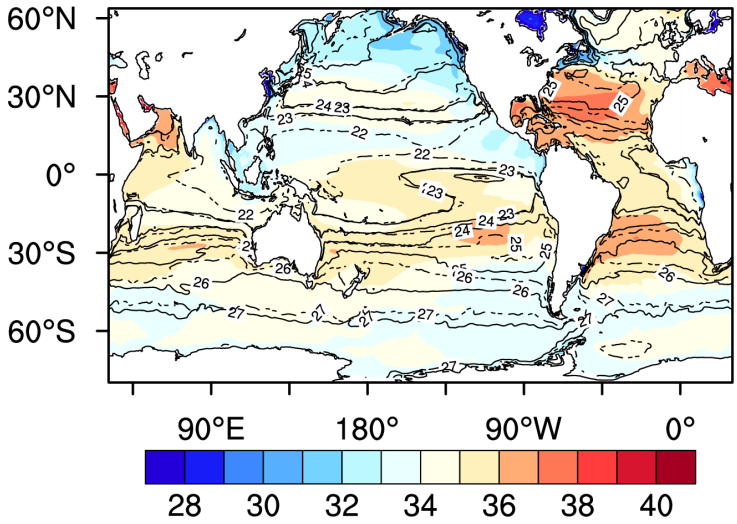

Figure 4.13: Surface winter density (kg m^{-3}) outcrop (contours) of the historical (dashed lines) and the RCP 8.5 (solid lines) runs overlaying the mean salinity (psu) for the period 1986−2100.

In order to obtain migration and freshwater term related salinity changes, we calculated changes during the March and September when the subduction occurs in the Northern and Southern hemispheres, respectively. This time selection facilitates a better understanding of changes in the subsurface driven by the changes at the surface by mean circulation. The isopycnal outcrop selection for the northern (March) and southern (September) hemispheres are such that they include depths with largest changes, which fall mostly in the upper 500 m. For presentation purpose, the outcrop values of migration-driven and freshwater-driven changes are averaged for every 10 degrees longitudinally.

Fig. 4.14 shows the salinity changes for March (left panel) and September (right panel) from the RCP8.5 period relative to the historical period. The circles represent the migration-driven salinity changes and the diamonds represent changes in SSS, including the changes driven by the surface FWF changes, referred to as freshwater-driven changes (Refer chapter 3, section 3.3.2).

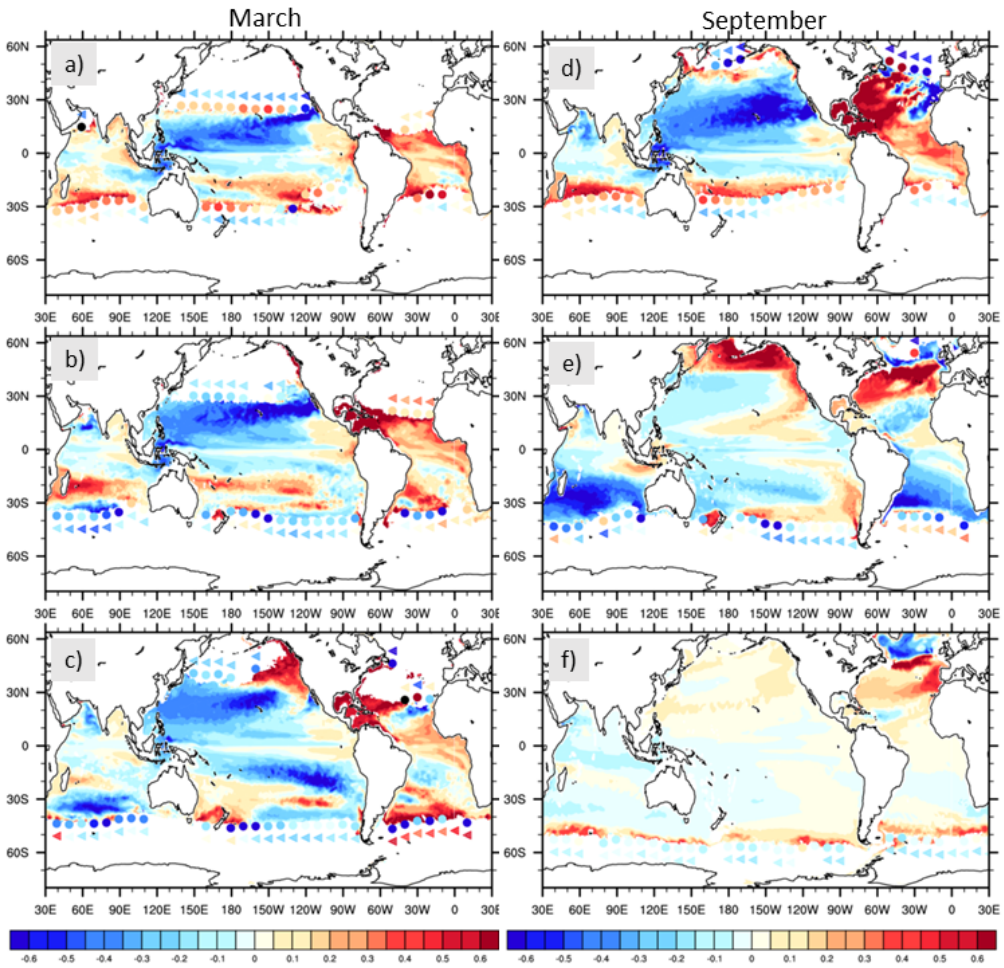

Figure 4.14: Salinity changes on isopycnal surfaces for March at (a) 23 kg m^{-3}, (b) 24 kg m^{-3}, and (c) 25 kg m^{-3} and for September at (d) 24 kg m^{-3}, (e) 26 kg m^{-3}, (f) 27 kg m^{-3}. Circles represent contribution from migration-term and triangles represent freshwater-term.

In the Atlantic basin, the outcrops in the tropical and subtropical latitudes of the North Atlantic (23 and 24 kg m^{-3}) show positive changes in salinity, which appear to be mostly freshwater-driven (Fig. 4.14 a, b), with some migration-driven dominance in the 25 kg m^{-3} (Fig. 4.14 c). This most likely indicates that the spice change attributed to an increase in the North Atlantic salinity, in the upper 100 m, is primarily driven by a substantial freshwater forcing at the surface, and warming-related SSS changes are negligible. Our result for the North Atlantic is in good agreement with Durack and Wijffels (2010) wherein most of the isopycnal salinity changes were driven by the freshwater component.

In the northern hemisphere, the isopycnal outcrop 23 kg m^{-3} of the North Pacific shows exclusive freshening, which is not entirely consistent with the dominance of the salinity increase visible in migration-driven changes (circles, Fig. 4.14 a). However, a small part of this isopycnal, in particular the region of the largest salinity change, is ventilated by the water near the strong negative migration signal off the west coast

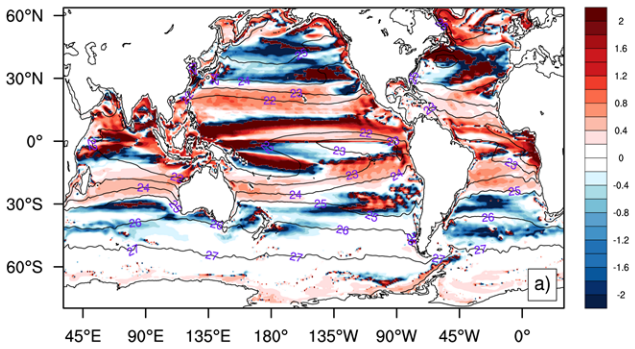

Figure 4.15: Changes in the surface salinity (psu) due to lateral migration of the isopycnal outcrops. Solid lines are the winter isopycnals calculated from the seasonal climatology of the data period (1986−2100).

of Baja California. A similar contribution coming from the freshwater-driven changes at this location suggests that a freshening of the North Pacific is driven by partial contribution from migration and freshwater-driven changes. However, in the South Pacific, a salinity increase in the upper thermocline water masses and freshening of mode water masses appear to be mostly migration-driven (Fig. 4.14 d, e). Moreover, a freshening in the intermediate waters of the South Indian Ocean corresponds with both freshwater and migration-driven changes at the outcrop (Fig. 4.14 e).

Given these migration-driven changes are largely from surface ocean warming, the warming-related isopycnal outcrop migration appears to influence salinity changes on isopycnal surfaces in the southern hemisphere more than in the northern hemisphere, with an exception in the higher latitude isopycnal, 27 kg m^{-3} (Fig. 4.14 f), where contributions are unclear. This could be due to the linearisation approach used in the migration-driven salinity changes to calculate the horizontal shift (δy), which is more in the northern hemisphere compared to the southern hemisphere. The meridional outcrop shift, δy, has unrealistic or very high values especially in certain regions of the tropical Pacific, the eastern part of the south and the north Pacific, the sub-tropical north and south regions of the Atlantic and the Indian Oceans, a result of abrupt change in gradients or due to large shifts in places where there are small gradients. Fig. 4.15 shows migration-driven salinity changes at the surface between RCP8.5 and the historical period. The regions where the migration of outcrops produces large salinity changes are regions such as the ITCZ band of the tropical ocean and the subtropical gyres. These are the regions near the maxima and minima of the density because in those regions small changes in density lead to large horizontal migration. In some regions, the concept of migration cannot be used as large positive signals exist inside of areas with large negative signals. Therefore, the disadvantage of this would

be that the migration-driven changes at a given surface outcrop could be overestimated in magnitude.

The migration and freshwater driven changes do not correspond well in many regions with the salinity changes on a given isopycnal surface, especially the regions away from the outcrop location. For instance, an increase in salinity in the tropical latitudes of the Pacific and Atlantic (e.g. Fig. 4.14 a, d, e), appears to be neither from the migration-term nor freshwater-term. The outcrop mismatch is more evident in the northern hemisphere than in the southern hemisphere due to large shifts in the density outcrops (Fig. 4.13).

4.4.3 Salinity changes due to pure warming, freshening and heave processes

The previous approach on decomposing the total salinity into heave and spice did not separate the impact of surface forcing signals on salinity. As the warming signal is masking the contributions on projected subsurface salinity changes, heave and spice signals lack clarity on the surface forcing dominating in each ocean basin. Hence, in an attempt to identify the contributions from warming, FWF and wind-stress changes, we used the method of Bindoff and Mcdougall (1994) to link salinity changes to the three processes, pure warming (PW), pure freshening (PF) and pure heave (PH), respectively, by an inverse approach. The description and mathematical equations of each process are provided in chapter 3, from which according to equation 3.12 to 3.16 the following part of this section describes the contributions from pure processes on total salinity on the depth and density levels.

The spice changes are a measure of salinity and temperature changes along a fixed neutral density surface. Therefore, spice changes result from changes in temperature and salinity, which could be connected to surface warming and FWF changes. By considering that the wind-stress changes do not create a modification in $\theta - S$ relationship, thereby not affecting the changes along a given isopycnal surface, the spice changes should explain the contribution from changes associated with surface FWF changes and surface warming.

Therefore, the spice signal can be represented as a sum of the PF and PW signals (Fig. 4.17 c, f, i). The PW process is defined such that it does not contribute to salinity changes at constant depth levels. However, PW changes the ocean temperature, which causes changes in the density field and thereby contributes to heave-related salinity changes shown in Figure 4.16. The PF process also results in the density changes due to changes in freshwater forcing and resulting redistribution of the freshwater. The difference between salinity changes on depth and those on density (mapped back to

depth) would give heave-related salinity changes (refer Eq. 3.5). With that in mind, the similarity between PF salinity changes on depth (Fig. 4.18a) and PF salinity changes on density (Fig. 4.17a) suggests that PF generates much less heave-related changes compared to the other surface fluxes.

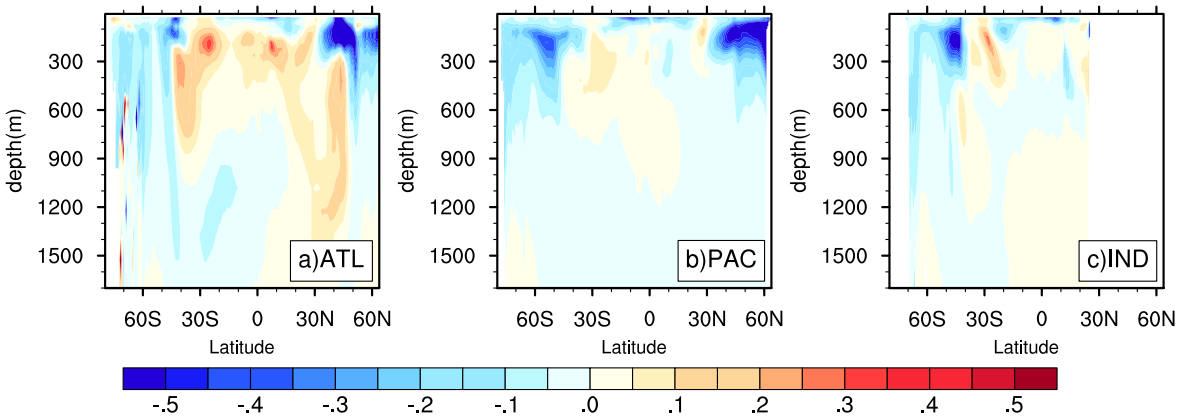

Figure 4.16: Zonal averages of heave contribution of salinity changes (psu) for pure warming process (PW) for the (a) Pacific Ocean, (b) the Indian Ocean and (c) the Atlantic Ocean basins.

The spice and heave contributions in the Atlantic Ocean are quite different from that of the Pacific and Indian oceans. As already alluded to in the discussion of Fig. 4.11, in the Atlantic Ocean, both PF and PH contribute to the increased salinity changes seen in the near-surface and subsurface depth levels. The salinity increase between 100−200 m of the tropics and at 300 m of the western subtropical North Atlantic falls in the mixed layer. Hence, as expected, the positive spice changes here associated with PF (Fig. 4.17g) is connected to a substantial increase in the surface FWF. This is also supported by our previous result on the dominance of freshwater-driven isopycnal salinity increase in the North Atlantic over the migration-driven changes. The pure heave and freshening processes also add to a freshening signal in the higher latitudes of the Atlantic basin.

The Atlantic basin seems to be an exception compared to other basins since PH appears to contribute significantly to the subsurface salinity changes causing an increase in salinity (Fig. 4.18h). These positive salinity changes in the North Atlantic seem to be consistent with the local negative wind-stress curl and associated Ekman downwelling in the Gulfstream and North Atlantic current (Fig. 4.8a,b). The North Atlantic Current and the Gulfstream regions have experienced isopycnal deepening in the past years (Häkkinen et al., 2016). Hence, the isopycnal deepening can be connected to a strengthening of the currents in the northern limb of the subtropical gyre, which probably drive a large part of the salinity increase at around 40°-50°N. A similar change in the South Atlantic associated with the positive wind-stress curl and Ekman downwelling in the southern limb of the subtropical gyre could be linked to the PH related

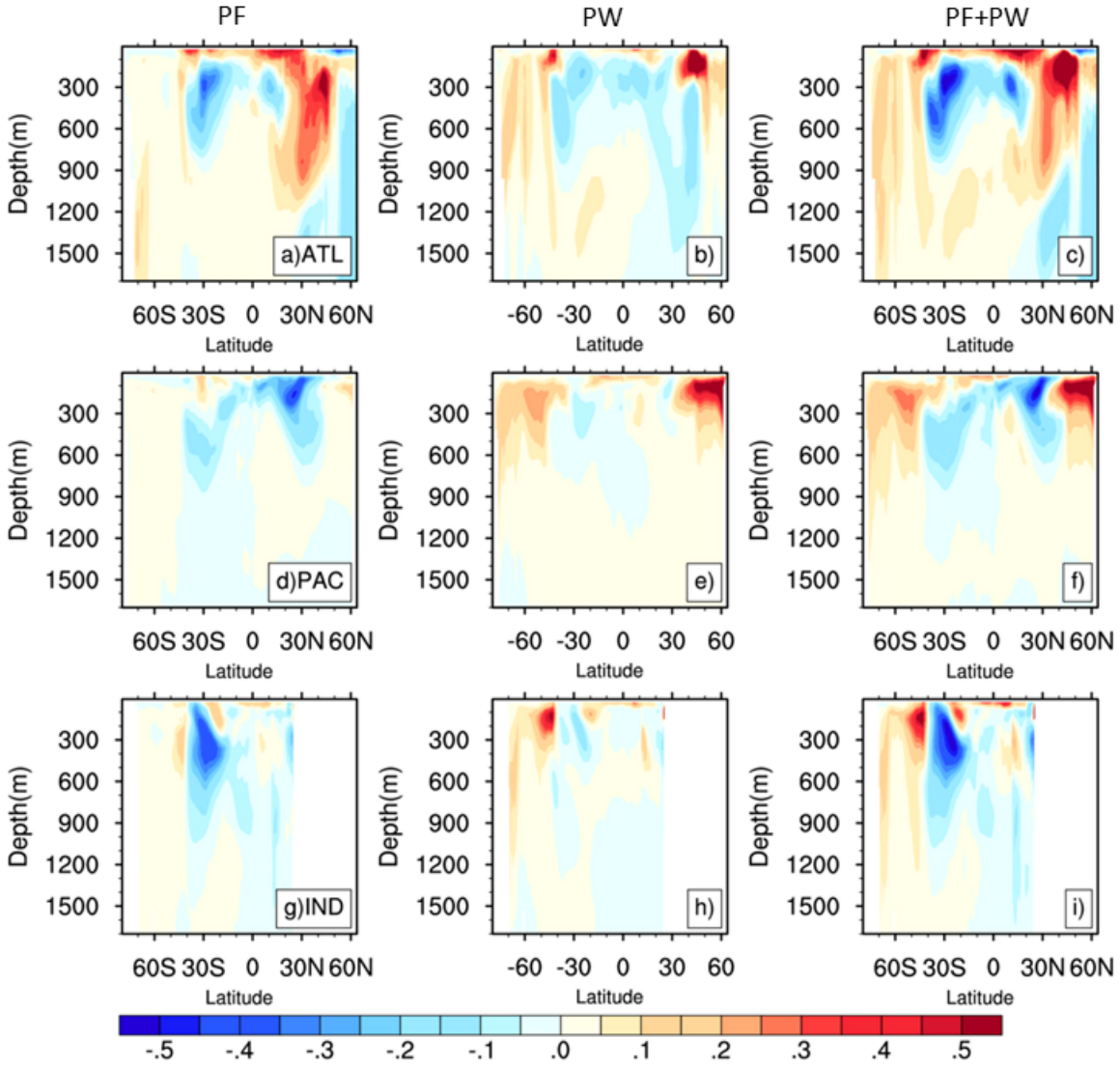

Figure 4.17: Zonal averages of spice contributions of salinity changes (psu) on isopycnal surfaces (represented on depth levels) for the (a, d, g) pure freshening process (PF), (b, e, h) pure warming process (PW) and spice signal given by PF+PW, in the (a, b, c) Atlantic Ocean, (d, e, f) the Pacific Ocean and (g, h, i) the Indian Ocean basins.

salinity increase in the South Atlantic. However, a deepening of the isopycnals does not exhibit a shoaling counterpart of similar magnitude, which is conflicting with the expected response to changes in wind-stress. This could be because the system is solved at every grid point for the global ocean without explicitly considering a constraint for zero global integral for the wind-stress heaving in the PH process (Lyu et al. 2020). In both hemispheres, the spice-related PF and PH together strengthen the subsurface salinity increase of the subtropical Atlantic Ocean.

The spice component which dominates the freshening in the upper 500 m of the subtropical North Pacific and the subtropical South Indian Ocean (Fig. 4.12) is dominated

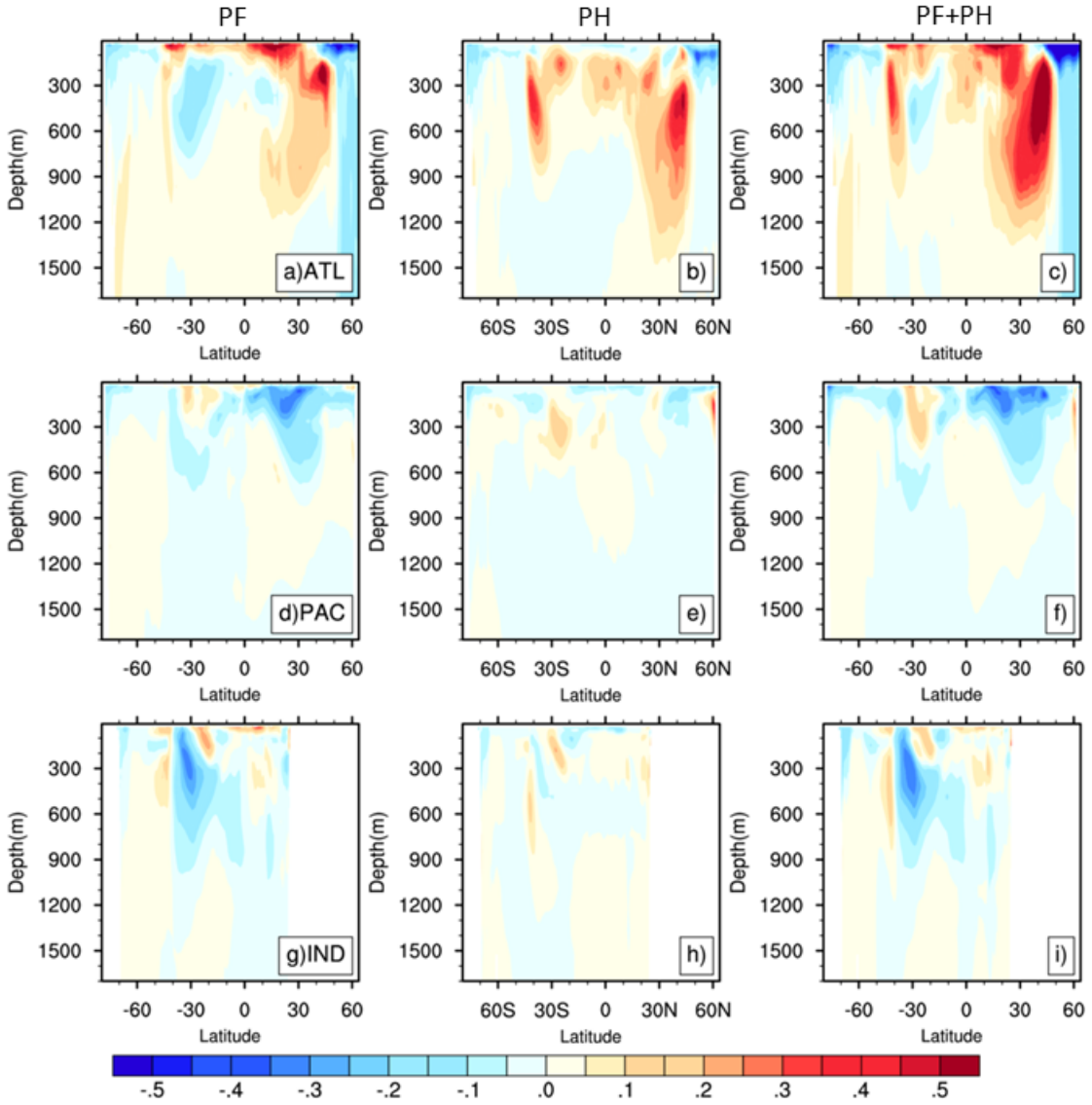

Figure 4.18: Zonal averages of depth contributions of salinity changes (psu) for the (a,d,g) pure freshening process (PF), (b,e,h) pure heave process (PH) and (c,f,i) salinity changes on depth given by PF+PH for the (a,b,c) Atlantic Ocean, (d,e,f) the Pacific Ocean and (g,h,i) the Indian Ocean basins.

by the PF process (Fig. 4.17 a, d). The positive slope in the $\theta - S$ relation (Fig. 3.3; Bindoff and Mcdougall (1994)) can explain the freshening of the subtropical gyres of the North Pacific and South Indian Oceans by the PF process, in which a surface freshening results in subducted water along an isopycnal to become cooler and fresher. Both the North Pacific and South Indian Ocean experience a freshening at the surface linked to an increase in surface FWF. Hence, there exists a good correspondence between the subsurface salinity contribution from PF and the increased freshening at the surface (Fig. 4.2 a). The spice-related PW subsurface contribution corresponds with migration-driven changes connected to warming; however, with weaker magnitudes.

As discussed before, the migration-driven changes have larger longitudinal variations, especially at the tropical and subtropical regions, so a zonal average could result in a weak signal. Nevertheless, the spice-related changes of the subsurface oceans potentially caused by lateral migration of isopycnals are compensated by the heave-related PW changes, leaving little or no salinity signal on total subsurface changes. As a result, the PF process tends to be responsible for the subsurface freshening in the North Pacific and South Indian Oceans.

On depth levels (Fig. 4.18), PF dominates a large part of the total salinity on depth levels (Fig. 4.7 e, f, g) in all the ocean basins contributing to the subsurface freshening in the tropical and subtropical North Pacific on depth levels. Since the subsurface salinity in these regions shows a freshening, the PF contribution is consistent with the subduction of the fresh surface signal. Moreover, a salinity increase in the subtropical South Pacific can also be linked to the PF process. However, PH shows slight freshening in the tropics and higher latitudes of Pacific and the tropical Indian Ocean. Therefore, PH contributes little to any changes in salinity in these two ocean basins.

The dominant contribution to total salinity on depth levels (Fig. 4.7e,f,g) of all ocean basins can be attributed primarily to the PF process. Pure heave plays a significant role in the Atlantic Ocean along with PF in the salinity changes of the tropical and subtropical Atlantic Ocean. The role PF plays in subsurface salinity changes corresponds well with the surface FWF changes in the global ocean. This signifies the importance of changes in the surface freshwater forcing on subsurface salinity changes under a global warming scenario. However, it is essential to remember that this is an underdetermined solution and does not provide us with an exact solution. In addition to that, we have applied this approach to the 20-year mean changes during the RCP8.5 and historical period. Hence, it is important to understand that the results represent contributions from a mean value of the changes related to each process, assuming they act linearly.

4.5 Discussion and concluding remarks

This chapter summarised analyses of the projected salinity changes of the global oceans in order to understand the impact of changes in surface forcings in a warming climate. The MPI-ESM-MR projections, with the historical and RCP 8.5 run, reveal that the inter-basin contrast will increase strongly by the end of the 21st century. By that time, the Pacific Ocean becomes fresher and the Atlantic Ocean becomes saltier in comparison with the historical period. The surface change in MPI-ESM-MR salinity agrees well with the CMIP5 model study by Levang and Schmitt (2015), which also include MPI-ESM-MR. We find that, while the projected surface FWF and SSS changes

show a good correspondence for the Atlantic Ocean, they do not correspond with each other in most regions of the Pacific and Indian oceans. On calculating the SSS pattern amplification (PA) defined by Durack and Wijffels (2010), we find an 18 % PA in the projected SSS with a correlation of 0.73 and a 19 % PA of the surface FWF (R=0.83). The SSS PA corresponds well with a study of Zika et al. (2018) where they find that the surface forcings act almost linearly to produce such a PA in SSS (13-15 %), with almost one half of the amplification, during the period 1957 to 2016, attributed to surface warming. Out of all three basins, the Atlantic Ocean exhibits the largest PA of 31 % with R value equals 0.88, whereas the Pacific and Indian Oceans have a 9 % SSS PA. Hence, the Atlantic ocean experiences the largest SSS changes in the projected ocean warming climate that closely resembles the mean climatological SSS in the Atlantic. The weaker PA and correlation in the Pacific in comparison to the Atlantic suggests that SSS changes are not closely related to the mean SSS pattern, which highlights the importance of other oceanic processes such as advection and mixing processes in the long-term salinity changes of the near-surface ocean despite the warming and changes in surface FWF.

Therefore, the resulting SSS changes cannot simply be rationalized as a result of the accumulation of freshwater changes, but follow from a new balance between the perturbed FWF and advection changes. In the tropics and mid-latitudes, the existence of such a balance could be demonstrated for a surface layer that includes the mixed layer, while for higher latitudes, the necessary inclusion of the mixing processes complicates the analysis. The advection term was decomposed into the contribution from salinity changes and the contribution from circulation changes. The resulting anti-correlation between these contributions reveal that near-surface salinity changes are also substantially driven by circulation changes. This holds, particularly on smaller spatial scales. However, the salinification of the subtropical regions most consistently is described by the changes in the surface FWF.

Several studies (e.g. Durack and Wijffels 2010; Skliris et al. 2014) report significant subsurface changes limited to the upper 500 m of the ocean. In a projected climate, our study similarly projects significant subsurface salinity changes in the ocean basins predominantly in the upper 500 m. While the Pacific and Indian oceans experience a freshening in the subsurface depth levels, the Atlantic Ocean experiences a basin-wide increase in salinity in the tropical and subtropical latitudes. A distinct positive salinity signal, extending to a depth of 1100 m, in the subtropical North Atlantic is noticeable throughout the depth range of central and intermediate water masses, with maximum salinity changes centred around 450 m at 45°N. A part of this increase appears to come from an increase in near-surface salinity of the western North Atlantic region, which corresponds well with a reduction in surface FWF. A projected shallowing of the MOW is a likely scenario at the end of the 21st century, associated with a reduction in MOW density owing to warming under increased greenhouse gas emissions (Thorpe and Bigg,

2000). In our study, a negative signal in the RCP8.5 period relative to the historical period, below the maximum salinity changes (around 700 m) in the North Atlantic MOW outlet region, suggests the possibility of such an upward shift. Hence, another part of the subtropical North Atlantic salinity increase can very likely be connected to the high saline MOW salinity increase noticed in this depth.

The subsurface salinity changes were explored by investigating the mechanisms driving those changes. The concept behind understanding these mechanisms is that in a global warming scenario the salinity changes are a result of changes in surface forcings such as changes in heat flux, FWF and wind-stress. A combination of these three forcings can very likely explain the salinity response. However, identifying the impact of each of these processes with absolute effectiveness is challenging. Nevertheless, we first use the approach of Durack and Wijffels (2010) that decomposes the total salinity into heave and spice components, and followed by the approach of Bindoff and Mcdougall (1994) that decomposes the total salinity into pure warming, pure freshening and pure heave components. The heave and spice decomposition enables us to identify a part of the subsurface changes in salinity associated with changes in the isopycnal, i.e. isopycnal movements due to wind-stress or circulation changes and another part due to changes in the $\theta - S$ relationship, respectively. The pure processes identified by pure warming, pure freshening and pure heave could link this heave and spice related subsurface salinity contributions to changes in warming, surface FWF and wind-stress.

The results obtained from the heave and spice decomposition appeared to exhibit a large anti-correlation between them. However, we could deduce that spice changes very likely play a dominating role in the upper few 100 m of the Atlantic Ocean. This contribution corresponds well with the large SSS changes in the Atlantic Ocean that are closely correlated to the surface FWF changes. In contrast, the heave component appeared to have a dominating role in the subtropical Atlantic, typically at depths below the mixed layer. (Häkkinen et al., 2016) claimed that, on multi-decadal timescales, the heaving of isopycnals is very likely a result of the warming of the global ocean, although there is some contribution from the dynamic processes such as changes in gyre circulation. However, along with warming, changes in the Ekman downwelling suggesting an increase in the gyre strength prompted us to a possible connection of the heave-driven salinity changes in the subtropical North Atlantic to changes in the wind-stress. The Pacific and Indian oceans largely depicted a spice dominance in the subsurface subtropical gyres in the upper 500 m, which experienced a freshening. In the high-latitude ocean basins, the freshening heave component appears to dominate, although a salty spice component counterbalances most of it.

The heave and spice decomposition of the total salinity might not be an effective method to identify the contributions from surface flux changes or wind-related changes. The presence of a large warming signal in the RCP8.5 scenario complicates the dynamic

association of heave to wind-driven changes while both warming and freshwater changes can attribute to the heave component as well. Hence, this decomposition method creates large signals in heave and spiciness that are real and important but contribute little to the understanding of salinity changes, especially on depth levels.

As a major advancement of the study by Durack and Wijffels (2010), we were able to estimate and distinguish the impact of warming, freshwater changes, wind-stress and circulation changes by applying the approach of Bindoff and Mcdougall (1994). This approach provides the attribution of salinity changes on depth levels to the pure freshening and pure heave processes. This method shows that surface FWF changes play a significant role and often a dominant role in driving salinity changes in the tropical and subtropical global oceans. A large part of the subsurface freshening in the North Pacific and South Indian Oceans could be connected to the pure freshening process, due to the substantial freshening at the surface which we link to being largely FWF driven. A contrast in the results of the pure process approach compared to Durack and Wijffels (2010) is the warming-driven contribution. The pure warming associated spice changes appear to be same as the changes connected to the poleward migration of surface isopycnal outcrop, referred as migration-driven changes, although the magnitudes are different due to the difference in the methods used. If that applies, the pure warming-related spice changes, contributing to a freshening of the subtropical waters, would be mostly compensated by the heave component of pure warming. Consequently, this suggests that pure warming results in little or no real impact on the total salinity in the subsurface depth levels.

The pure process analysis reveals that the pure heave seem to have a significant impact on salinity changes of the Atlantic Ocean but not much in case of the Pacific and Indian Ocean basins. The pure heave is representative of wind-stress and circulation related changes, the latter includes the contribution from other surface forcings, in particular warming. Therefore, it is also important to consider the role AMOC could play in this scenario. The AMOC weakens in the RCP8.5 scenario, which is very likely a result of warming (Levang and Schmitt 2020). As a result of this weakening, the northward salt transport could be reduced. This is supported by a strong dipole like salinity structure in the subsurface of the North Atlantic during the RCP8.5 period. Hence, this circulation reduction could also play a role in the distribution of salinity, and the role played by the AMOC is also important to consider in pure heave-related contribution to salinity changes.

In a warming scenario, our analyses provide an overview of the mechanisms governing the surface and subsurface salinity changes in each ocean basin and the processes dominating them. However, the pure process analysis provides an underestimated solution of subsurface salinity changes, along with the fact that the analysis is shown on zonal mean average. Moreover, the maximum emission scenario of RCP8.5 introduces sig-

nificant changes in surface forcing components and associated feedbacks, all of which influences the salinity changes. For instance, the pure heave-driven salinity changes can come from circulation changes generated by warming or FWF and not just wind-stress. Therefore, another way to interpret these results efficiently would be to perform this analysis on individual surface forcing experiments to differentiate between the differences and to analyse the salinity impacts with fewer uncertainties. Such an analysis is performed in chapter 5 of the salinity study using the Flux Anomaly Forced Model Intercomparison Project (FAFMIP) using the high resolution model data of MPI-ESM.

Chapter 5

Sensitivity experiments to understand the salinity response to different surface forcings[1]

5.1 Introduction

The global ocean salinity changes are driven by surface fluxes such as the heat flux, wind stress and FWF. Any changes in these surface fluxes affect the distribution of surface and subsurface salinities. The previous chapter described various mechanisms to identify and distinguish salinity contributions from surface fluxes under the high emission scenario of the coupled model - MPI-ESM-MR. In a high emission RCP8.5 scenario, investigated in chapter 4, all the surface forcings act to change the salinity simultaneously. The resulting salinity changes can be a result of collective contributions or impact of the individual surface fluxes. Upon investigating the mechanisms of spice and heave using Bindoff and Mcdougall (1994) method (BM's method), we decomposed subsurface salinity changes into the three pure processes of pure warming (PW), pure freshening (PF) and pure heave (PH). The results of this analysis provided a good insight into the global salinity changes under a warming climate. The surface FWF changes, resulting from an intensification of the global water cycle, play a dominant role in subsurface salinity changes on depth levels of the subtropical and tropical ocean basins. While the ocean warming appears to have more impact in the high-latitudes, wind-stress changes tend to play a strong role in the Atlantic Ocean (refer section 4.4.3).

The surface flux changes impact different ocean basins in different degree. In this chapter, we take a step further to confirm and to understand the similarities and dissimilarities in salinity responses to individually forced surface fluxes, by using sen-

sitivity experiments developed for the Flux-Anomaly-Forced Model Intercomparison Project (FAFMIP).

FAFMIP sensitivity experiments, designed to be a part of CMIP6, were set to study the climate change in oceans in a CO_2 forced climate change scenario (Gregory et al., 2016), in particular, to understand the sea-level and ocean circulation changes. The experiments are designed in a way that the flux from a coupled model is perturbed by a prescribed flux (momentum, heat and freshwater) in separate simulations of coupled models. In the CMIP5 studies, projected salinity responses in a warming climate has shown to be less consistent, specifically for different water masses (Sallée et al., 2013). The FAFMIP project was motivated by such uncertainties in projections, such as the sea-level changes, in response to climate change in different AOGCMs.

The main idea of FAFMIP experiments is to understand the ocean response to the surface flux changes induced by a CO_2-forced climate change. The surface flux perturbations for the FAFMIP experiments were calculated from the 61-80 year time-mean of 1pctCO2 experiments of CMIP5, which is representative of an anthropogenic climate change. The application of these surface flux perturbations (Chapter 3, section 3.2.2) on a model's respective surface fluxes ensures to understand different responses to the same forcing, which allows these experiment results to be compared and studied. Therefore, the oceanic changes due to changes in surface fluxes of heat, momentum and freshwater are separated in FAFMIP, thereby offering a simplified analysis on the ocean response.

Analysis of the FAFMIP experiments carried out until now focused on the sea-level changes, changes in ocean circulations and ocean heat uptake (Gregory et al. 2016; Griffies et al. 2016; Todd et al. 2020). Similarly, using the FAFMIP experiments for salinity study will aid in distinguishing the salinity responses under individual surface forcing corresponding to a warming climate. The different surface flux forcings and the related feedbacks can affect the salinity response to different forcings and oceanic changes; therefore, create uncertainties in their contribution. For instance, in chapter 4, we determined that a large contribution of the salinity increase in the North Atlantic comes from the pure heave process. According to BM's method, the pure heave process signifies changes connected to wind-stress and circulation. But in the RCP8.5, the circulation changes could come from changes in both temperature and salinity associated with heat flux and FWF changes. Therefore, by using the individually perturbed FAFMIP experiments, we expect to eliminate such uncertainties and provide a better estimation of salinity changes connected to individual forcing components.

This chapter is divided into two sections. The first part consists of using the individually perturbed FAFMIP high-resolution sensitivity experiments to analyse the salinity response for individual surface forcings. This is done by first discussing the changes in individual surface forcings for each experiment and their coupling impact on other sur-

face forcings. Followed by examining the salinity changes in each experiment, relative to the control run, and analyse the mechanisms attributing to these changes. From this, we can determine how robust are the salinity contributions obtained from the pure processes on the high emission MPI-ESM-MR run.

As a result of coupling, when an experiment is perturbed with one surface forcing it still results in some changes in the other surface forcings that can influence their contribution. Since in a warmer climate, freshwater forcing contributes significantly to the changes in surface and subsurface salinity, a passive tracer experiment is performed to assist in isolating the feedbacks. Hence, in the second part of this chapter, we analyse the passive tracer experiment results. The passive tracer experiment details are provided in chapter 3, section 3.2.3. However, for a brief review, we impose the FAFMIP surface FWF perturbation on our passive tracer, initialised with the control salinity value. This FWF perturbation is imposed only on the passive tracer field. Therefore, we define this as 'passive' tracer as this tracer does not affect the ocean density or circulation and does not have any effect on surface fluxes. Hence, this provides us with a pre-industrial control run where no surface forcing is applied and oceanic response is not affected. As a result, the changes and transport of passive tracer can be considered as a result of imposed surface FWF alone and does not involve density changes or feedback changes in any other surface fluxes.

5.2 Experiments

The FAFMIP experiments used in this study are the faf-water, faf-stress and faf-heatNA50pct (refer chapter 3, section 3.2.2). The perturbations for FAFMIP experiments were calculated at the time when the CO_2 concentration reaches double its concentration in the control state, which is in 61-80 years, i.e. centred at around 70 years, of the 1pctCO2 experiments taken from 13 CMIP5 models (Gregory et al., 2016). The prescribed perturbations are provided at the beginning of the simulation of MPI-ESM-HR, referred to as FAFMIP-HR from here on, and the model was integrated for 70 years. Since the perturbations are provided from the beginning of the simulation, the experiments produce significant results within a short time. Subsequently, we take the last twenty years with maximum changes for the analysis above. The methods used are similar to those of the previous chapter. To perform the analysis, time average of the last 20 years of the FAFMIP-HR runs, 51-70 years, are taken from which the mean of control run is removed.

5.2.1 FAFMIP surface flux changes

We start by revisiting and providing an overview of the surface forcing perturbations and the associated changes in surface fluxes of faf-water, faf-stress, faf-heat-NA50pct and faf-heat. The surface flux perturbations (Fig. 5.1a,b,c) applied at the beginning of the FAFMIP experiments have large signals exceeding the natural climate variability signals in most parts of the ocean (Fig. 5.1d,e,f). Therefore, the responses in salinity should leave strong signatures of a warming scenario in the FAFMIP experiments.

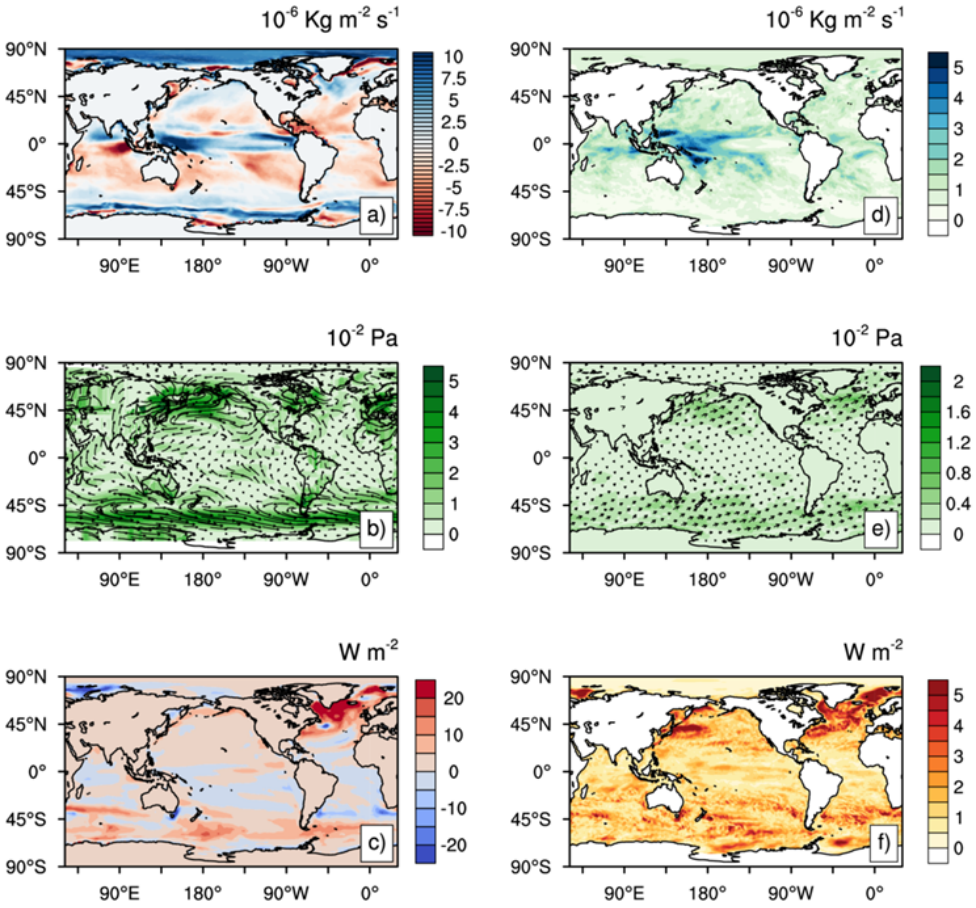

Figure 5.1: Prescribed surface flux perturbations (Left panel) and the standard deviations (20-year running mean) of the control run (Right panel) for (a, d) the FWF (10^{-6} kgm^{-2}s^{-1}), (b, e), the wind stress (10^{-2} Pa) and (c, f) the heat flux (Wm^{-2}).

The surface FWF perturbation is the sum of the precipitation, river run off, evaporation, water fluxes between the sea water and floating ice (Gregory et al. 2016). For faf-water, FWF perturbation or imposed flux, given by F_w (positive into the ocean), shows a positive FWF perturbation into the tropics and higher latitudes and negative FWF perturbation in the subtropical oceans (Fig. 5.1 a). For faf-stress, the predominant characteristic in the wind-stress perturbation is the strong westerlies in the southern

ocean. Similarly, the heat flux perturbation is strong in the southern ocean and also in the North Atlantic. The details on the application of the flux perturbation is provided by Gregory et al. (2016). We provided a brief overview on the heat flux perturbation in chapter 3, section 3.2.2.

The responses in other surface forcings, in each FAFMIP experiment, are a consequence of the coupled feedback. In a coupled ocean-atmospheric system, the changes in any surface forcings can result in oceanic response such as changes in the sea surface temperature (SST), ocean currents and salinity, which then feedback and result in surface forcing changes (Murtugudde and Busalacchi 1998; Yang et al. 1999; Dawe and Thompson 2006; Zhang and Busalacchi 2009).

faf-water

The total FWF changes, which is given by mean of last 20-years faf-water run minus control run, shows a positive change in the tropics and subpolar latitudes and negative in the subtropical latitudes (Fig. 5.2 a); however, much weaker in certain regions in comparison with the F_w. There are some changes in the wind-stress and heat flux in the faf-water run (Fig. 5.2b,c). Especially, the strengthening of the westerlies in the southern ocean. Though there may be several reasons, such as the changes in SST and associated atmospheric changes, to why this weakening is observed in certain regions, it is currently out of the scope of this research and hence not addressed here.

faf-stress

The wind stress perturbation (F_s) in the subtropics and higher latitudes, specifically in the Southern Ocean, is substantial. In general, there is a total weakening of the total wind stress in faf-stress run (Fig. 5.2e). The faf-stress run induces much less changes in FWF, especially in comparison with other runs. The FWF appears less sensitive to perturbed wind stress. However, faf-stress induces more changes in heat flux, especially over the Indian and the Atlantic basins. Therefore, with weak changes in wind-stress, it might be possible that the salinity response is more of a result of other oceanic changes due to changes in heat flux or related circulation, which is discussed in section 5.3.

faf-heat and faf-heat-NA50pct

Of all the tier-1 runs, faf-heat experiment induces substantial changes in all the surface forcings (Fig. 5.3 a, b). In faf-heat, the induced freshwater forcing and momentum changes are larger than in the individual forcings in faf-water and faf-stress and hence

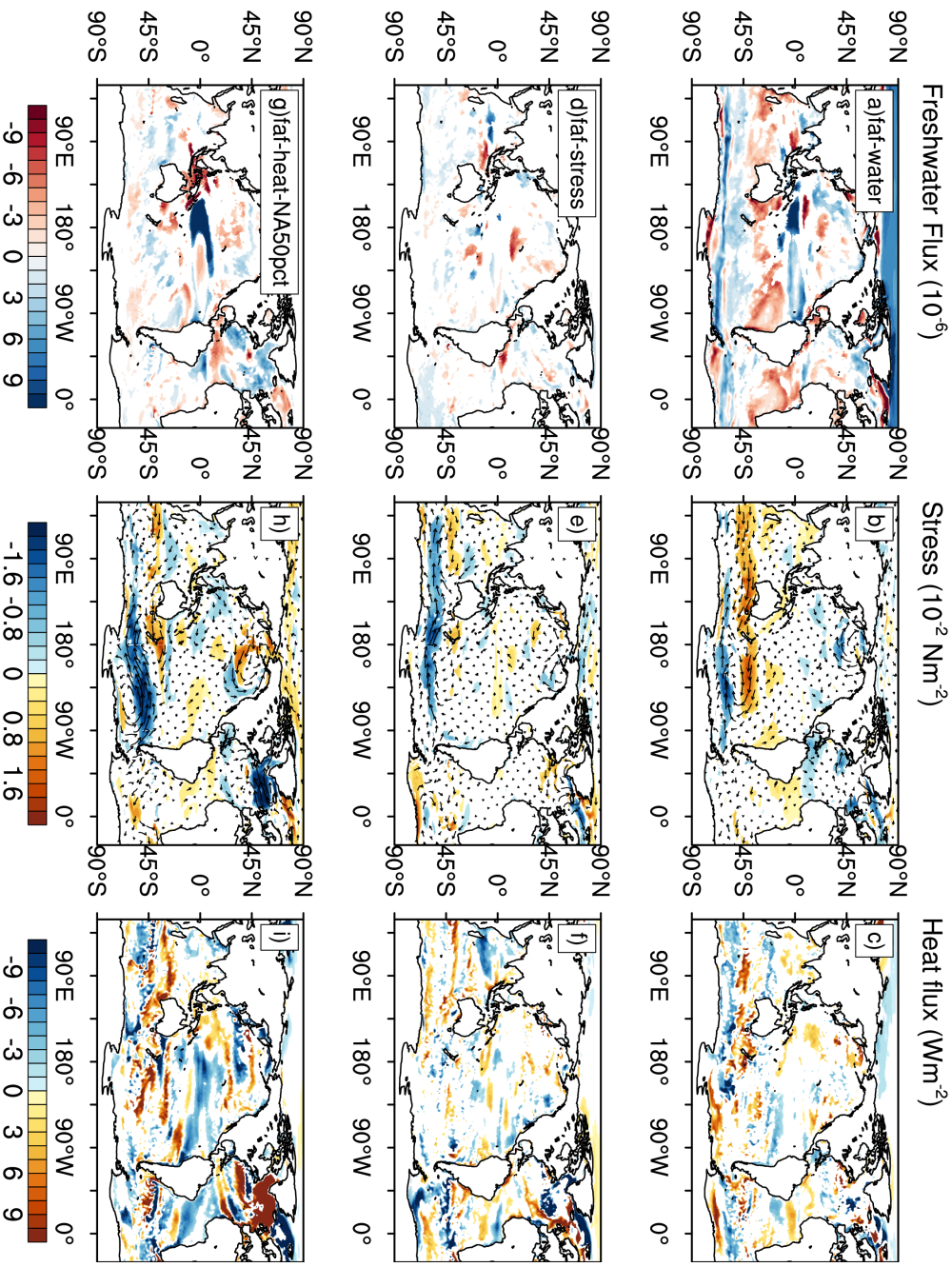

Figure 5.2: Changes in surface fluxes relative to the control run for the (a,b,c) faf-water, (d,e,f) faf-stress and (g,h,i) faf-heat-NA50pct runs. (a,d,g) is the FWF changes (10^{-6} kgm^{-2}s^{-1}), (b,e,h) is the wind-stress changes (10^{-2} Nm^{-2}) and (c,f,i) is the heat flux changes (Wm^{-2}). The regions with values less than 2 times the standard deviation of control run have been masked.

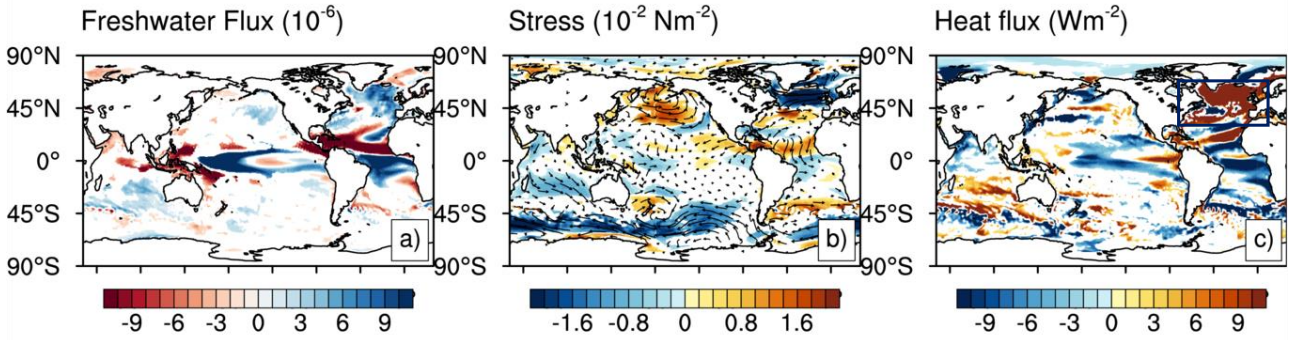

Figure 5.3: The faf-heat surface flux changes for (a) the FWF (10^{-6} kgm^{-2}s^{-1}), (b)the wind stress (10^{-2} Nm^{-2}) and (c)the heat flux (Wm^{-2}).

not very useful in determining individual impact on salinity response. In faf-heat-NA50pct, a 50 % reduction in the surface heat flux over the North Atlantic brought drastic changes in the response of surface forcings especially in the FWF of Atlantic and wind stress in the tropics and the Southern Ocean (Fig. 5.2 g, h). Therefore, in order to get a closer estimate of the salinity response to heat flux changes, we use faf-heat-NA50pct instead of faf-heat.

5.3 Salinity response

Figure 5.4 shows the surface salinity changes in each run relative to the control run. As intended from different surface perturbations, the SSS changes in the global ocean show significant differences in response to different surface flux perturbations. The faf-water run shows largely a decrease in the global SSS, except in the Atlantic Ocean where there is a slight increase in the SSS (Fig. 5.4 a). Meanwhile, faf-stress and faf-heat-NA50pct show either a SSS increase or decrease in various parts of the global ocean (Fig. 5.4b,c). Moreover, along with surface freshening, the global ocean shows a basin-wide cooling of the SST in faf-water, whereas the faf-stress and faf-heat-NA50pct runs show an increase (Fig. 5.5 a, b, c). A possible speculation of this SST cooling in faf-water could be due to a negative feedback caused by an amplification of the water cycle, which was identified in a study of Williams et al. (2007). According to that, a freshwater perturbation can cause an increase in surface salinity gradients. The ventilation of these gradients could lead to stronger density-compensating temperature gradients which can drive an increased downward isopycnal diffusive heat flux (Williams et al. 2007). The resulting net downward transfer of heat increases the temperature in the subsurface while causing

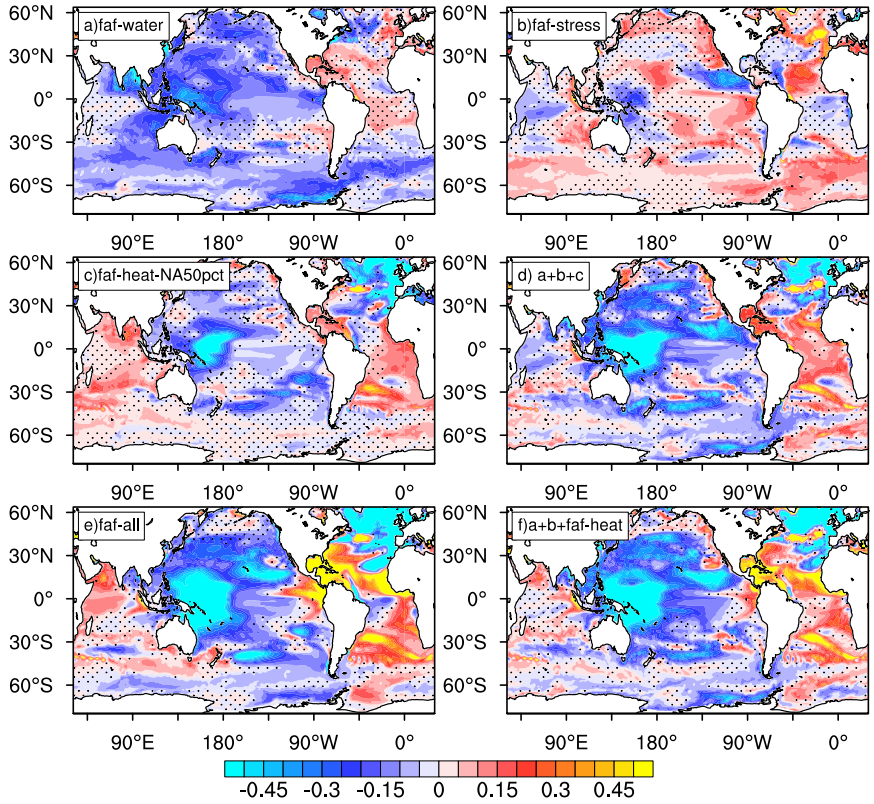

Figure 5.4: Changes in the SSS (psu) relative to control run for the (a) faf-water, (b) faf-stress (c) faf-heatNA50pct, (d) sum of faf-water, faf-stress and faf-heat-NA50pct (a+b+c), e) faf-all and (f) sum of faf-water,faf-stress and faf-heat (a+b+faf-heat). The regions with values less than 2 times the standard deviation of control run (20-year running mean) have been stippled.

a cooling at the surface. Such an increase in the subsurface temperature is evident in each ocean basin for faf-water (Fig. 5.5 d, e, f). It is a possibility that this mechanism is at work in faf-water. That being said, a reduction in SST might also be driving changes in the FWF and thereby influencing the SSS response indirectly. Such as a weakening of the SSS in the North Atlantic Ocean.

Considering that each perturbation causes changes in other surface forcings, especially for faf-heat-NA50pct, that could attribute to the SSS changes in those runs, the response in salinity in each run cannot be attributed perfectly to any one perturbation or surface forcing in FAFMIP experiments. Therefore, we focus on regions with major and similar changes projected across the RCP8.5 runs in CMIP5 models (Levang and Schmitt 2015) and MPI-ESM-MR in our previous chapter (chapter 4, fig.4.2 a) as a guide in an attempt to distinguish SSS changes dominated by each surface forcing.

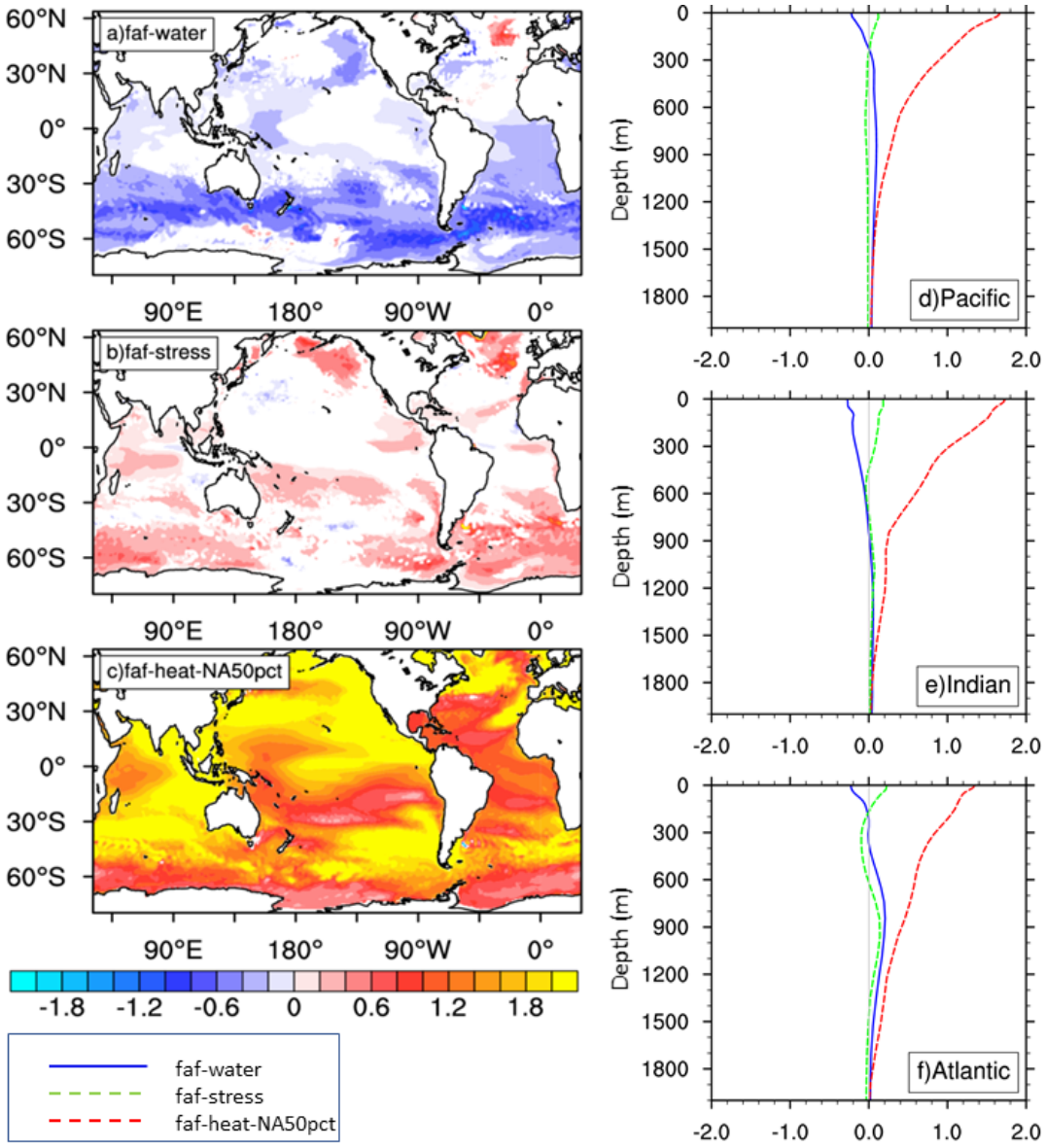

Figure 5.5: Changes in the SST (°C) relative to control run for (a) faf-water, (b) faf-stress (c) faf-heatNA50pct. The regions with values less than 2 times the standard deviation of control run (20-year running mean) have been stippled. d,e,f shows the vertical profile of the basin averaged potential temperatures (faf-water - blue, faf-stress-green, faf-heat-NA50pct - red) for the Pacific, Indian and Atlantic oceans, respectively.

In faf-water, the weak SSS increase in the Atlantic basin corresponds to a weak surface freshwater forcing changes in the basin. In the RCP8.5, SSS changes in the Atlantic Ocean was in a very good correspondence with the FWF changes (Chapter 4, fig. 4.1). However, a reduction in negative FWF changes in faf-water (Fig. 5.2 a), owing to an ocean-atmospheric feedback weakens the total FWF changes. As a result of this weakening of the FWF, the Atlantic SSS experiences only a weak increase in faf-water (Fig. 5.4 a). These surface changes are not much significant compared to the heat runs,

particularly in the South Atlantic.

A reduction in FWF intensification might not be the only reason attributed to a weak SSS increase in the Atlantic Ocean. In faf-heat and faf-heat-NA50pct, the induced changes in the freshwater forcing (Fig. 5.3a and Fig. 5.2g) are only slightly intense than faf-water (Fig. 5.2a) in the subpolar North Atlantic. However, they still result in substantial SSS changes (Fig. 5.4c,e). This increase in faf-heat-NA50pct SSS, despite a similar FWF change in faf-water, could be a result of changes in circulation due to warming (Fig. 5.5c), particularly changes in AMOC, which affects the transport of salt to higher latitudes (Levang and Schmitt 2020). Surface warming in heat perturbed runs, unlike in faf-water, could sustain and also further amplify the spatial pattern of SSS change by providing a stable upper ocean stratification (Zika et al. 2018).

For instance, we took a South Atlantic box (20°S-40°S, 55°W-5°W), which is a net evaporative region, has a consistent negative FWF throughout the 70-year experiment (Fig. 5.6). The time evolution of box area average shows that despite a similar time evolution of the changes in FWF for the faf-water and faf-heat-NA50pct runs, the SSS increase in faf-heat-NA50pct is substantial. Whereas, in faf-water, this region experiences little significant changes (Fig. 5.4a). A reduction in faf-water SSS may be connected to an increased mixing, which can be deduced from the increasing MLD (Fig. 5.6). The surface salinification due to a consistent negative FWF can destabilise the surface layers and thus drive more mixing. The wind-stress changes in these two runs are not substantially different to indicate their additional contribution to SSS increase in faf-heat-NA50pct. The surface warming in the faf-heat-NA50pct can maintain the upper ocean stratification, causing less mixing changes (Fig. 5.6). This could sustain the SSS anomalies formed at the surface due to a negative FWF, and without much decay SSS could amplify over the years.

The strong surface warming in faf-heat-NA50pct and associated SSS changes in the South Atlantic in comparison with faf-water SSS changes is suggestive of a larger role played by surface warming in defining the SSS changes in the subtropical Atlantic. However, this is not necessarily the same for all the basins. The increase in FWF along the ITCZ, especially in the western tropical Pacific corresponds to the decrease in SSS in the tropical Pacific, which is visible in both faf-water and faf-heat-NA50pct (Fig. 5.4a,c), implying these low salinities in the tropical Pacific could be largely due to an increased FWF. In faf-water, a freshening of the subtropical Pacific ocean and the eastern tropical Indian Ocean could be connected to an advection of the low saline surface waters from the tropical Pacific (Chapter 4, figure 4.6; Huang et al. 2005). Therefore, this almost basin-wide freshening of the Pacific suggests that oceanic freshening of the Pacific surface waters seems to be primarily driven by an increased freshwater input in the tropical Pacific, especially in the warm pool region.

Similarly, for the Indian Ocean, advection of these low pacific salinities via the ITF

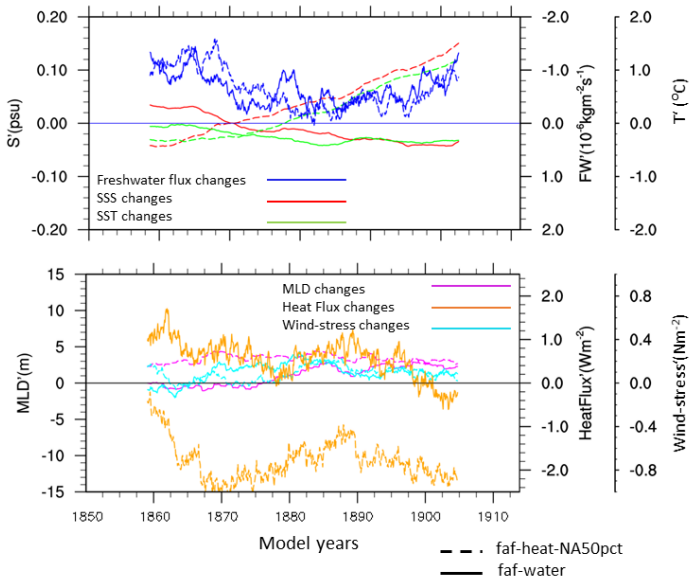

Figure 5.6: Time series of the South Atlantic region (20°S-40°S, 55°W-5°W) averaged SSS changes (S', red lines, psu), FWF changes (FW', blue lines, (10^{-6} kg m^{-2} s^{-1}) and temperature changes (T', green lines, °C) and (below) for the MLD changes (magenta, meter), heat flux changes (orange, $Wm10^{-2}$) and magnitude of wind-stress changes (cyan, 10^{-2} $Nm10^{-2}$). Solid lines denote faf-water and dashed lines denote faf-heat-NA50pct. The values are smoothed at a 20-year running time mean. Prime (') represents changes.

could result in the reduction of eastern tropical Indian Ocean SSS for faf-water. The Pacific freshening in freshwater imposed faf-water is in good agreement to our understanding of near-surface salinity changes in the RCP8.5 scenario from the previous chapter (chapter 4). In that chapter, we associated the changes in freshwater input to be the major driver of near-surface salinity changes in the eastern tropical Indian and subtropical Pacific oceans. In addition, despite no surface warming in the faf-water run, this large freshening in the Pacific Ocean reaffirms the dominant role of surface FWF changes in the Pacific SSS response. This could be connected to the stabilising effect of surface freshening that drives less mixing and hence sustain the freshwater for longer periods.

The SSS changes in faf-stress are far less significant than in faf-water and faf-heat-NA50pct (Fig. 5.4b). From faf-stress run, surface wind stress perturbation seems to have no considerable changes in the wind stress during the last 20 years. In addition, there is little or no induced surface freshwater forcing, but there are considerable changes in the heat flux (Fig. 5.2f). The substantial SSS changes in the north-eastern tropical Pacific and tropical North Atlantic oceans appear to contribute to the faf-all SSS signal (Fig. 5.4 e). However, in general, the SSS response in faf-stress seems to have

a dipole like pattern in most of the regions, with strong positive and negative changes both longitudinally and latitudinally. There appears no close direct relation with the surface FWF changes in most regions with substantial SSS changes (Fig. 5.2d and Fig. 5.4b), such as the north-eastern tropical Pacific. It is likely that the SSS changes are from the advection changes introduced by heat flux and freshwater changes or even from prolonged changes in the wind-stress. Despite the weak increase in FWF in the Southern Ocean, it is unclear why there is an increase in salinity in the Southern Ocean in faf-stress.

From a comparison of faf-all (Fig. 5.4e) and a sum of faf-water, faf-stress and faf-heat runs (Fig. 5.4f), we notice that the SSS difference between them is small and that the total SSS changes can be expressed as a sum of individual perturbations. However, each perturbation runs have induced changes in other surface forcings, particularly for faf-heat-NA50pct, that could attribute to the SSS changes in those runs. This may essentially get added to the faf-all run and makes it difficult to conclude whether the forcings act linear. Keeping that in mind, we add faf-water, faf-stress and faf-heat-NA50pct and is shown in Fig. 5.4d. Adding the SSS changes in each run show a spatial pattern reasonably similar to that of the spatial pattern of projected SSS changes in CMIP5 RCP8.5 runs, including MPI-ESM-MR (chapter 5.15, Fig. 4.2a; Levang and Schmitt 2015) with differences in some regions such as the western subtropical North Atlantic and in the south-western subtropical Pacific Oceans (Fig. 5.4d).

To compare the SSS amplification between the experiments, the global SSS pattern amplification (PA) is calculated. The PA is given by the linear regression of the global zonal SSS change against the mean climatological anomaly (Durack et al. 2012). On the total SSS signal in Fig. 5.4d, the global ocean experiences a PA of 3.5 % with a correlation (R) of .35, which is quite a weak correlation. This suggests that the global SSS changes do not closely resemble the mean climatological SSS. For the individual perturbations, the faf-water run shows a PA of ∼2 % (R=0.46) and a FWF PA of ∼6 % (R=0.73). On the other hand, the faf-heat-NA50pct run has a SSS PA of ∼5.5 % (R=0.53) with a PA of ∼3 % (R=0.49) for the FWF. The faf-stress run shows a negative PA of ∼3 % (R=0.65). This SSS PA for faf-heat-NA50pct and faf-water is interesting because despite a weaker FWF amplification in the heat run, it shows a much stronger SSS amplification with a stronger pattern correlation than in faf-water. This difference in SSS PA in faf-water and faf-heat-NA50pct, to a large extent, may be connected to surface warming in faf-heat-NA50pct. The faf-heat-NA50pct run has a global surface warming of 1.6°C, whereas the faf-water run has a global average of -0.21°C. Here, it is challenging to deconstruct the warming and freshwater contributions. However, a negative SST change and a weak SSS amplification despite a strong FWF amplification in faf-water suggests that the surface FWF intensification alone cannot produce a large SSS amplification in the global ocean.

The surface FWF and SSS changes in faf-water and faf-heat-NA50pct provide a clearer picture of the dominant role of surface FWF changes on SSS changes, especially in the tropical and subtropical Pacific and Indian oceans. In the subtropical and tropical Atlantic Ocean, faf-water related freshwater changes alone cannot sufficiently explain the negative SSS changes. Keeping in mind that the induced surface forcing changes in each experiment does have some influence on SSS response, the faf-water SSS changes together with faf-heat-NA50pct could closely represent for a similar spatial pattern of SSS changes projected in an RCP8.5 run for the Atlantic Ocean. That is, the Atlantic Ocean SSS response for global warming is better simulated when both faf-water and faf-heat-NA50pct runs are combined. This is indicative of surface warming having a larger role in the Atlantic SSS amplification than in the Pacific and Indian Oceans. The faf-heat run induces large changes in freshwater and wind-stress forcings (Fig. 5.3). The faf-heatNA50pct run also induces large changes, however, much less in comparison to faf-heat. Using faf-heat to study salinity response to heat flux changes are more challenging than in faf-heatNA50pct and hence not used further.

5.3.1 Subsurface changes

Surface salinity changes in the FAFMIP experiments show distinct responses, which influence the subsurface changes. In all 3 experiments (faf-water, faf-stress and faf-heatNA50pct), substantial subsurface changes are largely confined to the upper 500-600 m except for the Atlantic Ocean (Fig. 5.7).

In faf-water, with a significant freshening of the surface layers, the Pacific and Indian Oceans show a reduction in their subsurface salinities. In the southern hemisphere, a reduction in the salinities of intermediate water masses could be connected to a reduced SSS in their source regions (between 55°S-65°S)(Wong et al. 1999). This SSS reduction coincides with a significant increase in FWF in the Southern Ocean in faf-water (Fig.5.4 a). A strong freshening all over the surface at latitudes south of 30 °S indicate some other processes in play. A strengthening of the southern hemisphere westerlies in the faf-water run could mean that there is an increased northward Ekman transport from the Antarctic region towards the subtropical latitudes. As a result an additional change in SSS could be coming from the advection of these fresher waters into the subtropical oceans. It is more apparent from the significant fresher salinities in the South Indian Ocean which coincides with the strong westerlies induced there (Fig. 5.2b). Therefore, at latitudes south of 30 °S, a part of the subsurface salinity decrease in the southern oceans can be linked directly to the local surface FWF changes, while the other part of it might be a result of transport changes.

In the subtropical North Atlantic, faf-water shows positive salinity changes between the latitudes 20 °N-50 °N. This is extended down to a depth of 1100 m, with a maximum

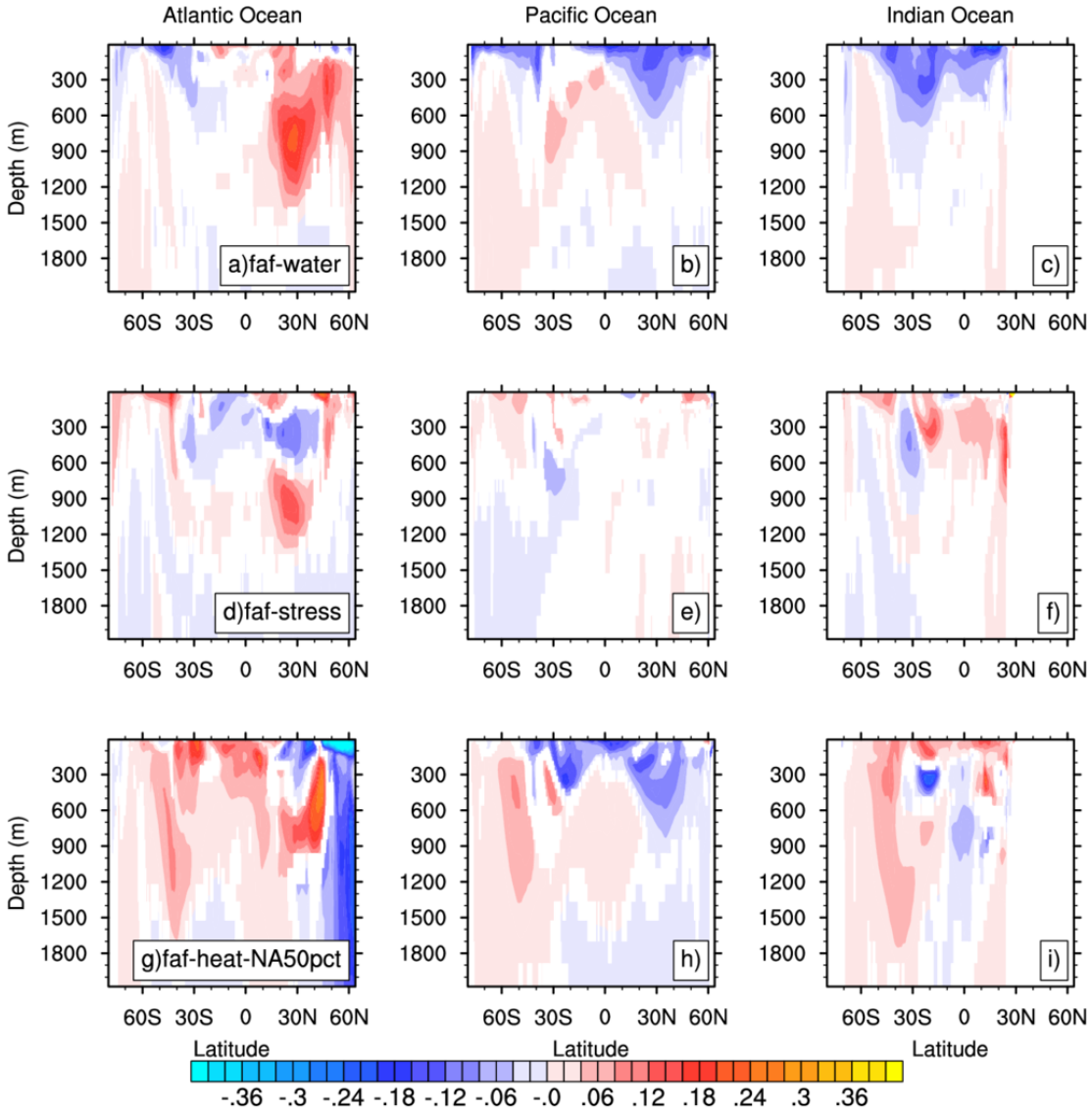

Figure 5.7: Zonal average of changes in subsurface salinity (psu) with respect to control run (a, b, c) for faf-water, (d, e, f) for faf-stress and (g, h, i) for faf-heat-NA50pct runs of the Atlantic, Pacific and Indian oceans. The regions with values less than 2 times the standard deviation of control run have been masked.

zonal positive salinity change at around 800 m. The increase in subsurface salinity at around 45 °N and 300 m, could be connected to an increase in salinity noticed in the eastern North Atlantic (Fig. 5.4a). Whereas the salinity increase below that, few latitudes south, appears to be much significant than the SSS changes simulated in this region. A similar positive signal, focused between 800-1200 m centered around 30 °N, is visible in faf-stress, denoting a possible signature of MOW changes. On a closer inspection of the depth-latitudinal profile of the MOW outlet region of the North Atlantic shows an increase in MOW salinity (not shown). Where we also notice that some part of the signal appears to come from the north-east North Atlantic with high

SSS (Fig. 5.4b). A subduction of this signal along the isopycnals and their subsequent southward movement would result in the observed positive signal at 30 °N. We describe these details in the following section on mechanisms.

Similar to the SSS changes, the subsurface changes in the Pacific and Indian Oceans of faf-stress are much weaker than in faf-water and faf-heat-NA50pct. Hence, in a realistic scenario where all the surface forcings come into play the wind stress related changes are likely to be overcompensated or weakly adds up.

Mechanisms

In scenarios of both warming (Fig. 5.5f; faf-heat-NA50pct) and cooling (Fig. 5.5f; faf-water) of the basin surface temperatures, the subtropical subsurface salinities in the North Atlantic follow a positive change pattern similar to the projected RCP8.5 scenario (Chapter 4, fig. 4.7e). This increase points to a dominating role played by surface FWF in driving the subsurface salinity response in the Atlantic Ocean. In contrast to the similarity mentioned above, between faf-water and the RCP8.5, faf-water shows a northward intergyre transport of the saline subtropical waters at the intermediate depths (below 300 m) (Fig. 5.7c). This increase can be connected to a slight increase in the AMOC (Fig. 5.8a). A strengthening of AMOC transports more salt into the high-latitudes.

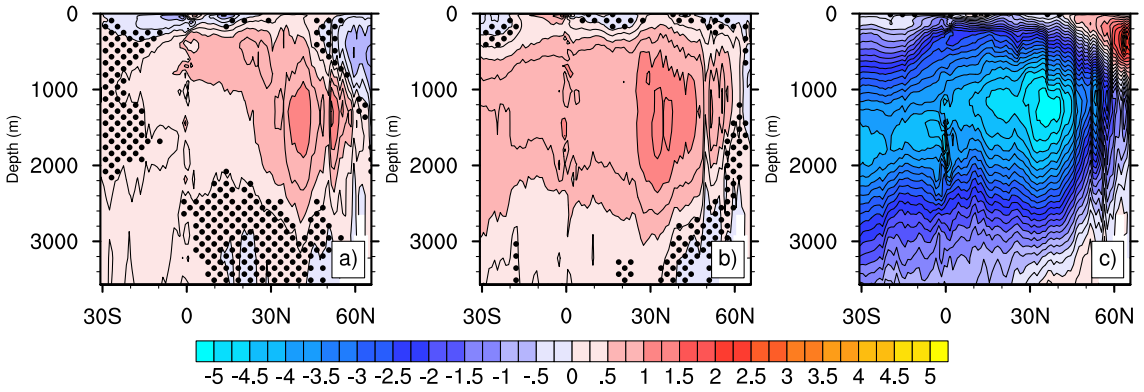

Figure 5.8: Meridional circulation changes (Sv) in the Atlantic Ocean in (a) faf-water, (b) faf-stress and (c) faf-heat-NA50pct runs relative to the control run. The values below 2 times standard deviation of the control run have been stippled.

As a result of possible contributions from induced changes in each FAFMIP run, we perform a decomposition of the subsurface salinity changes into heave and spice using BM's method. Given the induced heat flux and wind-stress are globally weak in faf-water compared to faf-heat-NA50pct, we expect to get a better decomposition signal from faf-water that is not masked by a warming signal. Therefore, details of the above introduced subsurface changes are further described in following section with respective to spice and heave related contributions.

In faf-water, the dominant part of the subsurface changes comes from the spice changes (Fig. 5.9a,b,c). The heave-related salinity changes for faf-water is mostly negligible, particularly in the upper 500 m (Fig. 5.10a,b,c). This indicates that the FWF pertur-

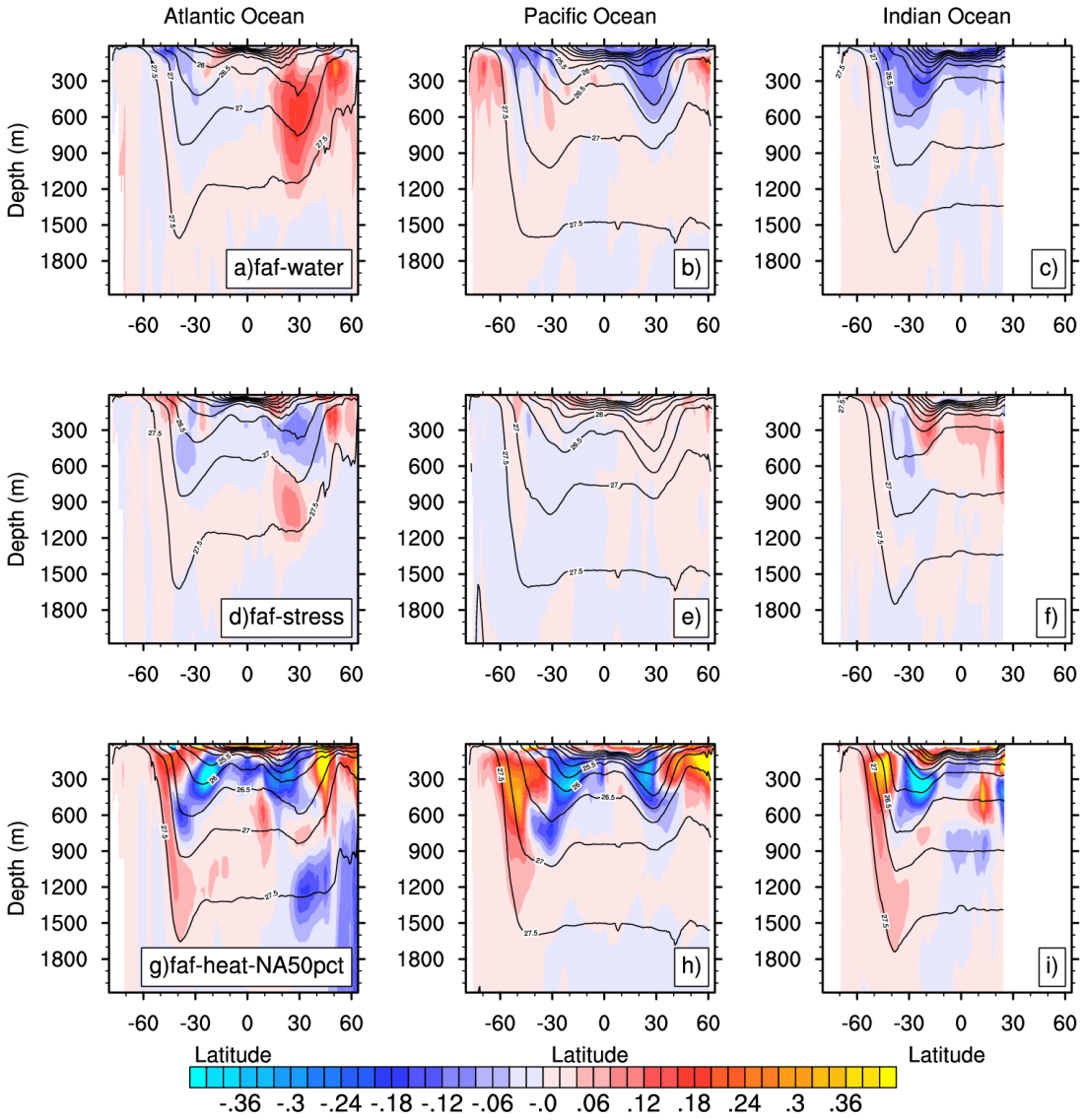

Figure 5.9: Zonal average of changes in subsurface salinity (psu) along isopycnals relative to the control run (a, b, c) for faf-water, (d, e, f) for faf-stress and (g, h, i) for faf-heat-NA50pct runs of the Atlantic, Pacific and Indian oceans. The salinity changes on density are mapped back to depth levels.

bation do not drive significant shifts in isopycnal surfaces or induce large circulation changes. In the North Atlantic, the increase in salinity due to spice contribution largely comes from the PF process (Fig. 5.11). In the absence of significant temperature changes, it is evident that a substantial increase in North Atlantic salinity under an enhanced FWF is driven by surface FWF changes. While there is a possibility that under a warming climate surface warming supports a SSS amplification. How-

ever, these results strongly suggests the role of FWF as the critical factor driving the North Atlantic salinity increase. A small PH salinity increase appears to contribute to the subsurface salinity increase in the 500-1000 m (Fig.5.12). However, the PH contribution is much weak in comparison with the large changes coming from PF.

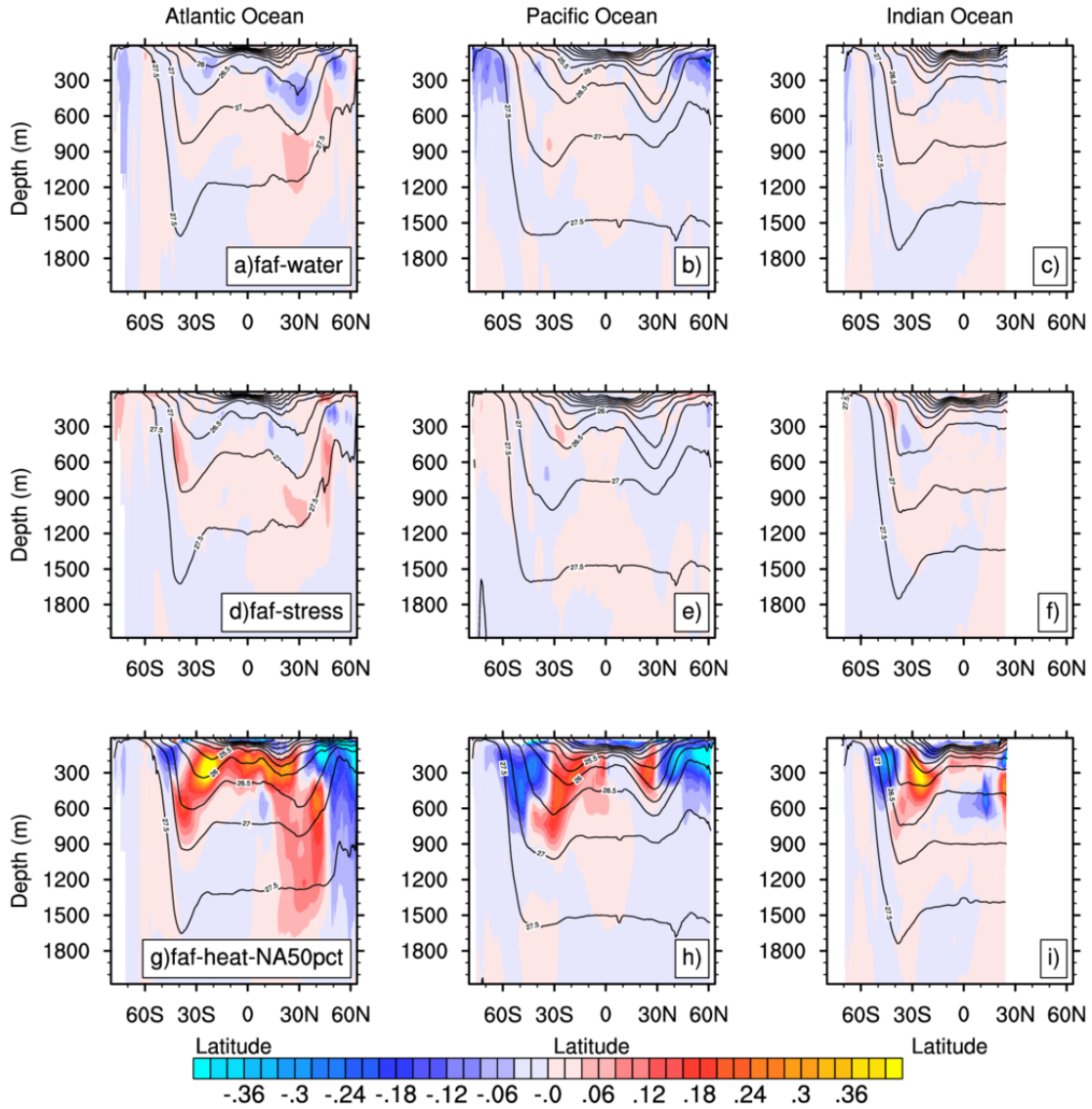

Figure 5.10: Zonal average of heave changes in subsurface salinity (psu) on depth levels relative to the control run (a, b, c) for faf-water, (d, e, f) for faf-stress and (g, h, i) for faf-heat-NA50pct runs of the Atlantic, Pacific and Indian oceans.

The Pacific and Indian oceans have significant freshening in the upper 500 m connected to spiciness changes (Fig. 5.9a,b,c). This spice contribution is dominated by the PF process (Fig. 5.11). This PF contribution can be linked to a reduced SSS in faf-water (Fig. 5.4a), which was connected to an increased freshwater input in the tropical and ITCZ regions of the Pacific (Huang et al. 2005). The above results suggest that an enhanced surface FWF is the dominant driver of subsurface freshening, particularly

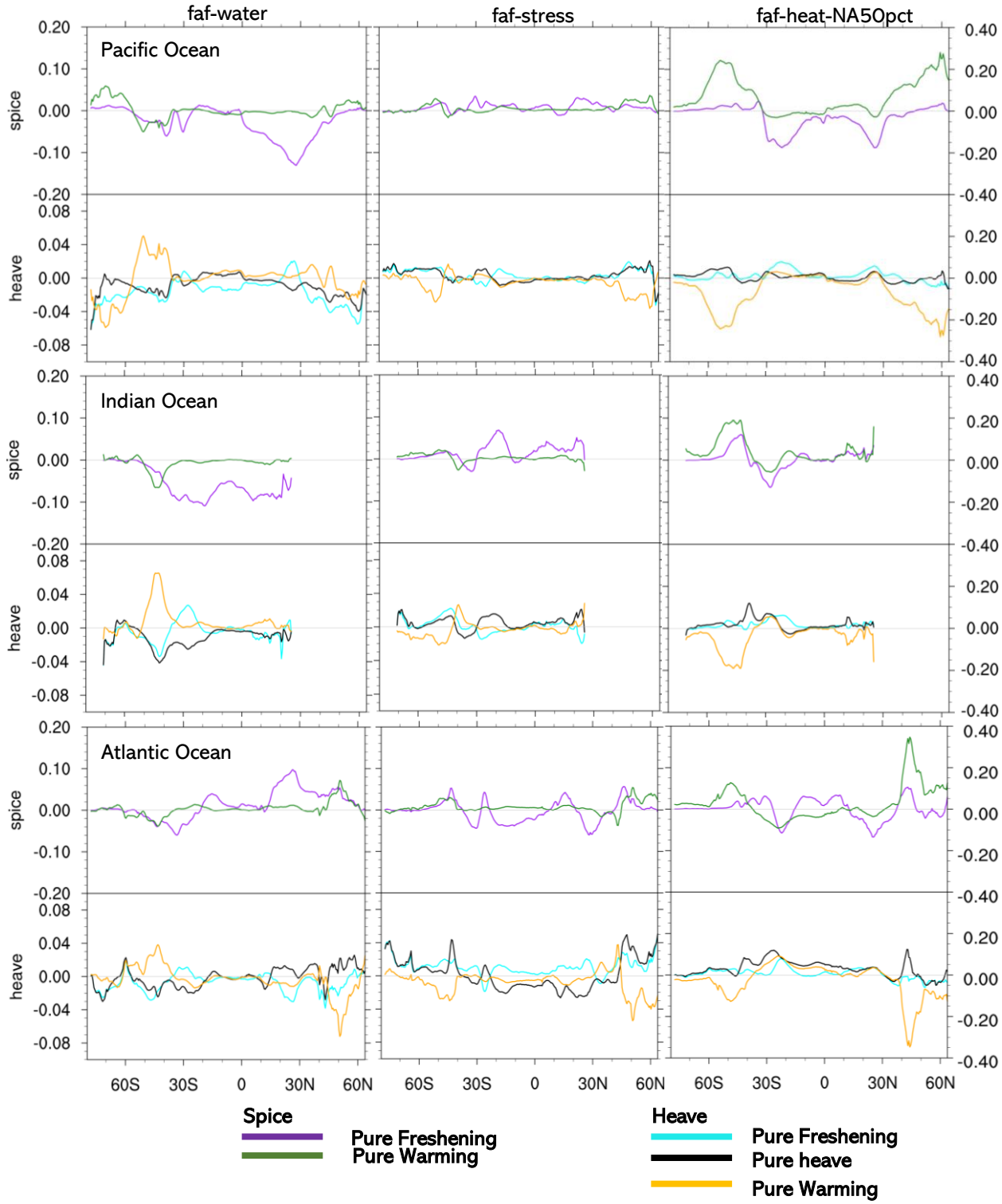

Figure 5.11: Longitude-depth (0-500 m) average of pure freshening, pure warming and pure heave salinity components expressed as components of spice and heave salinity contributions. Note the scale change in case of faf-heatNA50pct and heave axis of faf-water and faf-stress.

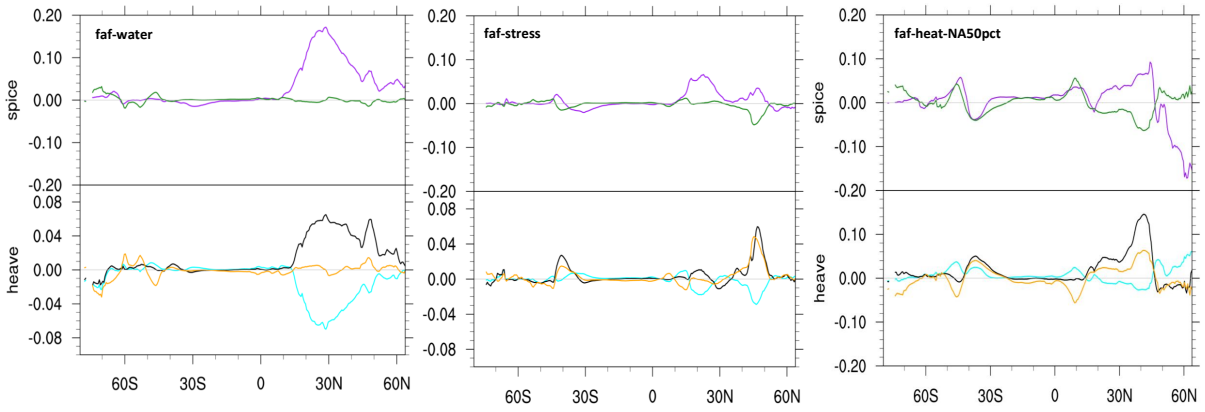

Figure 5.12: Similar to 5.11. Longitude-depth average of pure freshening, pure warming and pure heave expressed as components of spice and heave contributions for 500-1000 m of the Atlantic Ocean.

in the subtropical North Pacific. These results are consistent with our findings from the RCP8.5 projections analysed in chapter 4 (Fig. 4.17). It is interesting to note that there are no strong compensating signals observed in a faf-water run (Fig. 5.9a,b,c and Fig. 5.10a,b,c). However, we notice a strong compensation of spice and heave components of PW in all faf-runs (Fig. 5.11). The temperature changes appears to have a large compensating effect, especially in the high-latitudes.

Comparing with the faf-heat-NA50pct run, often spice and heave are showing large anti-correlation (Fig. 5.9g,h,i and Fig. 5.10g,h,i). This is similar to the RCP8.5 scenario discussed in chapter 4 (Fig. 4.11) where warming is prominent. This supports that warming largely creates a compensating masking signal on heave and spice which mostly do not contribute substantially to the total salinity signal on depth levels. Similarly, large changes in gyre circulation (Fig. 5.13c), especially in the Atlantic Ocean, appear to be leaving a similar signal on heave-related salinity changes. This structure is evident from the salinity slope, similar to faf-stress, seen in the subtropical gyres of the heave component of the North Atlantic (Fig. 5.10g).

In general, this confirms our results on the RCP8.5 salinity study where we had shown that surface FWF plays the dominant role in subsurface salinity changes in the upper 500 m of the subtropical ocean basins (Chapter 4; Fig. 4.17).

In faf-stress, the subsurface salinity changes dominated by spice signal suggest that the changes are mostly driven by the $\theta - S$ related changes rather than the wind-stress changes itself (Fig. 5.9d,e,f). The salinity increase in the spice signal of subtropical North Atlantic (Fig. 5.9e) dominate over the heave changes. The heave-driven changes are weak (Fig. 5.10e). As stated earlier, this region experiences an increase in MOW

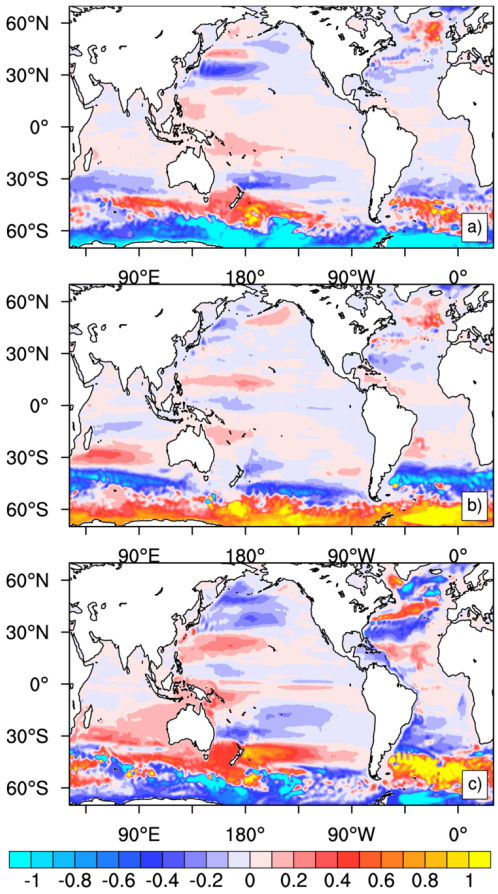

Figure 5.13: Changes in the barotropic streamfuction in (a) faf-water, (b) faf-stress and (c) faf-heat-NA50pct relative to the control run (10^{-10}kgs^{-1}).

salinity and the spice changes observed here can be connected to this MOW salinity increase. This coincides with the substantial increase observed in SSS of the Mediterranean Sea in faf-stress (Fig. 5.4 b). It appears challenging to attribute any faf-stress related salinity changes to wind-driven changes directly mostly due to the weak wind stress changes in faf-stress. In addition, the signals are too weak. However, the PH related salinity increase in the subtropical South and North Atlantic is largely heave-driven (Fig. 5.10d). These changes coincide with the spin-up of subtropical gyre in the South Atlantic and a slight increase in the Gulfstream-North Atlantic region in the North Atlantic (Fig. 5.13b). This leaves a signature similar to the PH contribution noted in the RCP8.5 scenario (chapter 4, Fig. 4.18b).

In the high latitudes, specifically of the southern hemisphere, FAFMIP experiments show large induced changes in the surface forcings (Fig. 5.2) in comparison to other regions. Therefore, large variations and contributions comes from each pure processes and it appears that PW related spice and heave contributions largely anti-correlate and PF and PF contributions also vary largely in these high latitudes, which makes it irrelevant to describe their effective contributions in FAFMIP experiments.

5.4 Tracer analysis

A surface flux perturbation can contribute to changes in the ocean circulation pattern and strength (Mikolajewicz and Voss, 2000). In faf-water, one way to understand and separate the oceanic response in salinity due to advective and ocean-atmospheric feedback is by introducing a passive salinity tracer. Some studies have shown the influence of surface FWF perturbations in weakening the meridional heat transport and increasing the heat content change in the Atlantic and also increasing the sea level (Bouttes and Gregory 2014; Sévellec et al. 2017). Our passive tracer, initialised with active control salinity, is perturbed with the prescribed FWF (F_w) from the beginning of the run similar to that of a faf-water run except that F_w will not affect the circulation and thermal changes in the ocean which might result from the oceanic feedbacks.

5.4.1 Evolution of the tracer

The surface pattern of the passive tracer is established within 20-30 years of the simulation after which the changes build up much slowly over the period of 150 years (Fig. 5.14). Even at 150-year, the passive tracer concentration has experienced a slight change from 20-year change indicating the surface has not reached complete saturation during our experiment period. The consistency in tracer pattern shown in 20^{th} and 150^{th} years, means the ocean reached a quasi-equilibrium state where the changes in salinity introduced by the imposed surface FWF and the near-surface ocean circulation related advection and mixing reaches a balance at certain period. The perturbed flux does not appear to affect the salinity response significantly afterward this roughly 20-30 year run. In certain regions, such as the South Indian and tropical and South Atlantic Oceans, there is a decrease in tracer values towards 150^{th} year. The tracer experiment induces no changes in ocean currents or any atmospheric feedbacks. Therefore, the reduction in passive tracer in the regions mentioned above for the last year could be a result of natural variabilities in transport or mixing. Apart from that, the tracer shows consistent pattern adherence depicts that fresh regions get fresher and salty regions to get saltier.

5.4.2 Comparison of faf-water and tracer experiment salinity responses

If there were no changes in any other surface forcings and ocean response, then the faf-water SSS changes should look similar to the tracer changes for the time average of 51-70 years of the experiment run. However, that is not the case and Fig. 5.15c shows the differences in SSS and tracer. Although the surface FWF perturbation introduced

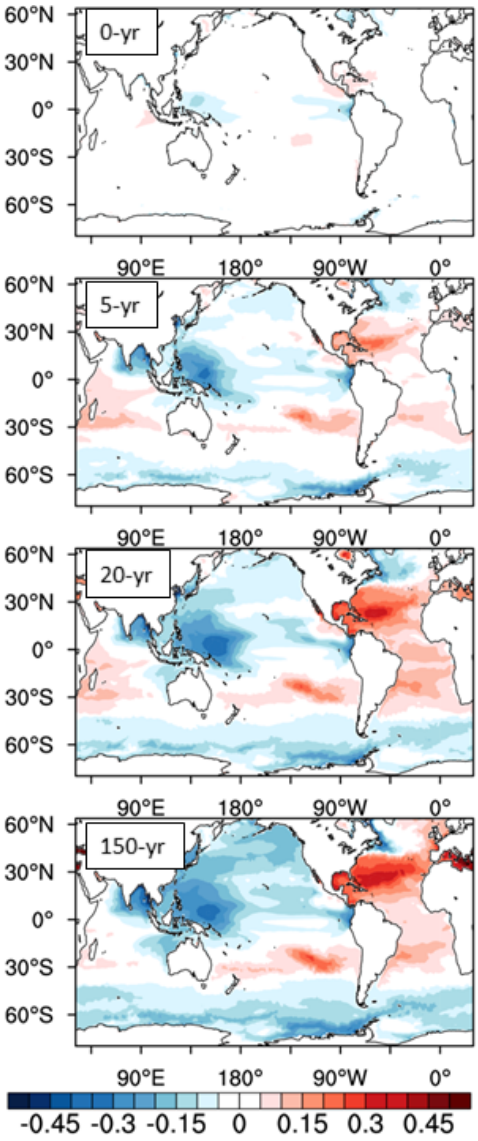

Figure 5.14: Surface evolution of passive tracer at 0, 5, 20, 150 years of the faf-passivesalt experiment. yr denotes year.

is same in these two experiments, the tracer and faf-water salinity changes and their differences (Fig. 5.15 c) is indicative of a substantial role of other processes in faf-water.

The difference is substantial, especially in the Atlantic, Indian and subtropical South Pacific Oceans, and of the same order of magnitude as the SSS changes. In the North Atlantic Ocean, a part of this difference can be attributed to the negative FWF feedback in faf-water, which weakens the negative FWF and reduces the SSS (Fig. 5.2 a). In passive tracer, the freshening of eastern tropical Indian Ocean is evident. As stated several times, this freshening can be connected to freshening of western Pacific source region (Valsala et al. 2011). However in faf-water, a positive FWF (Fig. 5.2 a) along with the advection of the fresher western Pacific anomalies appears to be driving an increased freshening of SSS in faf-water.

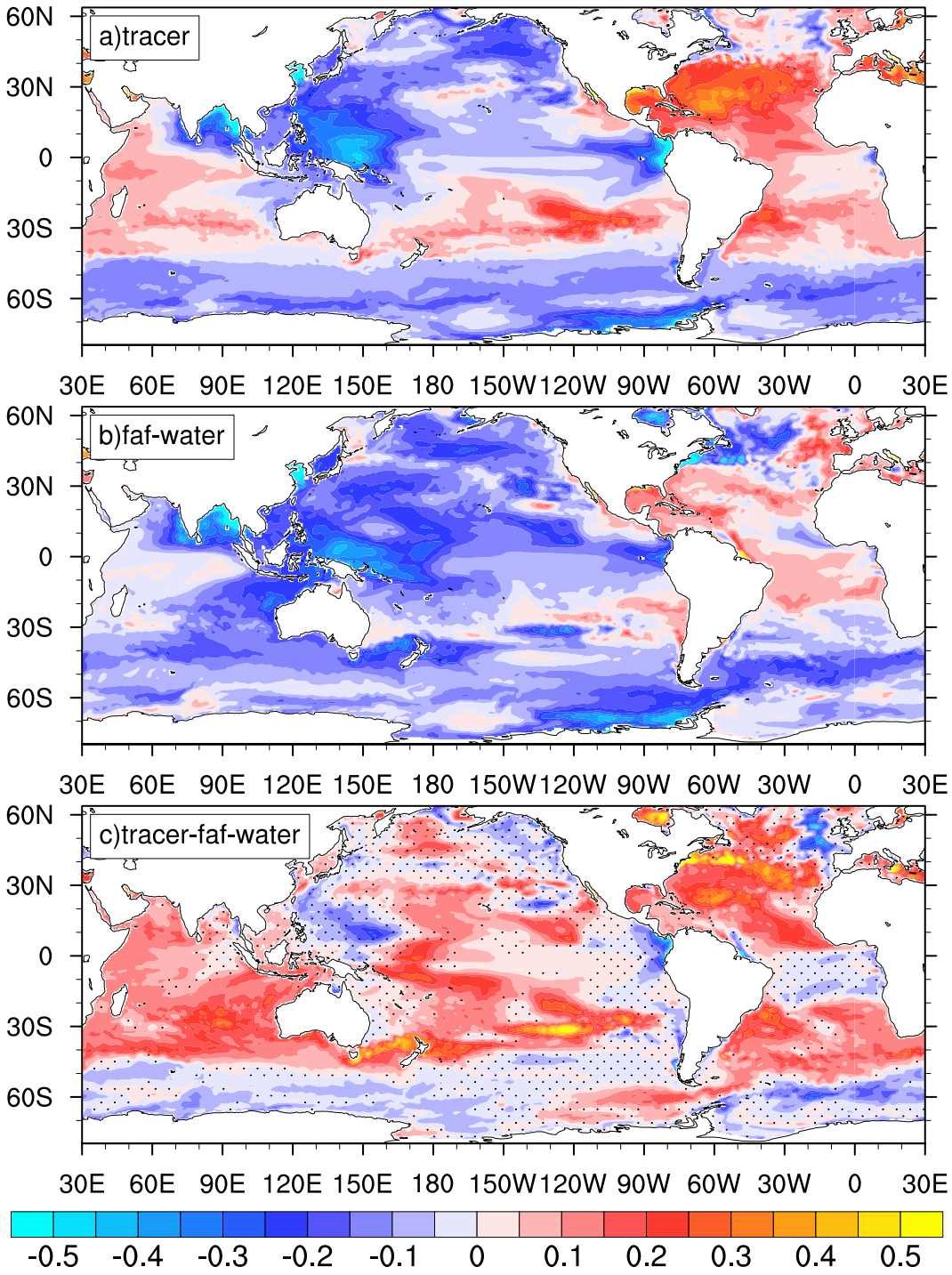

Figure 5.15: SSS changes for (a) tracer run (total tracer field (S_T) minus control run), (b) for faf-water run and (c) tracer minus faf-water for the global ocean. The values below 2 times standard deviation of the control run have been stippled for (c).

An increased FWF in the global ocean of faf-water experiment (Fig. 5.2 a) must be changing the stability of the upper ocean. Regions with increased freshwater input will freshen. As a result, the fresher surface waters stabilise the surface ocean and reduce vertical mixing. In effect, the surface salinity reduction is sustained for a longer time. On the other hand, net evaporation regions has increased salinities at surface, which destabilises the surface layer. By enabling more mixing of the saline waters, the the surface salinity reduces. This simple mechanism seems to be at work in the subtropical regions of faf-water.

In addition, a strengthening of the southern ocean westerlies in the faf-water run could also bring fresher waters from the Antarctic continent towards the subtropical latitudes (Fig. 5.2 b). The negative sign in Fig. 5.15c is indicative of a decrease in fresh water in the southern latitudes of faf-water. Hence, a large Ekman transport of freshwater from the high-latitude oceans towards subtropics cause an increase in salinity south of the westerly domain and a decrease in salinity north of it.

Propagation through subsurface ocean

The upper 500 m tracer changes for the 51-70$^{\text{th}}$ year average closely reflect the surface changes related to freshwater forcing (Fig. 5.16). As the passive tracer starts propagating below the MLD to deeper layers within a few decades of the experiment run, it is worth addressing the temporal tracer evolution in the subsurface of each ocean basin to distinguish the time and magnitude of changes occurring in faf-water.

In the initial decade, the subtropical salinities are seen to be subducted and slowly propagating equatorward (Fig. 5.17). The Atlantic basin exhibit largest changes of all the ocean basins, followed by the Pacific and Indian oceans. The higher salinities still remain in the first couple 100 m of the Atlantic basin during the few couple of decades. By approximately 20 years, the global surface tracer values has almost reached a balance state where no significant changes happen over the rest of the run (Fig. 5.14). In that same time, we already notice subsurface changes of the same order of surface magnitude at depths of 500 m (Fig. 5.17). In the faf-passivesalt experiment, a large surface FWF perturbation is switched on from the start of the run. This might be influencing the subsurface changes sooner than in a realistic scenario depending on the rate of intensification of the water cycle.

In the North Atlantic, the tracer evolution and propagation shows a part of the surface salinity increase in the subtropical North Atlantic being carried northward and another part carried equatorward in the first 40 years. Further, a third part continues to sink to form North Atlantic Deep Water (NADW) and reaches a depth of 3000 m after which they start propagating southward eventually becoming lighter and upwelling in the high-latitudes of the southern hemisphere (Fig. 5.17). A similar formation of fresher

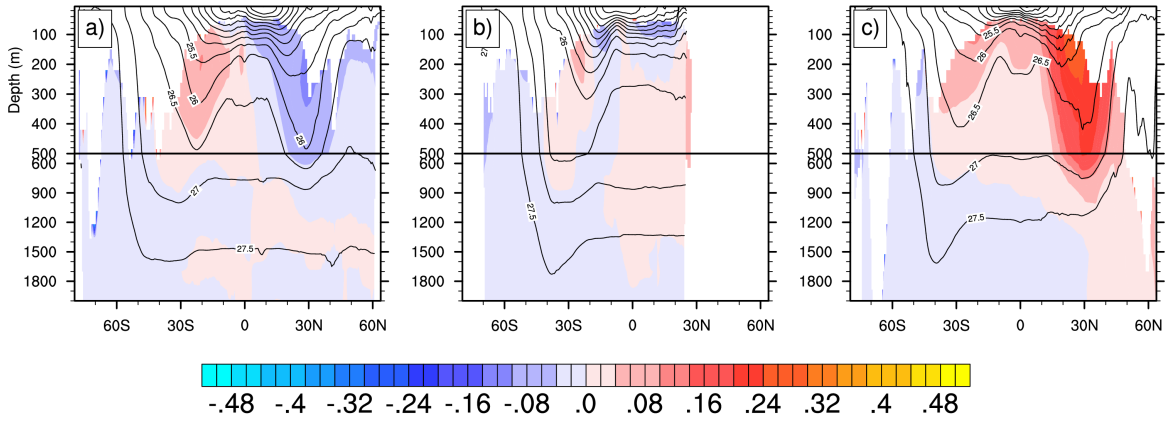

Figure 5.16: Zonal average of passive tracer changes for the mean period of 51-70 years for (a) the Pacific (b) the Indian and (c) the Atlantic Oceans. Values above the base of control run mixed layer is masked. Over-contoured with the mean neutral densities of the control run.

Antarctic Bottom Waters (AABW) propagates towards the north in the global ocean. However, the signal is much weaker. Note that the time change in the deeper layers is ongoing and have not reached an equilibrium. These changes are only a small fraction of the near-surface changes, which is modified by the mixing processes in the ocean interior, changing the actual properties of the subducted water. Also, the propagation time required for the surface changes to reach deeper layers is longer in the Pacific and Indian Oceans compared to the Atlantic due to their lesser densities and weaker circulation compared to the Atlantic.

Unlike tracer propagation, in faf-water, it appears that a large part of surface changes reaches the subsurface and propagates faster within the 1000 m (Fig. 5.18). In the Atlantic, in comparison to passive tracer, we earlier explained the large reduction in SSS (by 0.2-0.5 psu) to a possible increase in mixing due to buoyancy flux changes. From Fig. 5.18, it appears a larger fraction of the surface changes have subducted and

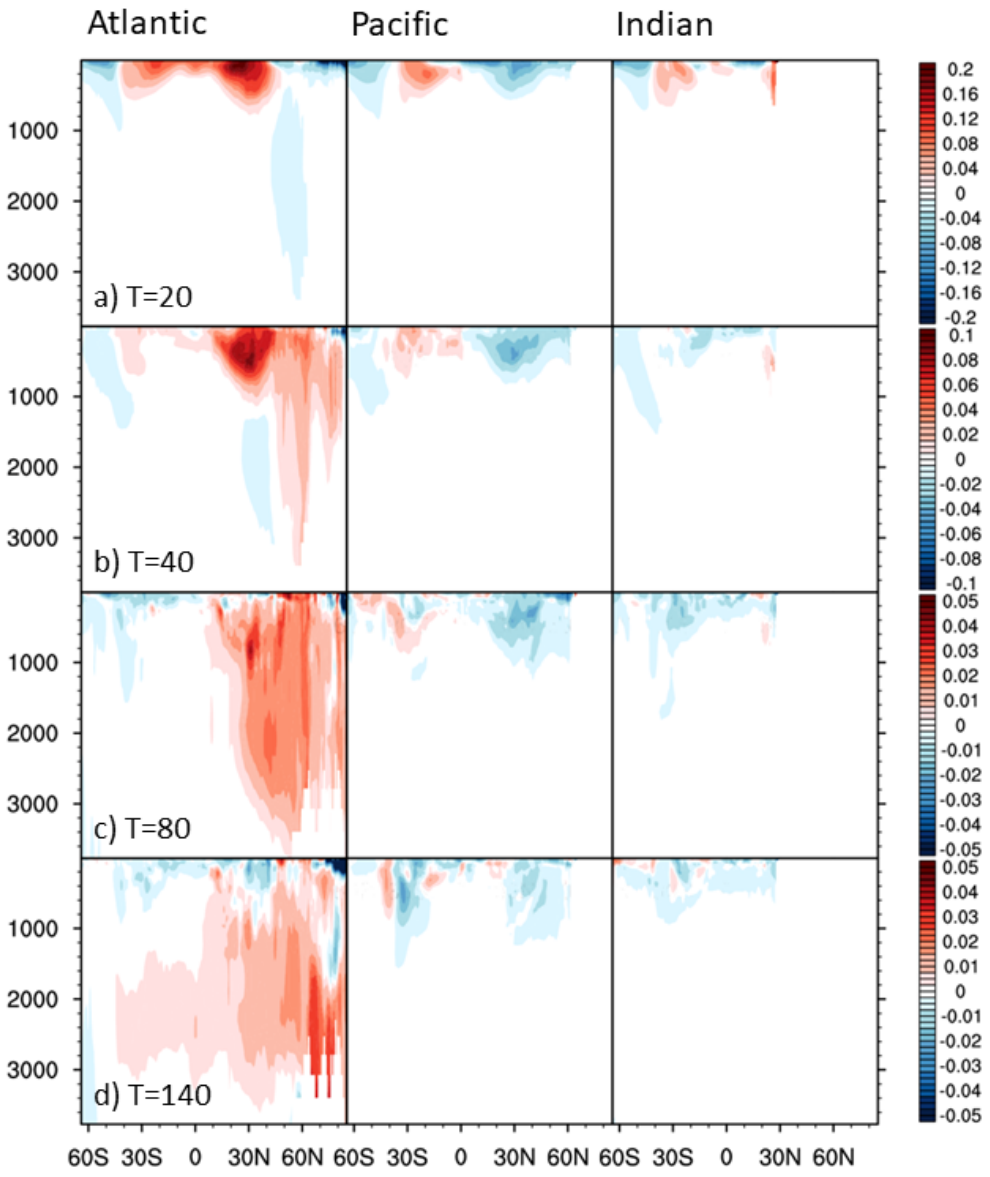

Figure 5.17: Passive tracer propagation through subsurface. Changes in tracer values relative to 20 years before that year, i.e T-20, where T is a given year starting from a) T=20 followed by b) T=40, c) T=80 and d) T=140. We have only shown those differences that show distinct propagation patterns throughout the time evolution. The propagation at each time step has different scales in order to show the changes clearly.

that the subducted salinity changes are propagating faster than in tracer run, often seen in dipole like pattern. This means a faster redistribution of the salinities occur both in surface and subsurface levels leading to a global reduction in salinity. In addition, the order of magnitude of the subducted changes remain the same over the entire period. That means the SSS changes at surface does not sustain longer and they subduct much faster in faf-water because of which the SSS response appears weak despite the

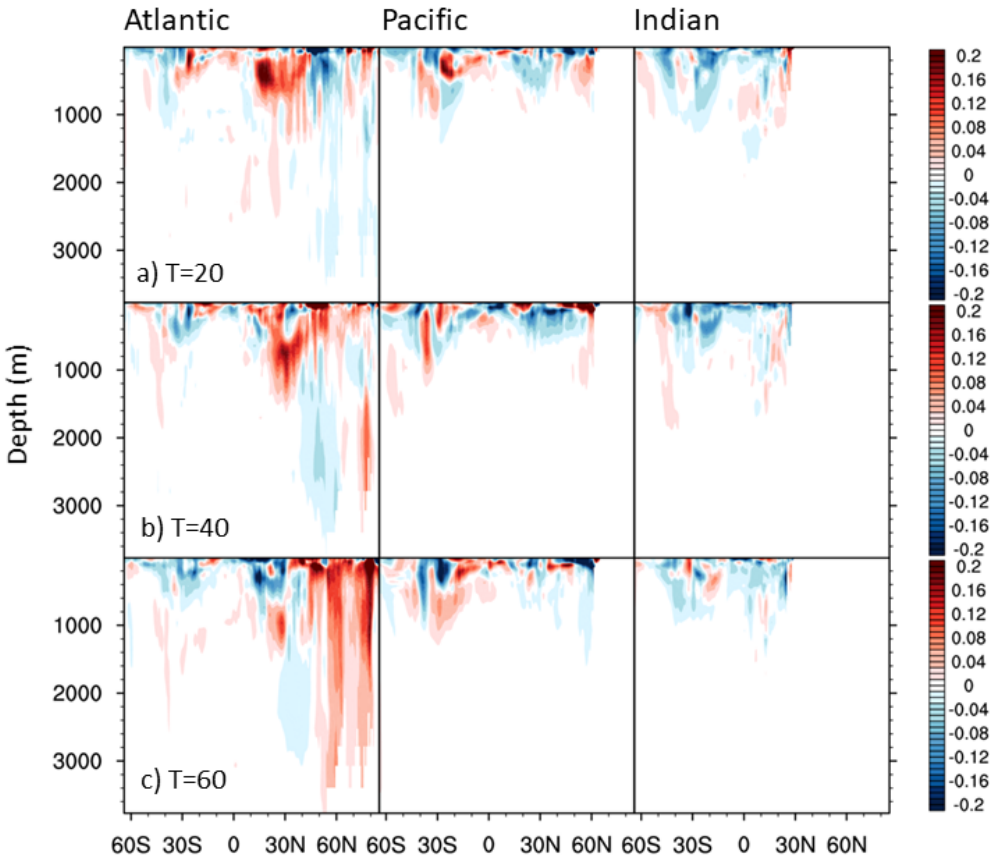

Figure 5.18: faf-water salinity propagation through subsurface, similar to Fig. 5.17.

strong FWF changes. This may be connected with an increase in gyre circulation in all the ocean basins, especially in the southern hemisphere (Fig. 5.13). These changes in circulation could be causing a redistribution of the salinity in comparison with the passive tracer run. In the northern hemisphere, there is an increase, however, with a slight equatorward shift, in the North Pacific subtropical gyre, marked by a dipole like pattern. On the other hand, the subtropical North Atlantic experience a decrease in gyre strength.

Typically at high temperatures, the variations in temperature dominate the buoyancy flux driven circulation changes, while salinity controls when the temperatures are low. Levang and Schmitt (2020) reported that positive salinity changes strengthen the AMOC and slightly oppose the warming-driven AMOC weakening. Therefore, in the absence of warming in faf-water, these subducted strong salinity changes likely drive a slight intensification of the AMOC in faf-water (Fig.5.8a). The AMOC strengthening explains the increased northward transport of positive salinity changes in the upper 300-400 m (Fig. 5.18b). An increased transport could explain why there is a decrease in salinity south of this region (Fig. 5.18b), in comparison with tracer where we do not

notice such a decrease (Fig. 5.17b). Therefore, increased gyre circulations combined with increased meridional circulation could be a large factor in salinity reduction and redistribution observed in faf-water.

5.5 Discussion and concluding remarks

In this chapter, the FAFMIP runs for the three separate surface flux perturbations, FWF, momentum and heat flux, are analysed to understand the impact of changes in each surface forcings on surface and subsurface salinity responses of the global ocean. The last 20 year time mean of the faf-runs relative to the control run have been analysed. We used the FAFMIP experiments to verify the salinity contributions obtained from an RCP8.5-forced run. Due to the ocean-atmospheric coupled feedback, each FAFMIP-HR experiments' flux data show changes in other surface forcings, in addition to changes in the original perturbation flux field. Therefore, in effect, surface flux contributions are not completely isolated in FAFMIP-HR, which makes it challenging to interpret salinity responses related to a given flux change in many regions, particularly for the heat flux perturbation experiment, faf-heat-NA50pct.

The faf-water and faf-stress flux output have the least amount of significant changes in other surface forcings, whereas the faf-heat-NA50pct flux output shows the most changes. The faf-stress run induces much less changes in the FWF over the global ocean. However, wind-stress changes in faf-stress is much less compared to faf-water and faf-heat-NA50pct. This seems to be a disadvantage in using faf-stress run in interpreting wind-related changes. The faf-heat-NA50pct experiment introduces significant changes in FWF in the tropics and subpolar latitudes and wind-stress changes over the high-latitudes.

The sum of individual salinity responses from faf-water, faf-stress and faf-heat is almost the same as the salinity response from simultaneous perturbation run, faf-all. Therefore, we added the faf-water, faf-stress and faf-heat-NA50pct to calculate the SSS pattern amplification and determine how much of the amplification comes from each experiment. The total SSS response PA was only 3.5 % which is less than the sum of individual SSS PA, which is 2 % for faf-water and 5.5 % for faf-heat-NA50pct. The faf-stress SSS PA is negative and about 3 %. Therefore, this lesser total SSS PA of 3.5 % is because the individual runs generate a lot of compensating signals when added, such as in the northern north Atlantic, subtropical Indian Ocean. In addition, the exact contributions from each surface forcing in FAFMIP can vary due to air-sea coupling, for example, a large part of the SSS changes in faf-heat-NA50pct is a result of induced FWF changes. Hence, it might not be a suitable way to access the amount of amplification connected to the total SSS signal as we cannot attribute this strictly to a given flux.

After taking into account the consistent and similar responses between the faf-water and faf-heat-NA50pct runs, the SSS reduction in the tropical Pacific, subtropical North Pacific and eastern tropical and north Indian oceans is consistent with the increase in FWF into the Pacific and north Indian oceans. Hence, these regions are indeed dominated by FWF changes. In that aspect, it gets complicated in the Atlantic basin. The SSS increase in the tropical and subtropical Atlantic is not significant in faf-water run. This shows that FWF change alone is not sufficient in generating large SSS anomalies in the Atlantic Ocean. It seems both warming and FWF changes together create the SSS increase. For instance, in the faf-water run, a negative FWF in the subtropical South Atlantic does not create positive SSS changes, whereas surface ocean warming in faf-heat-NA50pct shows an increase in SSS in the South Atlantic with similar changes in FWF. Given that the circulation changes are not significantly different in these runs, we have to consider that an increase in FWF does increase the SSS in the Atlantic, but surface warming helps to maintain these changes by reducing decay of surface salinities. We can explain this by the simple mechanism related to density. Increase in SSS causes an increase in density in a given region. Thus, salinification can cause the surface to destabilise and thereby cause more vertical mixing followed by an SSS reduction. In the presence of surface warming, the high temperatures compensates for the high density due to salinity and stabilise the surface (Levang and Schmitt 2020). Therefore, the surface warming can sustain the large SSS changes and drive an amplification over time.

A simple spice and heave decomposition of subsurface salinity in faf-water run showed that FWF perturbation does not cause much heave-driven changes. Most of the changes in the global ocean could be explained by the spice signal alone, and is consistent with the surface FWF changes. This is in agreement with our RCP8.5 study where we determined the spice component to be the major driver of subsurface salinity changes caused by surface FWF. Hence, these results together confirm that under an enhanced water cycle, the subsurface change in salinity is dominated by FWF changes, particularly in the subtropical oceans.

In addition, we noticed that warming in faf-heat-NA50pct mainly causes large signals in the heave and spice components that are almost anti-correlated. The warming in faf-stress is weak in comparison. Therefore, in the faf-stress and faf-water, this strong anti-correlated signal is absent. We can confirm that a substantial warming drive changes on salinity through heave and spice components. However, heave and spice signal in a global warming scenario are largely anti-correlated and masks the contributions from other surface forcings. As a result of which warming-driven changes on salinity are negligible.

The surface FWF is the dominating contributor to significant subsurface salinity changes in the Atlantic, Pacific and Indian oceans. Therefore, in order to understand

the feedbacks arising from the freshwater perturbation and to identify the changes in salinity response introduced by the oceanic responses and feedbacks, we performed a passive tracer experiment. A passive salinity tracer initialised with the control run salinity was perturbed with the same freshwater perturbation as in faf-water and run for 150 years.

The surface tracer pattern shows freshening in the Pacific and Indian Oceans and a strong salinification in the Atlantic Ocean. The tracer changes are considerably different from the SSS changes in faf-water, especially for the Atlantic Ocean, where the SSS increase is weak. There is a reduction (increase) in salinity (freshwater) at the surface of faf-water. The changes were as large as 0.5 psu in certain regions, such as in the subtropical North Atlantic and subtropical South Pacific. This indicated a strong redistribution of salinity in faf-water. In certain regions, such as the subtropical North Atlantic and eastern tropical Indian Ocean, this strong reduction coincided with a weakening and increase in surface FWF, respectively. However, in large parts this does not seem to hold true. In faf-water, the high-latitude southern hemisphere showed strong westerlies. The westerlies cause a northward Ekman transport that pushes fresh waters from the high-latitude oceans into the mid-latitudes. Hence, an increase in their strength drives more transport and thus, an enhanced freshening of the latitudes north of it. An increase in SSS in the southern ocean in faf-water compared to the passive tracer changes suggests this process could be driving the freshening in the subtropical oceans in the south.

Compared to the passive tracer subsurface propagation, the salinity propagation in faf-water showed drastic changes with larger magnitudes over the same timescales. The subducted salinity values in faf-water run were 2 times stronger than the passive tracer values by the end of faf-water run. These strong anomalies in the subsurface could be from the gyre circulation and/or AMOC changes. Firstly, AMOC is slightly intensified in the faf-water experiment. It is under the theory that AMOC is sensitive to freshwater changes in the northern North Atlantic which affects the sinking of salinity anomalies. A mechanism associated with this is the salt-advection feedback. An increase in the northern north Atlantic salinity when subducted along the isopycnals, causes an increase in the western Atlantic thermocline waters which comprises the upper limb of AMOC (Broecker et al. 1990). A salinity increase thus increases AMOC, which in turn causes salinity increase in the northern latitudes by an increased northward salt transport. This mechanism is supported in faf-water by an increase observed in northern latitude SSS in the North Atlantic and a northward increase in subsurface salinity. Secondly, the gyre circulation shows an increase, particularly in the southern hemisphere. These increased circulation replaces more water by causing more mixing. Thus, a redistribution of the salinity anomalies by changes in circulation together with induced FWF changes appears to be causing the significant reduction in faf-water SSS.

The passive tracer experiment is a preliminary step to understanding the extend at which other oceanic responses such as circulation changes affect the salinity response from enhanced water cycle. In future, a detailed analysis to determine the saturation time of the passive tracer at different depths could be performed to understand the time taken for the surface anomalies to reach different parts of the ocean. Along with that, a quantitative analysis on the oceanic contributions and feedbacks associated with an intensification of the water cycle would enhance our knowledge in how they affect the ocean and climate.

Chapter 6

Conclusions

We investigated the impact of surface forcings on salinity changes of the global ocean under a global warming scenario. The first set of objectives were to understand the mechanisms driving the salinity changes, thereby determine the major driver of the projected salinity changes, and to distinguish the salinity contributions from each surface forcing. In the second part of the study, we used salinity responses from the individually forced flux experiments in FAFMIP to verify the salinity contributions determined in the first part of the study.

6.1 Projected salinity changes under warming and their major drivers

The first part of the analysis used the MPI-ESM-MR to investigate the global salinity response in a high-emission RCP8.5 scenario (2081-2100) relative to the historical period (1986-2005). The RCP8.5 forced climate change scenario showed substantial changes in warming, freshwater flux and wind-stress forcings. The resulting SSS changes in the global ocean showed that the Atlantic Ocean may get saltier, and the Pacific and Indian Oceans may become fresher in comparison to the historical period.

A pattern amplification is a measure of intensification from the mean global pattern. For a global surface ocean warming of 2.3 °C, the projected global SSS pattern amplification in the RCP8.5 scenario is estimated to be 18 % with a pattern correlation of 0.73. This SSS amplification is accompanied with a pattern amplification of 19 % and a correlation of 0.83 in the surface freshwater flux. A large part of this SSS amplification occurs in the Atlantic Ocean (31 %), whereas the Pacific and Indian oceans experience much weaker amplification (9 % each) compared to the Atlantic. Hence, in a projected ocean warming scenario, the Atlantic Ocean is found to experience the most substantial salinity changes at the surface that closely resembles the mean climatological SSS.

A significant increase in subsurface salinity in the subtropical North Atlantic Ocean is noticed to a depth of ∼1100 m. The Pacific and Indian ocean basins do not experience similarly strong changes to that depth and are mostly limited to the upper 500 m. These subsurface salinity changes can be associated with the mechanisms of water-mass changes (spice) and the vertical shift of isopycnals (heave). We found that, in the presence of warming, a decomposition of subsurface salinity into spice and heave components produced mutually opposing signals, which could not be used to distinguish the contributions from warming, freshwater or wind-stress related changes. However, from this decomposition we found that spice and heave together dominated salinity changes in the upper 1000 m of the subtropical Atlantic Ocean, whereas the spice changes dominated in the upper 500 m of the subtropical North Pacific and South Indian oceans. We also noted that a freshening in the upper 500 m of the high-latitude ocean basins were dominated by the heave component.

The contributions from each surface forcing were determined from the approach of pure warming, pure freshening and pure heave processes developed by Bindoff and Mcdougall (1994). Using this approach, we found that changes in surface freshwater flux are the primary driver of the subsurface salinity changes in the tropical and subtropical Atlantic, subtropical North Pacific and subtropical South Indian oceans. The surface freshwater flux changes drive major subsurface changes by modifying the water-mass along isopycnals.

Another major advancement in this study, in the area of multidecadal salinity changes, is that the wind-stress and circulation changes are found to be one of the major drivers of subsurface salinity changes in the subtropical Atlantic Ocean. This is a result of a strengthening of the subtropical gyre circulation connected to an increase in the Gulfstream North Atlantic currents drove a deepening of the isopycnals. However, the wind-stress and circulation changes played no significant role in the Pacific and Indian Oceans. Although wind-stress related isopycnal deepening drive some freshening in the high-latitudes, the contribution was weak.

Surface warming was found to cause salinity changes by isopycnal deepening and by water-mass changes. However, these heave and spice components attributed to warming compensated each other. As a result, the depth level salinity contributions from warming of the surface ocean are found to be negligible in most parts of the ocean, especially in the subtropical ocean basins. A dominant part of the freshening in the high-latitude ocean comes from warming, along with minor contributions from wind-stress and freshwater flux changes.

In essence, our study concludes that, under a global warming scenario, the subsurface salinity changes in the world oceans occur primarily from the intensification of the surface freshwater flux. In the Atlantic Ocean, however, the contributions from wind-stress and circulation changes play an equally important role as the surface freshwater

flux changes. Moreover, warming-driven salinity changes are found to have played no significant role in the salinity changes on depth levels.

6.2 Salinity response to surface flux-forced runs

In the second part of this thesis, a set of surface flux-forced FAFMIP experiments performed on MPI-ESM-HR were used to compare the salinity responses to individual forcings from the section 6.1. The surface flux-forced runs enabled to isolate salinity contributions from each of the surface fluxes. The FAFMIP results were largely consistent with our findings from section 6.1. This study also confirms that the warming largely produced an anti-correlated signal on spice and heave.

For the South Atlantic box, the SSS response in the Atlantic Ocean depicted a stronger connection to surface warming compared to the freshwater flux perturbation experiment (faf-water). In the absence of warming in faf-water, a decrease in surface freshwater flux alone could not cause a large SSS amplification in the South Atlantic box.

The disadvantage of the FAFMIP experiments were the changes induced in other surface forcings due to the coupled ocean-atmosphere feedback. To some extent, this limited the interpretation of salinity response to attribute it to corresponding surface flux changes of the experiment. This limitation was found to be largest in heat flux perturbation experiment.

To identify the extent of feedback and circulation changes driving the salinity changes in a perturbed freshwater run, a salinity passive tracer experiment was performed in the last part of this study. The passive tracer evolution showed that the surface changes in most parts of the global ocean closely resembles the projected SSS changes in an RCP8.5 scenario with a freshening of the tropical and subtropical North Pacific Ocean and salinification of the Atlantic Ocean.

A comparison between the passive tracer experiment and faf-water showed a significant reduction in SSS in most parts of the faf-water run. A part of this difference was arising from the changes in the surface freshwater flux owing to a negative atmospheric feedback in the faf-water run. In addition, the subsurface salinity changes propagating in the faf-water experiment were stronger than in the passive tracer experiment at least by a factor of 2, especially in the Atlantic Ocean. This faster propagation could be linked to an increased circulation. Therefore, another part of the reduced SSS in the faf-water run was most likely arising from the circulation changes. However, this is a qualitative assessment and a detailed quantitative analysis was not performed in this study. Such an analysis would be required to determine the salinity reduction from circulation changes and flux changes.

This whole study investigated the contributions on the zonal average of the ocean basins. Therefore, caution should be taken while interpreting the subsurface salinity changes, especially at smaller spatial scales.

6.3 Implications and future research

The salinity changes and their response to different surface forcings in this thesis trigger new questions which require further investigation. In view of the projected intensification of the water cycle, a domination of the surface freshwater flux on salinity changes implies that, under global warming, salinity changes would continue to be a good indicator to obtain a detailed understanding of the water cycle changes. Additionally, the results also imply that the more the water cycle intensifies under global warming, the more the salinity changes. Such large and fast changes in salinity can cause significant changes in the ocean circulation and thereby have implications on the heat transport and ultimately on climate.

Our study shows a clear difference in contributions and mechanisms between the Atlantic Ocean and the Pacific-Indian oceans. The major contribution from spice component is connected to surface freshwater flux and warming, with the assumption that wind-stress changes are not contributing to the spice component. However, a surface shift in isopycnal outcrop locations may come from the wind-stress changes that get subducted along isopycnals (Durack and Wijffels (2010)). Since the RCP8.5 forcing scenario has large variations in the wind-stress and gyre circulation changes, one could make an attempt to determine if wind-stress changes can indeed contribute to spice component of the salinity signal. Such an analysis would be important on smaller timescales where wind-driven changes are often dominating (Bindoff and McDougall 2000).

Moreover, the pure heave process is defined as wind-stress and circulation related changes. The circulation changes can also result from the salinity and temperature changes. Since pure heave is a dominant contributor to salinity changes in the $500-1000$ m of the subtropical Atlantic, one can distinguish the circulation components from the wind-stress changes and temperature-salinity changes and separate the salinity contributions coming from both components. An expected weakening of the future AMOC associated with warming (Levang and Schmitt 2020) and the projected strong North Atlantic salinity increase could have implications on each other. Therefore, a detailed analysis to determine the circulation components could provide new insights into the AMOC related salinity distribution in the future.

The passive salinity tracer experiment forces the tracer field with the freshwater-flux perturbation equivalent in a CO_2 forced climate change scenario. With this perturba-

tion, we understand that the upper 500 m of the ocean reach a stable state in salinity change within in a couple of decades of the run. With that in mind, we could perform an experiment forced with constant salinity at the surface that could probably help us to determine if there is an optimal salinity pattern to force subsurface salinity changes. Williams et al. (2010) performed an ocean salinity experiment where they forced global ocean salinity with an additional 35 psu everywhere. They claim that such a salinity increase does not have substantial consequences on the thermohaline circulation. Therefore, it would be interesting to see whether there is a certain spatial salinity pattern that could drive significant oceanic responses.

References

Abdalati, W. and Steffen, K. (1997). Snowmelt on the greenland ice sheet as derived from passive microwave satellite data. *Journal of Climate*, 10(2):165–175.

Allen, M. R. and Ingram, W. J. (2002). Constraints on future changes in climate and the hydrologic cycle. *Nature*, 419(6903):228–232.

Antonov, J. I., Levitus, S., and Boyer, T. P. (2002). Steric sea level variations during 1957–1994: Importance of salinity. *Journal of Geophysical Research: Oceans*, 107(C12):SRF–14.

Baumgartner, A. and Reichel, E. (1975). *The world water balance: mean annual global, continental and maritime precipitation and run-off*. Elsevier.

Béthoux, J.-P., Gentili, B., and Tailliez, D. (1998). Warming and freshwater budget change in the mediterranean since the 1940s, their possible relation to the greenhouse effect. *Geophysical Research Letters*, 25(7):1023–1026.

Bhowmick, M., Sahany, S., and Mishra, S. K. (2019). Projected precipitation changes over the south asian region for every 0.5 c increase in global warming. *Environmental Research Letters*, 14(5):054005.

Bindoff, N. L. and Mcdougall, T. J. (1994). Diagnosing climate change and ocean ventilation using hydrographic data. *Journal of Physical Oceanography*, 24(6):1137–1152.

Bindoff, N. L. and McDougall, T. J. (2000). Decadal changes along an indian ocean section at 32 s and their interpretation. *Journal of Physical Oceanography*, 30(6):1207–1222.

Bindoff, N. L., Willebrand, J., Artale, V., Cazenave, A., Gregory, J. M., Gulev, S., Hanawa, K., Le Quere, C., Levitus, S., Nojiri, Y., et al. (2007). Observations: oceanic climate change and sea level.

Bingham, F. M., Foltz, G. R., and McPhaden, M. J. (2010). Seasonal cycles of surface layer salinity in the pacific ocean. *Ocean Science*, 6(3):775–787.

Bouttes, N. and Gregory, J. (2014). Attribution of the spatial pattern of co2-forced sea level change to ocean surface flux changes. *Environmental Research Letters*, 9(3):034004.

Boyer, T. P., Levitus, S., Antonov, J., Locarnini, R., and Garcia, H. (2005). Linear trends in salinity for the world ocean, 1955–1998. *Geophysical Research Letters*, 32(1).

Caesar, L., Rahmstorf, S., Robinson, A., Feulner, G., and Saba, V. (2018). Observed fingerprint of a weakening atlantic ocean overturning circulation. *Nature*, 556(7700):191.

Chen, J.-F., Zhou, M.-Y., Shao, L., Wang, Y.-Y., Yun, J., Chew, N. Y., and Chan, H.-K. (2004). Feasibility of preparing nanodrugs by high-gravity reactive precipitation. *International journal of pharmaceutics*, 269(1):267–274.

Cravatte, S., Delcroix, T., Zhang, D., McPhaden, M., and Leloup, J. (2009). Observed freshening and warming of the western pacific warm pool. *Climate Dynamics*, 33(4):565–589.

Curry, R., Dickson, B., and Yashayaev, I. (2003). A change in the freshwater balance of the atlantic ocean over the past four decades. *Nature*, 426(6968):826.

Curry, R. and Mauritzen, C. (2005). Dilution of the northern north atlantic ocean in recent decades. *Science*, 308(5729):1772–1774.

Dai, A., Trenberth, K. E., and Qian, T. (2004). A global dataset of palmer drought severity index for 1870–2002: Relationship with soil moisture and effects of surface warming. *Journal of Hydrometeorology*, 5(6):1117–1130.

Dawe, J. T. and Thompson, L. (2006). Effect of ocean surface currents on wind stress, heat flux, and wind power input to the ocean. *Geophysical Research Letters*, 33(9).

De Ruijter, W., Biastoch, A., Drijfhout, S., Lutjeharms, J., Matano, R., Pichevin, T., Van Leeuwen, P., and Weijer, W. (1999). Indian-atlantic interocean exchange: Dynamics, estimation and impact. *Journal of Geophysical Research: Oceans*, 104(C9):20885–20910.

Delcroix, T., Alory, G., Cravatte, S., Corrège, T., and McPhaden, M. (2011). A gridded sea surface salinity data set for the tropical pacific with sample applications (1950–2008). *Deep Sea Research Part I: Oceanographic Research Papers*, 58(1):38–48.

Delcroix, T., Henin, C., Porte, V., and Arkin, P. (1996). Precipitation and sea-surface salinity in the tropical pacific ocean. *Deep Sea Research Part I: Oceanographic Research Papers*, 43(7):1123–1141.

Dickson, B., Yashayaev, I., Meincke, J., Turrell, B., Dye, S., and Holfort, J. (2002). Rapid freshening of the deep north atlantic ocean over the past four decades. *Nature*, 416(6883):832.

Dickson, R., Osborn, T., Hurrell, J., Meincke, J., Blindheim, J., Adlandsvik, B., Vinje, T., Alekseev, G., and Maslowski, W. (2000). The arctic ocean response to the north atlantic oscillation. *Journal of Climate*, 13(15):2671–2696.

Donat, M. G., Lowry, A. L., Alexander, L. V., O'Gorman, P. A., and Maher, N. (2016). More extreme precipitation in the world's dry and wet regions. *Nature Climate Change*, 6(5):508–513.

Drijfhout, S. S., Marshall, D. P., and Dijkstra, H. A. (2013). *Ocean Circulation and Climate: Chapter 11. Conceptual Models of the Wind-Driven and Thermohaline Circulation*, volume 103. Elsevier Inc. Chapters.

Durack, P. J. and Wijffels, S. E. (2010). Fifty-year trends in global ocean salinities and their relationship to broad-scale warming. *Journal of Climate*, 23(16):4342–4362.

Durack, P. J., Wijffels, S. E., and Gleckler, P. J. (2014). Long-term sea-level change revisited: the role of salinity. *Environmental Research Letters*, 9(11):114017.

Durack, P. J., Wijffels, S. E., and Matear, R. J. (2012). Ocean salinities reveal strong global water cycle intensification during 1950 to 2000. *science*, 336(6080):455–458.

Evans, D. G., Toole, J., Forget, G., Zika, J. D., Naveira Garabato, A. C., Nurser, A. G., and Yu, L. (2017). Recent wind-driven variability in atlantic water mass distribution and meridional overturning circulation. *Journal of Physical Oceanography*, 47(3):633–647.

Giorgetta, M. A., Jungclaus, J., Reick, C. H., Legutke, S., Bader, J., Böttinger, M., Brovkin, V., Crueger, T., Esch, M., Fieg, K., et al. (2013). Climate and carbon cycle changes from 1850 to 2100 in mpi-esm simulations for the coupled model intercomparison project phase 5. *Journal of Advances in Modeling Earth Systems*, 5(3):572–597.

Gordon, A. L., Weiss, R. F., Smethie Jr, W. M., and Warner, M. J. (1992). Thermocline and intermediate water communication between the south atlantic and indian oceans. *Journal of Geophysical Research: Oceans*, 97(C5):7223–7240.

Gregory, J. M., Bouttes, N., Griffies, S. M., Haak, H., Hurlin, W. J., Jungclaus, J., Kelley, M., Lee, W. G., Marshall, J., Romanou, A., et al. (2016). The flux-anomaly-forced model intercomparison project (fafmip) contribution to cmip6: investigation of sea-level and ocean climate change in response to co forcing. *Geoscientific Model Development*, 9(11):3993–4017.

Griffies, S. M., Winton, M., Donner, L. J., Horowitz, L. W., Downes, S. M., Farneti, R., Gnanadesikan, A., Hurlin, W. J., Lee, H.-C., Liang, Z., et al. (2011). The gfdl cm3 coupled climate model: characteristics of the ocean and sea ice simulations. *Journal of Climate*, 24(13):3520–3544.

Griffies, S. M., Winton, M., and Hurlin, W. J. (2016). Detailing the heat tracers in fafmip.

Gupta, A. S., McGregor, S., Van Sebille, E., Ganachaud, A., Brown, J. N., and Santoso, A. (2016). Future changes to the indonesian throughflow and pacific circulation: The differing role of wind and deep circulation changes. *Geophysical Research Letters*, 43(4):1669–1678.

Häkkinen, S. (2002). Surface salinity variability in the northern north atlantic during recent decades. *Journal of Geophysical Research: Oceans*, 107(C12):SRF–4.

Häkkinen, S., Rhines, P. B., and Worthen, D. L. (2016). Warming of the global ocean: Spatial structure and water-mass trends. *Journal of Climate*, 29(13):4949–4963.

Harris, T. (1972). Sources of the agulhas current in the spring of 1964. In *Deep Sea Research and Oceanographic Abstracts*, volume 19, pages 633–650. Elsevier.

Haumann, F. A., Gruber, N., Münnich, M., Frenger, I., and Kern, S. (2016). Sea-ice transport driving southern ocean salinity and its recent trends. *Nature*, 537(7618):89–92.

Hegerl, G. C., voN SToRcH, H., Hasselmann, K., Santer, B. D., Cubasch, U., and Jones, P. D. (1996). Detecting greenhouse-gas-induced climate change with an optimal fingerprint method. *Journal of Climate*, 9(10):2281–2306.

Held, I. M. and Soden, B. J. (2006). Robust responses of the hydrological cycle to global warming. *Journal of climate*, 19(21):5686–5699.

Helm, K. P., Bindoff, N. L., and Church, J. A. (2010). Changes in the global hydrological-cycle inferred from ocean salinity. *Geophysical Research Letters*, 37(18).

Holland, M. M., Finnis, J., Barrett, A. P., and Serreze, M. C. (2007). Projected changes in arctic ocean freshwater budgets. *Journal of Geophysical Research: Biogeosciences*, 112(G4).

Holland, M. M., Finnis, J., and Serreze, M. C. (2006). Simulated arctic ocean freshwater budgets in the twentieth and twenty-first centuries. *Journal of Climate*, 19(23):6221–6242.

Hosoda, S., Suga, T., Shikama, N., and Mizuno, K. (2009). Global surface layer salinity change detected by argo and its implication for hydrological cycle intensification. *Journal of Oceanography*, 65(4):579.

Hsu, P.-c., Li, T., Luo, J.-J., Murakami, H., Kitoh, A., and Zhao, M. (2012). Increase of global monsoon area and precipitation under global warming: A robust signal? *Geophysical Research Letters*, 39(6).

Huang, B., Mehta, V. M., and Schneider, N. (2005). Oceanic response to idealized net atmospheric freshwater in the pacific at the decadal time scale. *Journal of physical oceanography*, 35(12):2467–2486.

Huntington, T. G. (2006). Evidence for intensification of the global water cycle: review and synthesis. *Journal of Hydrology*, 319(1-4):83–95.

Ilyina, T., Six, K. D., Segschneider, J., Maier-Reimer, E., Li, H., and Núñez-Riboni, I. (2013). Global ocean biogeochemistry model hamocc: Model architecture and performance as component of the mpi-earth system model in different cmip5 experimental realizations. *Journal of Advances in Modeling Earth Systems*, 5(2):287–315.

Jackett, D. R. and McDougall, T. J. (1997). A neutral density variable for the world's oceans. *Journal of Physical Oceanography*, 27(2):237–263.

Jacobs, S., Giulivi, C., and Mele, P. (2002). Freshening of the ross sea during the late 20th century. *Science*, 297(5580):386–389.

Johnson, E. S., Lagerloef, G. S., Gunn, J. T., and Bonjean, F. (2002). Surface salinity advection in the tropical oceans compared with atmospheric freshwater forcing: A trial balance. *Journal of Geophysical Research: Oceans*, 107(C12):SRF–15.

Jungclaus, J., Fischer, N., Haak, H., Lohmann, K., Marotzke, J., Matei, D., Mikolajewicz, U., Notz, D., and Von Storch, J. (2013). Characteristics of the ocean simulations in the max planck institute ocean model (mpiom) the ocean component of the mpi-earth system model. *Journal of Advances in Modeling Earth Systems*, 5(2):422–446.

Jungclaus, J., Keenlyside, N., Botzet, M., Haak, H., Luo, J.-J., Latif, M., Marotzke, J., Mikolajewicz, U., and Roeckner, E. (2006). Ocean circulation and tropical variability in the coupled model echam5/mpi-om. *Journal of climate*, 19(16):3952–3972.

Kara, A. B., Rochford, P. A., and Hurlburt, H. E. (2003). Mixed layer depth variability over the global ocean. *Journal of Geophysical Research: Oceans*, 108(C3).

Lagerloef, G., Schmitt, R., Schanze, J., and Kao, H.-Y. (2010). The ocean and the global water cycle. *Oceanography*, 23(4):82–93.

Lago, V., Wijffels, S. E., Durack, P. J., Church, J. A., Bindoff, N. L., and Marsland, S. J. (2016). Simulating the role of surface forcing on observed multidecadal upper-ocean salinity changes. *Journal of Climate*, 29(15):5575–5588.

Ledwell, J. R., Watson, A. J., and Law, C. S. (1993). Evidence for slow mixing across the pycnocline from an open-ocean tracer-release experiment. *Nature*, 364(6439):701.

Levang, S. J. and Schmitt, R. W. (2015). Centennial changes of the global water cycle in cmip5 models. *Journal of Climate*, 28(16):6489–6502.

Levang, S. J. and Schmitt, R. W. (2020). What causes the amoc to weaken in cmip5? *Journal of Climate*, 33(4):1535–1545.

Levitus, S., Antonov, J., Boyer, T., Baranova, O., Garcia, H., Locarnini, R., Mishonov, A., Reagan, J., Seidov, D., Yarosh, E., et al. (2017). Ncei ocean heat content, temperature anomalies, salinity anomalies, thermosteric sea level anomalies, halosteric sea level anomalies, and total steric sea level anomalies from 1955 to present calculated from in situ oceanographic subsurface profile data (ncei accession 0164586).

Lutjeharms, J. (1988). Remote sensing corroboration of retroflection of the east madagascar current. *Deep Sea Research Part A. Oceanographic Research Papers*, 35(12):2045–2050.

Lyu, K., Zhang, X., Church, J. A., and Wu, Q. (2020). Processes responsible for the southern hemisphere ocean heat uptake and redistribution under anthropogenic warming. *Journal of Climate*, 33(9):3787–3807.

Maiyza, I. and Kamel, M. (2010). Climatological trend of sea surface salinity anomalies in the south eastern mediterranean sea. *Journal of King Abdulaziz University*, 21(2):63.

Marshall, J., Kushnir, Y., Battisti, D., Chang, P., Czaja, A., Dickson, R., Hurrell, J., McCARTNEY, M., Saravanan, R., and Visbeck, M. (2001). North atlantic climate variability: phenomena, impacts and mechanisms. *International Journal of Climatology: A Journal of the Royal Meteorological Society*, 21(15):1863–1898.

McDougall, T. J. (1987). Neutral surfaces. *Journal of Physical Oceanography*, 17(11):1950–1964.

Mikolajewicz, U. and Voss, R. (2000). The role of the individual air-sea flux components in co 2-induced changes of the ocean's circulation and climate. *Climate Dynamics*, 16(8):627–642.

Moss, R. H., Edmonds, J. A., Hibbard, K. A., Manning, M. R., Rose, S. K., Van Vuuren, D. P., Carter, T. R., Emori, S., Kainuma, M., Kram, T., et al. (2010). The

next generation of scenarios for climate change research and assessment. *Nature*, 463(7282):747–756.

Müller, W. A., Jungclaus, J. H., Mauritsen, T., Baehr, J., Bittner, M., Budich, R., Bunzel, F., Esch, M., Ghosh, R., Haak, H., et al. (2018). A higher-resolution version of the max planck institute earth system model (mpi-esm1. 2-hr). *Journal of Advances in Modeling Earth Systems*, 10(7):1383–1413.

Murtugudde, R. and Busalacchi, A. J. (1998). Salinity effects in a tropical ocean model. *Journal of Geophysical Research: Oceans*, 103(C2):3283–3300.

O'Gorman, P. A., Allan, R. P., Byrne, M. P., and Previdi, M. (2012). Energetic constraints on precipitation under climate change. *Surveys in geophysics*, 33(3-4):585–608.

Painter, S. C. and Tsimplis, M. N. (2003). Temperature and salinity trends in the upper waters of the mediterranean sea as determined from the medatlas dataset. *Continental Shelf Research*, 23(16):1507–1522.

Perner, K., Moros, M., Otterå, O. H., Blanz, T., Schneider, R. R., and Jansen, E. (2019). An oceanic perspective on greenland's recent freshwater discharge since 1850. *Scientific reports*, 9(1):1–10.

Peterson, B. J., Holmes, R. M., McClelland, J. W., Vörösmarty, C. J., Lammers, R. B., Shiklomanov, A. I., Shiklomanov, I. A., and Rahmstorf, S. (2002). Increasing river discharge to the arctic ocean. *science*, 298(5601):2171–2173.

Peterson, B. J., McClelland, J., Curry, R., Holmes, R. M., Walsh, J. E., and Aagaard, K. (2006). Trajectory shifts in the arctic and subarctic freshwater cycle. *Science*, 313(5790):1061–1066.

Pierce, D. W., Gleckler, P. J., Barnett, T. P., Santer, B. D., and Durack, P. J. (2012). The fingerprint of human-induced changes in the ocean's salinity and temperature fields. *Geophysical Research Letters*, 39(21).

Polson, D., Hegerl, G., Allan, R., and Sarojini, B. B. (2013). Have greenhouse gases intensified the contrast between wet and dry regions? *Geophysical Research Letters*, 40(17):4783–4787.

Ponte, R. and Vinogradova, N. (2016). An assessment of basic processes controlling mean surface salinity over the global ocean. *Geophysical Research Letters*, 43(13):7052–7058.

Ramaswamy, V., Schwarzkopf, M., Randel, W., Santer, B., Soden, B. J., and Stenchikov, G. (2006). Anthropogenic and natural influences in the evolution of lower stratospheric cooling. *Science*, 311(5764):1138–1141.

Rao, R. and Sivakumar, R. (2003). Seasonal variability of sea surface salinity and salt budget of the mixed layer of the north indian ocean. *Journal of Geophysical Research: Oceans*, 108(C1):9–1.

Reick, C., Raddatz, T., Brovkin, V., and Gayler, V. (2013). Representation of natural and anthropogenic land cover change in mpi-esm. *Journal of Advances in Modeling Earth Systems*, 5(3):459–482.

Rhein, M., Rintoul, S., Aoki, S., Campos, E., Chambers, D., Feely, R., Gulev, S., Johnson, G., Josey, S., Kostianoy, A., et al. (2013a). Climate change 2013: The physical science basis. *Contribution of Working Group*, 1.

Rhein, M., Rintoul, S. R., Aoki, S., Campos, E., Chambers, D., Feely, R. A., Gulev, S., Johnson, G. C., Josey, S. A., Kostianoy, A., et al. (2013b). Observations: ocean.

Richter, I. and Xie, S.-P. (2010). Moisture transport from the atlantic to the pacific basin and its response to north atlantic cooling and global warming. *Climate dynamics*, 35(2-3):551–566.

Roether, W., Manca, B. B., Klein, B., Bregant, D., Georgopoulos, D., Beitzel, V., Kovačević, V., and Luchetta, A. (1996). Recent changes in eastern mediterranean deep waters. *Science*, 271(5247):333–335.

Sætre, R. and Da Silva, A. J. (1984). The circulation of the mozambique channel. *Deep Sea Research Part A. Oceanographic Research Papers*, 31(5):485–508.

Sallée, J.-B., Shuckburgh, E., Bruneau, N., Meijers, A. J., Bracegirdle, T. J., Wang, Z., and Roy, T. (2013). Assessment of southern ocean water mass circulation and characteristics in cmip5 models: Historical bias and forcing response. *Journal of Geophysical Research: Oceans*, 118(4):1830–1844.

Santer, B. D., Taylor, K., Wigley, T., Johns, T., Jones, P., Karoly, D., Mitchell, J., Oort, A., Penner, J., Ramaswamy, V., et al. (1996). A search for human influences on the thermal structure of the atmosphere. *Nature*, 382(6586):39–46.

Santer, B. D., Wehner, M. F., Wigley, T., Sausen, R., Meehl, G., Taylor, K., Ammann, C., Arblaster, J., Washington, W., Boyle, J., et al. (2003). Contributions of anthropogenic and natural forcing to recent tropopause height changes. *science*, 301(5632):479–483.

Schmitt, R. W. (2008). Salinity and the global water cycle. *Oceanography*, 21(1):12–19.

Schneck, R., Reick, C. H., and Raddatz, T. (2013). Land contribution to natural co2 variability on time scales of centuries. *Journal of Advances in Modeling Earth Systems*, 5(2):354–365.

Serreze, M. C. and Stroeve, J. (2015). Arctic sea ice trends, variability and implications for seasonal ice forecasting. *Philosophical Transactions of the Royal Society A: Mathematical, Physical and Engineering Sciences*, 373(2045):20140159.

Sévellec, F., Fedorov, A. V., and Liu, W. (2017). Arctic sea-ice decline weakens the atlantic meridional overturning circulation. *Nature Climate Change*, 7(8):604.

Skliris, N., Marsh, R., Josey, S. A., Good, S. A., Liu, C., and Allan, R. P. (2014). Salinity changes in the world ocean since 1950 in relation to changing surface freshwater fluxes. *Climate dynamics*, 43(3-4):709–736.

Solomon, S., Manning, M., Marquis, M., Qin, D., et al. (2007). *Climate change 2007-the physical science basis: Working group I contribution to the fourth assessment report of the IPCC*, volume 4. Cambridge university press.

Sterl, A., Bintanja, R., Brodeau, L., Gleeson, E., Koenigk, T., Schmith, T., Semmler, T., Severijns, C., Wyser, K., and Yang, S. (2012). A look at the ocean in the ec-earth climate model. *Climate Dynamics*, 39(11):2631–2657.

Stevens, B., Giorgetta, M., Esch, M., Mauritsen, T., Crueger, T., Rast, S., Salzmann, M., Schmidt, H., Bader, J., Block, K., et al. (2013). Atmospheric component of the mpi-m earth system model: Echam6. *Journal of Advances in Modeling Earth Systems*, 5(2):146–172.

Stramma, L. and Lutjeharms, J. R. (1997). The flow field of the subtropical gyre of the south indian ocean. *Journal of Geophysical Research: Oceans*, 102(C3):5513–5530.

Stroeve, J., Markus, T., Boisvert, L., Miller, J., and Barrett, A. (2014). Changes in arctic melt season and implications for sea ice loss. *Geophysical Research Letters*, 41(4):1216–1225.

Taylor, K. E., Stouffer, R. J., and Meehl, G. A. (2012). An overview of cmip5 and the experiment design. *Bulletin of the American Meteorological Society*, 93(4):485–498.

Terray, L., Corre, L., Cravatte, S., Delcroix, T., Reverdin, G., and Ribes, A. (2012). Near-surface salinity as nature's rain gauge to detect human influence on the tropical water cycle. *Journal of Climate*, 25(3):958–977.

Tesdal, J.-E., Abernathey, R., Goes, J. I., Gordon, A. L., and Haine, T. W. (2018). Drivers of recent salinity trends in the subpolar north atlantic. In *AGU Fall Meeting Abstracts*.

Thorpe, R. and Bigg, G. (2000). Modelling the sensitivity of mediterranean outflow to anthropogenically forced climate change. *Climate dynamics*, 16(5):355–368.

Todd, A., Zanna, L., Couldrey, M., Gregory, J. M., Wu, Q., Church, J. A., Farneti, R., Navarro-Labastida, R., Lyu, K., Saenko, O. A., et al. (2020). Ocean-only fafmip: Understanding regional patterns of ocean heat content and dynamic sea level change.

Trenberth, K., Jones, P., Ambenje, P., Bojariu, R., Easterling, D., Klein Tank, A., Parker, D., Rahimzadeh, F., Renwick, J., Rusticucci, M., et al. (2007). Observations: surface and atmospheric climate change. chapter 3. *Climate change*, pages 235–336.

Trenberth, K. E. (2011). Changes in precipitation with climate change. *Climate Research*, 47(1-2):123–138.

Valsala, V., Maksyutov, S., and Murtugudde, R. (2011). Interannual to interdecadal variabilities of the indonesian throughflow source water pathways in the pacific ocean. *Journal of Physical Oceanography*, 41(10):1921–1940.

Vavrus, S. J., Holland, M. M., Jahn, A., Bailey, D. A., and Blazey, B. A. (2012). Twenty-first-century arctic climate change in ccsm4. *Journal of Climate*, 25(8):2696–2710.

Vinogradova, N. T. and Ponte, R. M. (2017). In search of fingerprints of the recent intensification of the ocean water cycle. *Journal of Climate*, 30(14):5513–5528.

Wentz, F. J., Ricciardulli, L., Hilburn, K., and Mears, C. (2007). How much more rain will global warming bring? *Science*, 317(5835):233–235.

Willett, K. M., Jones, P. D., Gillett, N. P., and Thorne, P. W. (2008). Recent changes in surface humidity: Development of the hadcruh dataset. *Journal of Climate*, 21(20):5364–5383.

Willett, K. M., Jones, P. D., Thorne, P. W., and Gillett, N. P. (2010). A comparison of large scale changes in surface humidity over land in observations and cmip3 general circulation models. *Environmental Research Letters*, 5(2):025210.

Williams, P. D., Guilyardi, E., Madec, G., Gualdi, S., and Scoccimarro, E. (2010). The role of mean ocean salinity in climate. *Dynamics of Atmospheres and Oceans*, 49(2-3):108–123.

Williams, P. D., Guilyardi, E., Sutton, R., Gregory, J., and Madec, G. (2007). A new feedback on climate change from the hydrological cycle. *Geophysical research letters*, 34(8).

Wong, A. P., Bindoff, N. L., and Church, J. A. (1999). Large-scale freshening of intermediate waters in the pacific and indian oceans. *Nature*, 400(6743):440.

Yang, S., Lau, K.-M., and Schopf, P. S. (1999). Sensitivity of the tropical pacific ocean to precipitation-induced freshwater flux. *Climate dynamics*, 15(10):737–750.

Zhang, R.-H. and Busalacchi, A. J. (2009). Freshwater flux (fwf)-induced oceanic feedback in a hybrid coupled model of the tropical pacific. *Journal of climate*, 22(4):853–879.

Zhang, X., Zwiers, F. W., Hegerl, G. C., Lambert, F. H., Gillett, N. P., Solomon, S., Stott, P. A., and Nozawa, T. (2007). Detection of human influence on twentieth-century precipitation trends. *Nature*, 448(7152):461–465.

Zika, J. D., Skliris, N., Blaker, A. T., Marsh, R., Nurser, A. G., and Josey, S. A. (2018). Improved estimates of water cycle change from ocean salinity: the key role of ocean warming. *Environmental Research Letters*, 13(7):074036.

List of Acronyms

SSS	Sea Surface Salinity
E	Evaporation
P	precipitation
R	River runoff
CC	Clausius–Clapeyron
SST	Sea Surface Temperature
RSW	Red Sea Water
PGW	Persian Gulf Water
AAIW	Antarctic Intermediate Water
SMW	Subtropical Mode Water
WP	Warm Pool
IPCC	Intergovernmental Panel on Climate Change
ITCZ	Intertropical Convergence Zone
SPCZ	South Pacific Convergence Zone
NAO	North Atlantic Oscillation
CMIP	Coupled Model Intercomparison Project
CMIP5	CMIP Phase 5
CMIP6	CMIP Phase 6
MPI-ESM	Max Planck Institute - Earth System Model
MPI-ESM-MR	MPI-ESM-Mixed Resolution
MPI-ESM-HR	MPI-ESM-High Resolution
RCP	Representative Concentration Pathways
MPIOM	Max Planck Institute Ocean Module
FAFMIP	Flux-Anomaly-Forced Intercomparison Project
FWF	freshwater flux
PW	Pure Warming
PF	Pure Freshening
PH	Pure Heave
IFREMER	French Research Institute for Exploitation of the Sea

List of Figures

List of Tables

Acknowledgment

I would like to express sincere gratitude to my supervisor Prof. Dr. Detlef Stammer for giving me the opportunity to do research and providing his guidance and motivation throughout my PhD. I am deeply grateful to my co-supervisor Dr. Armin Köhl for providing his invaluable support, for the constructive criticisms, and for his patience at times when I was truly stupid. Without their mentoring and inspiration, I could not have finished this work.

I am extending my heartfelt thanks to Dr. Johann Jungclaus for being my panel chair and providing me with insightful comments during the course of my work. I also owe a great debt of gratitude to Dr. Helmuth Haak for helping me set up the experiment for my study and providing his complete support in learning the MPI-Earth system model.

I am truly happy and thankful to be a part of the Remote Sensing and Assimilation Group from the Institute of Oceanography. It was a pleasure to benefit from their collective experience and to make acquaintance with their exceptional personalities.

I would like to thank the Deutsche Forschungsgemeinschaft (DFG) funded Forschergruppe 1740 and the University of Hamburg for supporting this research work. A special thanks to SICSS graduate school for providing a joyful and learning environment during PhD.

I have received endless support from my friend Saurabh through all the brainstorming discussions. My friend J örg provided me with incredible support throughout my PhD and especially during the writing of my thesis. Manita, Sayantani, Sebastian and Mark helped to refine the dissertation through their constructive comments. My fellow colleague and friend Song helped me during my difficult times coding MATLAB. I cannot express enough thanks to all of them.

My gratitude goes to all my family and friends who gave me all their love and support throughout my life. At last but not least, to my husband Ajith, without whom I could not have possibly come this far in life.

Aus dieser Dissertation hervorgegangene Vorveröffentlichungen
List of Publications

To be submitted
Sathyanarayanan A., Köhl A. and Stammer D.,2020 : Mechanisms for salinity change in the global ocean under global warming conditions.

Eidesstattliche Versicherung
Declaration on Oath

Hiermit versichere ich an Eides statt, dass ich die vorliegende Dissertation mit dem Titel: „Understanding projected salinity changes in the global ocean of the MPI-Earth system model under a global warming scenario“ selbstständig verfasst und keine anderen als die angegebenen Hilfsmittel – insbesondere keine im Quellenverzeichnis nicht benannten Internet-Quellen – benutzt habe. Alle Stellen, die wörtlich oder sinngemäß aus Veröffentlichungen entnommen wurden, sind als solche kenntlich gemacht. Ich versichere weiterhin, dass ich die Dissertation oder Teile davon vorher weder im In- noch im Ausland in einem anderen Prüfungsverfahren eingereicht habe und die eingereichte schriftliche Fassung der auf dem elektronischen Speichermedium entspricht.

I hereby declare an oath that I have written the present dissertation on my own with the title: “Understanding projected salinity changes in the global ocean of the MPI-Earth system model under a global warming scenario” and have not used other than the acknowledge resources and aids. All passages taken literally or analogously from other publications are identified as such. I further declare that this thesis has not been submitted to any other German or foreign examination board and that the submitted written version corresponds to that on the electronic repository.

Hamburg, den 9. Juni 2020

Anju Sathyanarayanan